AIR CONDITIONER CONDENSER OPTIMIZATION

A THESIS

Presented to

The Faculty of the Division

of Graduate Studies

By

James Lawson Propst

In Partial Fulfillment

of the Requirements for the Degree

Master of Science in Mechanical Engineering

Georgia Institute of Technology

August, 1975

AIR CONDITIONER CONDENSER

OPTIMIZATION

Approved:

S. V. Shelton, Chairman

R. B. Evans

P. V. Kadaba

D. Young

Date approved by Chairman: 8/28/75

ACKNOWLEDGMENTS

I wish to express special gratitude to Dr. Shelton, my advisor, for suggesting this study. Then, for his expertise, insights, enthusiasm, and guidance in developing this work I am truly grateful. It was a pleasure working with Dr. Shelton.

A special word of thanks to Dr. Young for his role on the reading committee and for his helpful comments and suggestions concerning the economic analysis. I appreciate Dr. Evans and Dr. Kadaba's willingness to serve on the committee and their constructuve review of this thesis.

Lastly, my appreciation to others who have made completion of this work possible.

This work is dedicated to my dear mom and dad whose love, prayers, and encouragement have been a source of continual inspiration to me.

TABLE OF CONTENTS

LIST OF ILLUSTRATIONS

Figure Page

Figure | Page

LIST OF TABLES

SUMMARY

This study develops a methodology for determining the minimal annual cost condenser (amortized equipment cost and operating cost) for an air conditioning system. First the condenser and A/C system are modeled so that the system coefficient of performance can be evaluated as a function of the condenser design parameters: air flow area, number of fins per inch, fin depth, working fluid saturation temperature, air inlet temperature, and air velocity.

Secondly, the model is combined with an economic analysis in order to minimize total cost. This allows the optimal air velocity and condenser configuration to be found for various combinations of energy cost and annual hours of operation. The methodology is applied to the solution of optimal condensers for several locations in the United States.

The results indicate potential savings are possible in selection of the condenser configuration and air velocity. However, the savings associated with optimizing the configuration are generally small since it is shown that the configuration can deviate from the optimum over quite a wide range without affecting the total cost significantly, i.e. there are any number of condenser configurations that are nearly equal in cost-effectiveness.

Of much greater importance in reducing the cost

(operating cost) is the air velocity. The study shows that, in general, A/C units should be operated at significantly higher velocities than is the common practice. The model predicts reductions in operating cost ranging from 5 percent to over 50 percent for typical units currently on the market by increasing velocity to the optimal value for a given configuration. This velocity optimization is applicable to existing A/C units by changing only the condenser fan system.

The study's results are embodied in a few key equations describing the system coefficient of performance and a number of curves and tables which are intended as a guide and reference for the technical designer and interested customer.

NOMENCLATURE

Symbol	Refers to:
A	frontal area of the condenser (ft^2)
A_f	total fin surface area (ft^2)
A_i	inside tube surface area (ft^2)
A_o	total air-side heat transfer surface area (ft^2)
$A/Q_e opt$	optimal condenser frontal area per ton (ft^2/ton) as shown in Appendix D
A_t	outside tube surface area (ft^2)
a	a constant dependent upon mode of air flow through heat exchanger
b	exponent on Reynolds number, dependent upon geometry and regime of flow field
C_f	average friction coefficient. By definition $C_f = \frac{2\tau}{\rho v^2}$
COP_{com}	conventional coefficient of performance for the compressor
COP_s	A/C system coefficient of performance. Includes compressor and heat exchanger fan work rate
C_p	specific heat of air at constant pressure (Btu/lb_m-°R)
C_{oper}	annual operating cost of A/C system per ton of cooling ($/ton)
C_{cap}	capital cost of A/C system ($)
$\overline{C}_{cap}$	amortized cost of A/C system ($)
C_T	total annual cost--annual operating cost plus amortized incremental cost of the condenser on a per ton basis ($/ton)

Symbol	Refers to:
D_H	hydraulic diameter. By definition: $D_H = 4 \frac{\text{flow cross-sectional area}}{\text{wetted perimeter}}$ $D_H \cong 2/\eta$ (in)
E_{com}	compressor effectiveness (efficiency)
E_{fc}	condenser fan efficiency
$\bar{h}$	average heat transfer coefficient for air in a duct of infinite length (Btu/ft^2-sec-°R)
$\bar{h}_\ell$	average heat transfer coefficient for air corrected for entrance effects in a duct of finite length (Btu/ft^2-sec-°R)
$\bar{h}_r$	average heat transfer coefficient for refrigerant in a tube (Btu/ft^2-hr-°R)
$\dot{m}$	mass flow rate of air through the heat exchanger (lb_m/sec)
Pr	Prandtl number for air
$\dot{Q}_c$	heat flow rate from condenser to air (ton)
$\dot{Q}_e$	heat flow rate from air to evaporator (ton)
Re	Reynolds number based on hydraulic diameter
T_1	air inlet temperature to condenser (°R)
T_2	air exit temperature from condenser (°R)
T_{rc}	refrigerant saturation temperature in condenser (°R)
T_{re}	refrigerant saturation temperature in evaporator (°R)
t	fin gauge thickness (in)
U_o	overall heat transfer coefficient for condenser (Btu/ft^2-sec-°R)
V	air face velocity at condenser (ft/sec)
V_{opt}	optimal air velocity (ft/sec)

CHAPTER I

INTRODUCTION

As of 1968, an estimated 3.4 percent (4.915×10^{14} Btu/yr) of the electricity generated in the United States was consumed by the residential air conditioning sector. Furthermore, this consumption grew at an annual geometric rate of 14.6 percent for the period 1960-1968 [31]. Assuming continuation of this growth rate from 1968 to the present, an estimate of 1975 energy consumption for residential air conditioning is 1.3×10^{15} Btu/yr (7×10^{5} barrels/day). Taking into account the highly seasonal demand for air conditioning, the consumption during the summer months is about 2.1 million barrels/day. Total daily energy consumption in the United States is about 17 million barrels/day. Thus, in the summer, residential air conditioning accounts for about 12.3 percent of total daily U. S. energy consumption.

In 1968 the energy consumption for commercial air conditioning was slightly more than double that for the residential sector [31]. Although most large units in the commercial sector use water tower cooling methods (to which this study does not apply), it is clear that energy consumption for standard vapor-compression air conditioning is significant.

Even small percentage reductions in this energy usage can result in large savings. Taking the 1.3×10^{15} Btu/yr for the residential sector, a decrease of even 1 percent in consumption would save 1.3×10^{13} Btu/yr and, at a rate of 1.0¢/1000 Btu (2.9¢/kw-hr), a savings of $130 million/yr. The incentive for increasing the efficiency of residential air conditioning systems is apparent.

Of the several components comprising an air conditioning system, any one, or a combination, might be chosen for special consideration. This study is restricted to the condenser and the optimization of its function in the system.

Basic Operation of the Vapor-Compression Cycle

To familiarize the reader with the air conditioning system being studied, a brief explanation of the cycle operation and system follows.

The vapor-compression cycle is the most widely used air conditioning cycle. A schematic diagram of a typical vapor-compression air conditioning system is shown in Figure 1. The system consists of the following major components: compressor, condenser, evaporator, expansion device, and fans. The first four items listed comprise a closed loop in which a fluid alternately evaporates and condenses, with the intervening processes being compression and expansion. It is this cycle through which the fluid

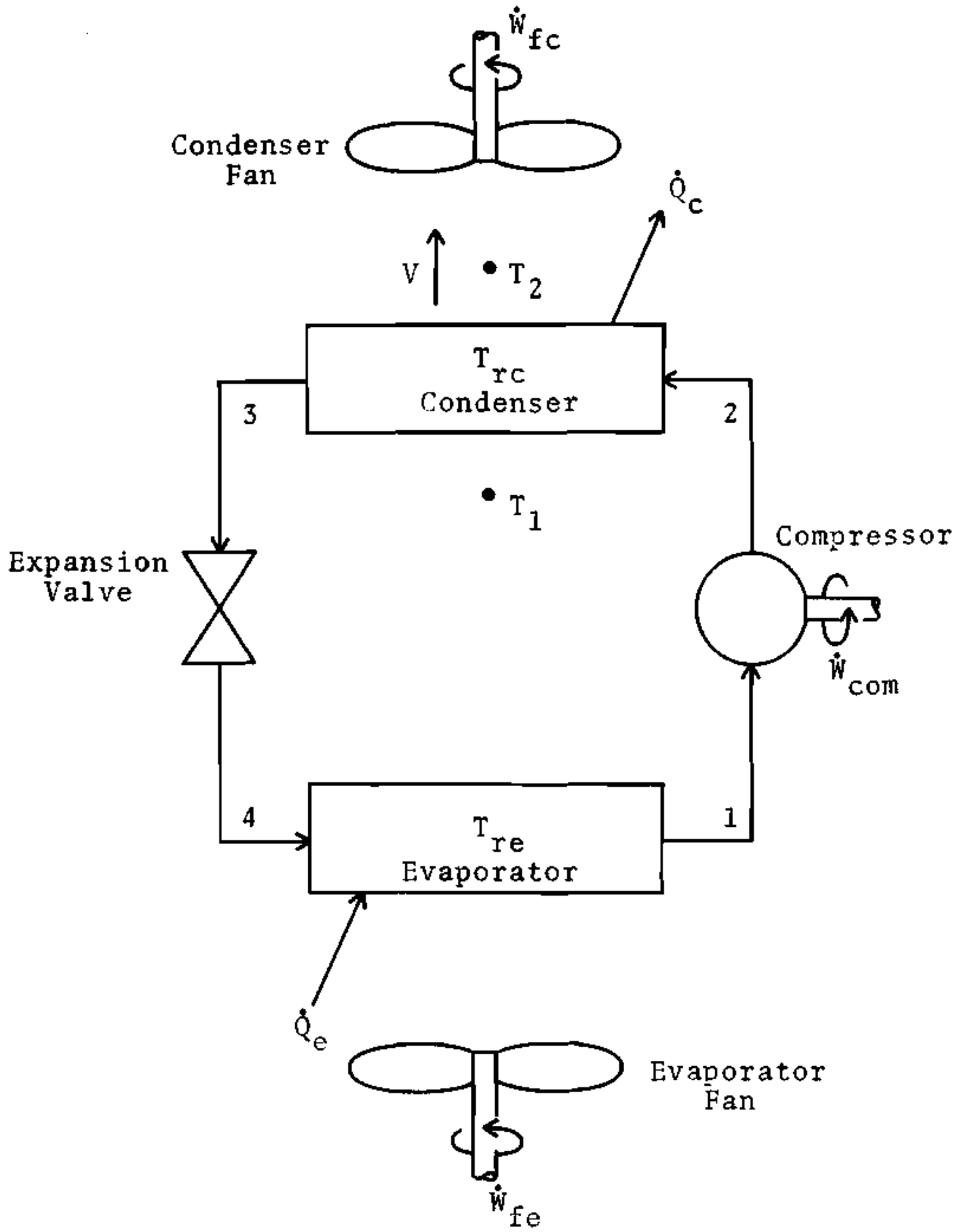

Figure 1. Schematic Diagram of a Vapor-Compression A/C System

passes that produces the desired cooling effect.

Boiling fluid at low pressure and temperature in the evaporator absorbs heat from air which is passed through the evaporator heat exchanger. The resulting vapor is then compressed to high pressure and temperature and enters the condenser. In the condenser, the hot vapor gives up its heat to air flowing through the heat exchanger. As the vapor gives up heat it condenses to a liquid and flows to the expansion device. The pressure drop across the expansion device allows the liquid to expand rapidly and partially vaporize with a drop in temperature. The cool fluid enters the evaporator and the cycle is complete.

The major energy flow rates into and out of the system are the two heat flows at the heat exchangers and the mechanical power inputs at the compressor and fans. These energy flow rates are also shown in Figure 1.

The corresponding ideal and actual cycles for the vapor-compression cycle are depicted in Figure 2. The numbered points on the cycle correspond to the numbers in Figure 1. In actuality, the so-called ideal cycle is not ideal thermodynamically in that the entropy increases during the expansion process. The essential differences between the actual and ideal cycles are

(1) Pressure drops across the heat exchangers due to refrigerant flow losses in the tubes.

(2) Subcooling of the refrigerant liquid in the

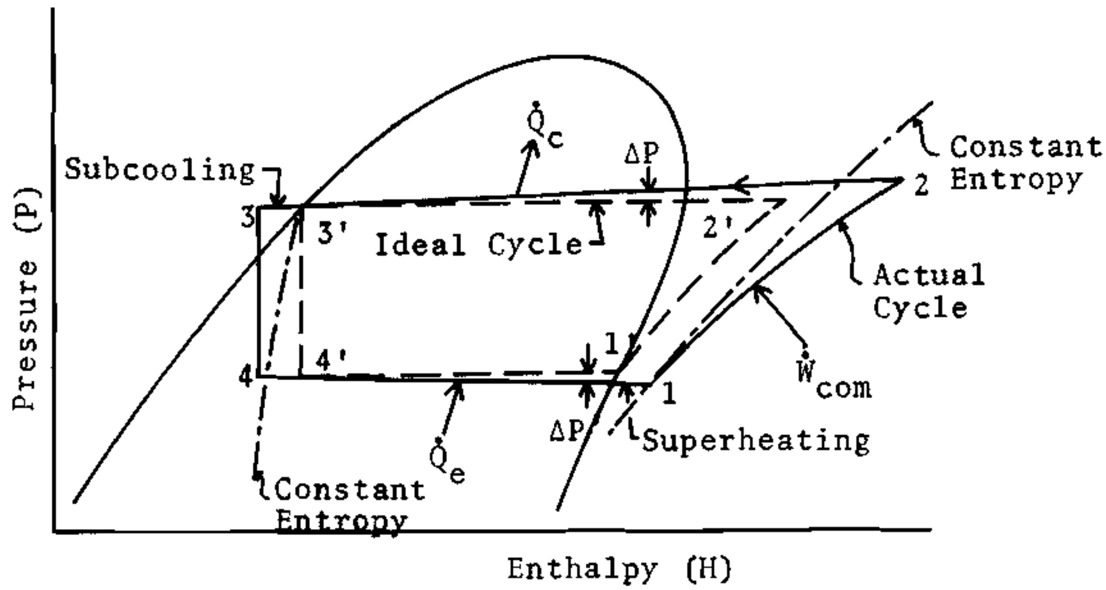

Figure 2. Actual Vapor-Compression Cycle Compared to Ideal Cycle

condenser to ensure 100 percent liquid entering the expansion valve.

(3) Superheating of the vapor in the evaporator to ensure that no droplets of liquid reach the compressor.

(4) Nonisentropic compression due to mechanical friction, valve pressure drops, and heat transfer.

The condenser and evaporator are usually of the tube and fin type. An illustration of an air-cooled heat exchanger is shown in Figure 3. The refrigerant is circuited through the tubes to which are attached the fins. As the resistance to heat flow into the air is much greater than that of heat flow from the refrigerant fluid, the air-side contact area is increased by means of the fins to aid in

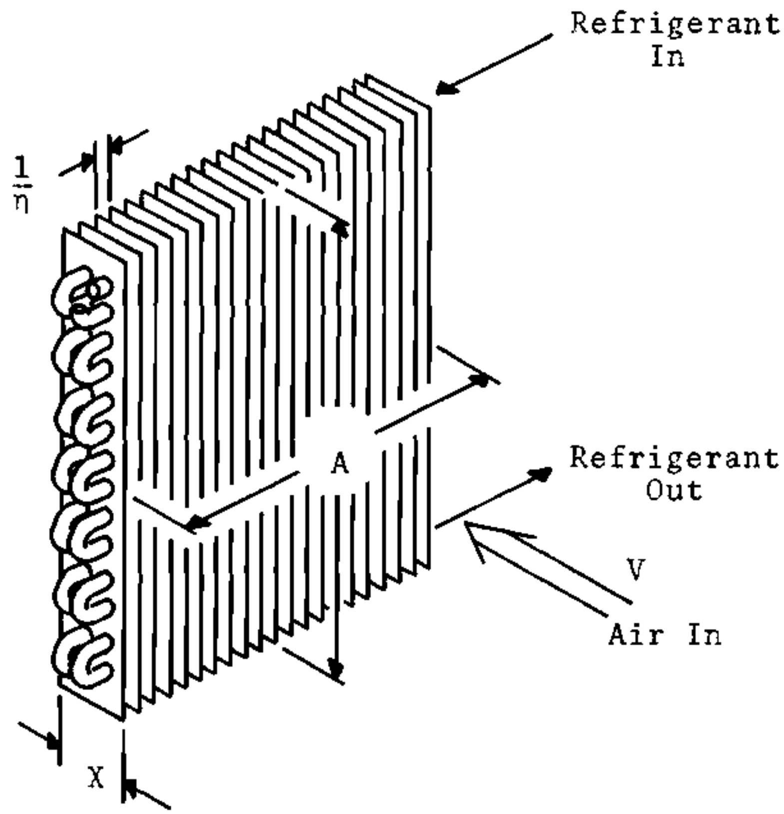

Figure 3. Tube and Fin Heat Exchanger

the heat transfer. Air drawn between the fins by the action of the fan is either heated or cooled as the case may be.

Literature Survey

As the vapor-compression cycle and air conditioning system (Figure 1) have been in use for many years, a large volume of research and study has been conducted on the separate components of the system. The literature on heat exchangers is extensive. One of the most complete studies was conducted by Kays and London [18]. Over a period of 15 years they compiled a large amount of experimental heat-transfer and flow-friction data for over 90 different compact heat exchanger configurations. However, data on the tube and continuous plate-fin exchanger of interest here was confined to only two specific configurations. Their work did not involve any optimization of the heat transfer surfaces.

Other investigators have studied the tube and continuous fin heat exchanger. Shepherd [28] experimentally tested one row-coils as the fin spacing, fin depth, tube spacing and location were varied. He found that the air-side heat transfer coefficient, for a given face velocity, increased only slightly with fin pitch. The coefficient decreased as fin depth and tube pitch increased, other things being equal. Rich [24] studied the heat transfer and friction performance of multi-row coils as the fin spacing was varied. He found that the air-side heat transfer coefficient and friction factor were independent of fin pitch over the range from three to fourteen fins per inch. This is due to the fact that the heat transfer was based on a boundary layer over a flat plate. Neither of these studies involved an optimization of heat exchanger parameters.

McQuiston and Tree [22] optimized heat exchanger core geometries for the criteria of minimum volume and minimum face area heat exchangers at a specified heat rejection rate, air pressure drop, and air inlet conditions. The effect of fin and tube radius, fin thickness and spacing, and heat transfer coefficient on the exchanger volume per unit of heat transfer was studied. The minimal volume core was found to be very thin with a large face area, while the opposite was true of the minimal face area core. The flow rates and exit air conditions were practically the same for the two cases indicating that either of the cores would produce practically the same results in a given system.

The most complete studies of heat exchanger optimization have been conducted for automotive air conditioning systems. Zahn [37] reports on a computer program developed at the York Division, Borg-Warner Corp. for optimizing automotive A/C evaporator coils. The program is set up to calculate either the size of the coil given specific operating conditions, or the core capacity given a specific geometry, air in, and refrigerant leaving conditions. At fixed depth and fins per inch optimizations for the tube diameter and spacing with respect to face area and core weight are shown for the case where air pressure drop is not considered and for the case where it is assumed constant. Mention is made of the need to balance blower pumping cost with core cost, but no calculations are given. A maximum velocity of 10 ft/sec was taken to eliminate water blow-off problems.

Conklu [10] describes a computer program developed by the Ford Motor Company for determining performance characteristics of automotive condenser coils. The air-side and refrigerant-film heat transfer coefficents are found from empirical formulas. The program calculates the steady heat rejection rate for a given core geometry, condensing temperature, and air inlet temperature and velocity. Alternately, it optimizes the condenser with respect to limits (selected by the designer) on a performance parameter for a specific rejection rate, condensing temperature, and air inlet conditions. Simulations of the heat rejection rate are within three to seven percent of test data. No mention is made of fan power requirements, nor are economic considerations addressed.

Davis et al. [12] discuss work at the Chrysler Corporation where the entire refrigerant loop (condenser, expansion valve, evaporator, compressor) has been modeled for computer simulation. The blowers are apparently not modeled. The program calculates the exchanger capacity from given air and working fluid inlet states, air mass flow rate, and coil geometry. The balance point to assure matched conditions for evaporator and condenser side is also computed. Mention is made of optimizing system performance with respect to design loads and economic considerations, but no data is presented. The system simulation correlates well with test data.

Schoonman [27] offers a good discussion of the economic optimization of a large multi-section aircooler system for industrial applications. His study includes an optimization of the heat transfer surfaces and consideration of capital, installation, and operating costs. He shows the savings gained by fan control.

Very little information was found in the open literature dealing with A/C system performance of residential and room units. Wrench [35] discusses a number of areas impacting on system efficiency such as, type of compressor motor, compressor design, the path for circuiting the refrigerant in the coil, and the effect of coil design on fan power requirements, but offers little analytical data or methodology for improving performance. Hamilton and Pearson [15] indicate desirable goals for system performance by comparing typical performance with that of an ideal system based on the ideal vapor-compression cycle. A simple model including the efficiency of the electrical-mechanical drive processes for the compressor and fans is stated from which the COP for an actual cycle is computed. They conclude that there is a tremendous potential for improvement in present day equipment. They do not attempt any optimization, nor do they suggest how this might be done.

Objective

First, the heat exchanger (condenser) and A/C system are modeled so that the system's coefficient of performance can be evaluated as a function of the heat exchanger design. The heat exchanger design variables considered are the air flow area (A), number of fins per inch (η), fin depth (X), working fluid saturation temperature (T_{rc}), air inlet temperature (T_1), and air velocity (V).

Secondly, the model of system performance is coupled with an economic analysis in order to minimize the total annual cost (amortized equipment cost and operating cost) of the system per ton of cooling. With the aid of the model and economic considerations, a parametric study is performed for a number of different annual hours of operation and electrical rates. This allows the optimal operating air velocity and minimal cost heat exchanger configuration to be specified for various combinations of these parameters.

It is intuitively clear that the economic optimums indicated above exist. The compressor work can be reduced by lowering the temperature of the condenser. Lowering the condenser temperature can be accomplished by providing a greater heat transfer area, i.e., increasing the frontal area of the heat exchanger while holding all other parameters constant. This will also increase fan power requirements. However, at some point the savings associated with a reduction in compressor work will be more than offset by the increased fan power. Also capital expenditure associated with the condenser increases eventually offsetting any savings in operational cost. Alternatively, for a fixed condenser configuration, the heat transfer rate can be increased by increasing the air velocity. It is advantageous to increase the heat transfer rate but, here again, this effect will be offset by the increased fan energy consumption. It is obvious there are trade-offs among various variables. It is the objective of this study to determine the trade-offs that minimize the system's total cost.

The results of the study are embodied in: Equations (31)-(35) which are expressions for determining the total system coefficient of performance; Tables 1 and 2 which give nominal values (taken as constants) for various quantities in these equations; Equation (45) from which the system's total annual cost is evaluated; and the curves presented in the appendices which show the optimization of air velocity and condenser frontal area. The curves are intended as a guide and reference for the technical designer involved in the manufacture and specification of A/C heat exchangers. The interested customer would also find the curves helpful in evaluating the effectiveness of the numerous A/C units currently on the market.

CHAPTER II

ANALYTICAL MODEL OF THE CONDENSER AND AIR CONDITIONING SYSTEM

In order to achieve the stated objectives of this study, an analytical model of the condenser and A/C system is developed from which the performance of the system can be evaluated with varying condenser designs. This model of the system's operating characteristics is then made use of in the economic analysis of Chapter III.

In developing the model, the following procedure is taken:

(1) State the basic assumptions underlying the model.

(2) State the fundamental equations describing the various devices and processes in the A/C system.

(3) Present the analytic expressions derived from the fundamental equations and discuss the insights to the system's performance as predicted by the model.

Basic Assumptions Underlying the Model

The formulation of the model is based upon the following assumptions:

(1) Steady-state operating conditions.

(2) Uniform refrigerant saturation temperature and pressure throughout the condenser and evaporator tubes.

(3) The heat transfer resistances of the desuperheated and subcooled regions in the condenser tubes tend to counteract each other's effect on the overall heat transfer coefficient of the condenser and are neglected. (This assumption was made in the study reported by Conklu [10]. It was found that, over the practical range of condensing temperatures, neglecting the above effects did not seriously effect the accuracy of the model in that predicted results were within three to seven percent of test results).

(4) The thermal resistances of the tube material and tube-fin joints are assumed small compared to the heat transfer resistances of the air-film, refrigerant-film, and fins.

(5) The exterior tube area is small compared to the total fin area. Therefore, the air-side heat transfer is based solely on the total fin surface area.

(6) In considering the fan work, the air drag due to the tubes is neglected as small compared to the drag produced by the fins.

Fundamental Equations

The fundamental equations are derived from an analysis of the thermal and mechanical processes of the system at equilibrium. The theory of cross-flow heat exchangers is employed as well as standard methods for describing the mechanical devices such as the compressor and fan. (A description of the symbols used in the following equations is given in the nomenclature.)

An equilibrium energy balance on the condenser yields the following,

$$\left\{\begin{array}{l}\text{Rate of heat rejected}\\\text{by the hot refrigerant}\\\text{in the condenser tubes}\end{array}\right\} = \left\{\begin{array}{l}\text{Rate of heat absorbed}\\\text{by the air passing}\\\text{through the condenser}\end{array}\right\}$$

In symbol form this can be expressed as,

$$\dot{Q}_c = \dot{m}C_p \ (T_2 - T_1) \tag{1}$$

An additional relation making use of Equation (1) can be obtained from the equilibrium energy balance,

$$T_{rc} - T_2 = (T_{rc} - T_1)\exp\left(\frac{-2U_oA \ X\eta}{\dot{m} \ C_p}\right) \tag{2}$$

where the heat transfer is based on the total fin surface area (see Appendix H for the development of Equation (2)). The mass flow rate of air is given by,

$$\dot{m} = \rho VA \ (1 - \eta t) \tag{3}$$

where the factor $(1-\eta_c t)$ accounts for the reduction of air flow area due to the fin material thickness.

The overall heat transfer coefficient for the heat exchanger is given by,

$$U_o = \left(\frac{1}{\bar{h}} + \frac{A_o}{A_i \bar{h}_r} + \frac{1-\phi}{\bar{h}\left(\frac{A_t}{A_f} + \phi\right)}\right)^{-1} \tag{4}$$

where $\frac{1}{\bar{h}}$ is the average air-film resistance; $\frac{A_o}{A_i \bar{h}_r}$ is the resistance due to the refrigerant-film; and $\frac{1-\phi}{\bar{h}\left(\frac{A_t}{A_f} + \phi\right)}$ is the resistance for a non-ideal fin [1, page 12; 10].

To express the heat transfer from the fins to the air, Reynolds analogy is used. According to the analogy, heat and momentum are transferred by analogous processes. This relationship can conveniently be expressed as,

$$StPr^{2/3} = \frac{\bar{h}\ Pr^{2/3}}{\rho V C_p} = \frac{C_f}{2} \tag{5}$$

where $Pr^{2/3}$ is a modifying factor proposed by Colburn [9] to account for fluids with Prandtl numbers ranging from 0.6 to about 50.

The friction coefficient is related to the flow field by,

$$C_f = \frac{a}{Re^b} \tag{6}$$

where the Reynolds number is based upon the significant length scale for a specific flow situation and a and b are constants dependent on the flow geometry and flow regime.

The condenser fan work rate is equal to the drag force exerted on the air by the fins times the air velocity. Introducing a fan efficiency factor, the fan work rate is given by

$$\dot{W}_{fc} = C_f \rho V^3 X \eta \; A/E_{fc} \tag{7}$$

In Figure 4 the actual vapor-compression cycle and corresponding Carnot cycle are shown on a temperature-entropy diagram. The conventional coefficient of performance COP, based on the compressor work,

$$COP_{com} = \dot{Q}_e/\dot{W}_{com} \tag{8}$$

can be expressed in terms of the COP for a Carnot cycle if it is modified by a factor, E_c, to account for nonisentropic compression and the behavior of actual refrigerants. The mechanical efficiency, E_m, of the compressor can be lumped with the cycle efficiency, E_c, to obtain the compressor effectiveness, E_{com},[7, Chapter 7]. Hence,

$$COP_{com} = COP_{Carnot} \; E_c E_m = \left(\frac{T_{re}}{T_{rc} - T_{re}}\right) E_{com} \tag{9}$$

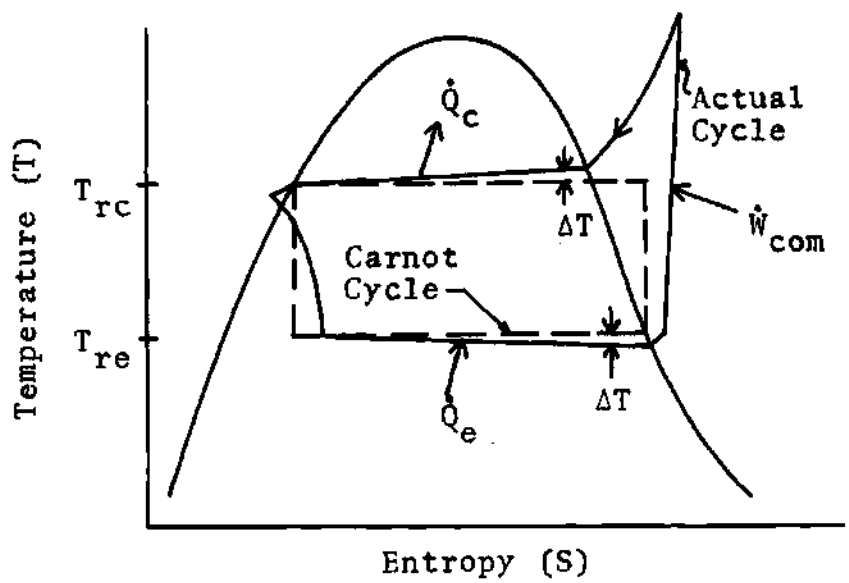

Figure 4. Actual Vapor-Compression Cycle Compared to Carnot Cycle

With regard to the compressor it is assumed that the clearance volume is very small, therefore, the compressor pumping capacity is independent of the condenser saturation temperature for the condition of a fixed suction temperature.

An energy balance on the entire refrigerant loop yields,

$$\dot{Q}_c = \dot{W}_{com} + \dot{Q}_e \tag{10}$$

The ratios of condenser and evaporator fan work rates to compressor work rate are defined as,

$$\beta_c = \frac{\dot{W}_{fc}}{\dot{W}_{com}} \tag{11}$$

$$\beta_e = \frac{\dot{W}_{fe}}{\dot{W}_{com}} \tag{12}$$

A coefficient of performance for the total system, COP_s, including compressor and heat exchanger fan work rates, is defined as,

$$COP_s = \text{Ratio of } \frac{\{\text{Cooling Rate}\}}{\text{Total Input } \{\text{Work Rate to}\} \text{ the System}}$$

Symbolically this becomes,

$$COP_s = \frac{\dot{Q}_e}{\dot{W}_{com} + \dot{W}_{fc} + \dot{W}_{fe}} \tag{13}$$

The Analysis

The basic equations presented in the previous section are now combined algebraically to yield an expression for COP_s (see Appendix H for details). With the 13 equations, 13 of the variables can be eliminated. Initially, the following variables are eliminated.

U_o	$\bar{h}$	C_f	$\dot{W}_{com}$	COP_{com}
$\dot{m}$	$\dot{Q}_c$	$\dot{W}_{fc}$	β_c	
T_2	$\dot{Q}_e$	$\dot{W}_{fe}$	A	

This results in the following expression for system performance,

$$\frac{1}{COP_s} = \frac{aV^2X\eta\left(1 + \frac{T_{rc}}{E_{com}\,T_{re}} - \frac{1}{E_{com}}\right)}{E_{fc}Re^bC_p(1-\eta t)(T_{rc}-T_1)[1-\exp(-k)]}$$

$$+ (1+\beta_e)\left[\frac{T_{rc}}{E_{com}\,T_{re}} - \frac{1}{E_{com}}\right] \tag{14}$$

where

$$k = \frac{a X\eta/(1-\eta t)}{Re^bPr^{2/3}\left[1+\frac{1-\phi}{A_t/A_f+\phi}\right] + \frac{a\rho\, VC_p\, A_o}{2\,\bar{h}_r\, A_i}} \tag{15}$$

A more useful COP_s expression can be obtained if T_{rc} is eliminated and frontal area, A, retained. From the fundamental equations this can be accomplished but the variable $\dot{Q}_e$ is reintroduced. Although the model does not consider the evaporator design, $\dot{Q}_e$ is an important quantity as the system's purpose is to produce a cooling effect. Hence, $\dot{Q}_e$ can be considered a fixed quantity for which the planner designs a particular system. The resulting COP_s expression is,

$$\frac{1}{COP_s} = \frac{aX\eta}{E_{fc}} \frac{\rho V^3}{Re^b} \frac{A}{\dot{Q}_e}$$

$$+ (1+\beta_e) \frac{(1-\frac{T_{re}}{T_1})[1-\exp(-k)] + \frac{\dot{Q}_e}{\rho VC_p T_1 A(1-\eta t)}}{E_{com} \frac{T_{re}}{T_1} [1-\exp(-k)] - \frac{\dot{Q}_e}{\rho VC_p T_1 A(1-\eta t)}} \qquad (16)$$

where k is again given by Equation (15). Equations (14), (15), and (16) yield the operational performance of the system model. The system's performance may now be evaluated in terms of the quantities and design variables appearing in (14), (15), and (16).

Theoretical Analysis

In this section consideration is given to the theoretical optimal design for the condenser first for the situation where no design constraints whatsoever are imposed and secondly for the criterion of a fixed-volume heat exchanger. The purpose for this is to gain insight into the COP_s expressions given in (14)-(16) and to be able to compare the theoretical optimal design with the analysis of real condenser design.

The "Ideal" Heat Exchanger. For the immediate discussion, the complexity of (15) is reduced by assuming ideal fins ($\phi=1$) and a zero refrigerant-film resistance. Thus, the heat transfer coefficient is based solely on the air-side resistance, and (14) condenses to the following,

$$\frac{1}{COP_s} = \frac{aV^2X\eta\left(1 + \frac{T_{rc}}{E_{com}T_{re}} - \frac{1}{E_{com}}\right)}{E_{fc}Re^bC_p(1-\eta t)(T_{rc}-T_1)\left[1-\exp\left(\frac{-aX\eta}{Re^bPr^{2/3}(1-\eta t)}\right)\right]}$$

$$+ (1+\beta_e)\left[\frac{T_{rc}}{E_{com}T_{re}} - \frac{1}{E_{com}}\right] \tag{17}$$

Suppose quantities at the evaporator are fixed, i.e., a constant cooling load and evaporator temperature. If no constraints (physical size, cost, etc.) are placed on the condenser heat exchanger, what condenser design would optimize the system's performance? In Equation (17) the following non-dimensional groups appear,

$$\frac{1}{M} = \frac{V^2}{C_p(T_{rc}-T_1)}; \quad N = \frac{T_{rc}}{E_{com}T_{re}}; \quad P = \frac{aX\eta}{Re^b(1-\eta t)}$$

Equation (17) can be written in terms of the non-dimensional variables, M, N, and P.

$$\frac{1}{COP_s} = \frac{P\left(1+N - \frac{1}{E_{com}}\right)}{E_{fc}M[1-\exp(-PC)]} + (1+\beta_e)\left[N-\frac{1}{E_{com}}\right] \tag{18}$$

where $C = \frac{1}{Pr^{2/3}}$ is constant. This reduces the number of independent variables on which system performance depends.

Recalling the definition of COP_s, the optimum will be realized as $1/COP_s$ becomes as small as possible. Thus, if the partial derivatives of $1/COP_s$ with respect to one of the above groups is evaluated and set equal to zero, the optimal value of that group results. Taking the partial of (18) with respect to M,

$$\frac{\partial}{\partial M}\left(\frac{1}{COP_s}\right) = -\frac{P(1+N-\frac{1}{E_{com}})}{E_{fc}M^2[1-\exp(-PC)]} = 0 \tag{19}$$

Equation (19) is satisfied as $M \to \infty$. The partial of (18) with respect to N is,

$$\frac{\partial}{\partial N}\left(\frac{1}{COP_s}\right) = \frac{P}{E_{fc}M[1-\exp(-PC)]} + (1+\beta_e) = 0 \tag{20}$$

Since (20) is independent of N, Equation (18) can be inspected to determine the effect of N and find its optimal value. It is noticed that $1/COP_s$ is linear with N and becomes small when N is small. For the optimum, N should be as small as possible. Taking the partial of (18) with respect to P and setting to zero,

$$\frac{\partial}{\partial P}\left(\frac{1}{COP_s}\right) =$$

$$\frac{(1+N-\frac{1}{E_{com}})E_{fc}M[1-\exp(-PC)]-P(1+N-\frac{1}{E_{com}})[-E_{fc}M\exp(-PC)](-C)}{(E_{fc}M[1-\exp(-PC)])^2} = 0 \tag{21}$$

Examining the numerator of (21) for its zero value,

$$\frac{1}{C}\,(1+N - \frac{1}{E_{com}})E_{fc}M[1-\exp(-PC)] =$$

$$P(1+N - \frac{1}{E_{com}})\,[E_{fc}M\exp(-PC)] \qquad (22)$$

Rearranging (22),

$$\frac{E_{fc}M}{C} - \frac{E_{fc}M}{C}\exp(-PC) = PE_{fc}M\exp(-PC) \qquad (23)$$

$$\frac{1}{C} = \exp(-PC)[P + \frac{1}{C}] \qquad (24)$$

Letting Y = PC, and substituting into (24),

$$\frac{1}{C} = \exp(-Y)[Y/C + 1/C] \qquad (25)$$

$$1 = (Y+1)\exp(-Y) \qquad (26)$$

Equation (26) has only one root at Y = 0 or P = 0. To determine whether $1/COP_s$ is a maximum or minimum at P = 0, Equation (18) is studied with the help of L'Hospital's rule by forming the derivative of numerator and denominator with respect to P and taking the limit,

$$\text{Lim}\left(\frac{1}{COP_s}\right) = \text{Lim}\,\frac{1+N-\dfrac{1}{E_{com}}}{CE_{fc}M\exp(-PC)}$$

$$= \begin{cases} \dfrac{1+N-\dfrac{1}{E_{com}}}{CE_{fc}M}, & \text{as } P\to 0 \\ \\ \infty, \text{ as } P\to\infty \end{cases} \qquad (27)$$

Hence, P equal to zero is the optimum.

In summary the conclusions for the condenser design producing the maximum system COP_s are:

(1) $\dfrac{V^2}{C_p(T_{rc}-T_1)} \to 0$, implies V as small as possible.

(2) $\dfrac{T_{rc}}{E_{com}\,T_{re}} \to$ small, implies T_{rc} as small as possible. (It is noticed that the lower limit for T_{rc} is T_1 if the condenser is to continue rejecting heat. Hence, $T_{rc} \to T_1$.)

(3) $\dfrac{aX\eta}{Re^b(1-\eta t)} \to 0$, implies $X\eta \to 0$. (Since $R_e = \dfrac{\rho VD_H}{\mu}$, V must remain finite.)

(4) From the fundamental equations it can be shown that, as condition (2) above is approached, $A \to \infty$.

Applying these conclusions to (14), it is seen that the total system COP_s approaches the modified Carnot efficiency given by (9) because the refrigerant condenser temperature approaches the ambient air temperature and the fan work approaches zero. This occurs for a condenser with infinite frontal area, very small depth or sparsely spaced fins, and a very small but finite air velocity.

Constant-Volume Heat Exchanger. The previous optimization was carried out with no constraints placed on the condenser design variables. Suppose the constraint of a fixed volume heat exchanger is introduced. As in the previous analysis, the heat transfer coefficient is based only on the air-side resistance. Letting A = Vol/X where Vol is fixed, and substituting into Equation (16),

$$\frac{1}{COP_s} = \frac{a\eta \ \rho V^3 Vol}{E_{fc} \ Re^b \ \dot{Q}_e}$$

$$+ (1+\beta_e) \frac{(1-\frac{T_{re}}{T_1})[1-\exp(\frac{-aX\eta}{Re^b Pr^{2/3}(1-\eta t)})] + \frac{\dot{Q}_e X}{\rho V C_p T_1 Vol(1-\eta t)}}{E_{com} \frac{T_{re}}{T_1} [1-\exp(\frac{-aX\eta}{Re^b Pr^{2/3}(1-\eta t)})] - \frac{\dot{Q}_e X}{\rho V C_p T_1 Vol(1-\eta t)}} \tag{28}$$

Holding everything else constant, X is varied to determine the effect on $1/COP_s$. As $X \to 0$ or $X \to \infty$ Equation (28) is undefined. For convenience let,

$$B = \frac{a\eta}{Re^b Pr^{2/3}(1-\eta t)} \ ; \quad C = \frac{\dot{Q}_e}{\rho V C_p T_1 Vol(1-\eta t)}$$

and apply L'Hospital's rule by differentiating with respect to X.

$$\operatorname{Lim}\left(\frac{1}{COP_s}\right) = \operatorname{Lim}(1+\beta_e)\,\frac{\left(1 - \frac{T_{re}}{T_1}\right)B\exp(-BX)+C}{E_{com}\,\frac{T_{re}}{T_1}\,B\exp(-BX)-C}$$

$$= \begin{cases} (1+\beta_e)\,\dfrac{\left(1 - \frac{T_{re}}{T_1}\right)B+C}{E_{com}\,\frac{T_{re}}{T_1}\,B-C}, & \text{as } X \to 0 \\ -(1+\beta_e), \text{ as } X\to\infty \end{cases} \tag{29}$$

In the limit as $X \to \infty$, negative $1/COP_s$, the heat exchanger is absorbing heat, i.e., $T_{rc} < T_1$. Thus, the $1/COP_s$ versus X curve has gone through an asymptote. If Equation (29) is plotted the form of the curve is shown in Figure 5. The portion of the curve in Figure 5 where $1/COP_s$ is negative indicates heat pump action since $T_{rc} < T_1$. Therefore, the portion of the curve where $1/COP_s$ is positive, $T_{rc} > T_1$, is the region of interest for A/C systems. The same is true of Figure 6. The same conclusion is reached as for the ideal case. A heat exchanger with small depth gives the best A/C system performance. The effect of varying frontal area, A, with a fixed volume is just the reverse of the above as shown in Figure 6. A fixed-volume heat exchanger with large frontal area and small depth gives the best A/C system performance. Since volume is a good indication of cost, this is a good rule of thumb for a fixed cost condenser also.

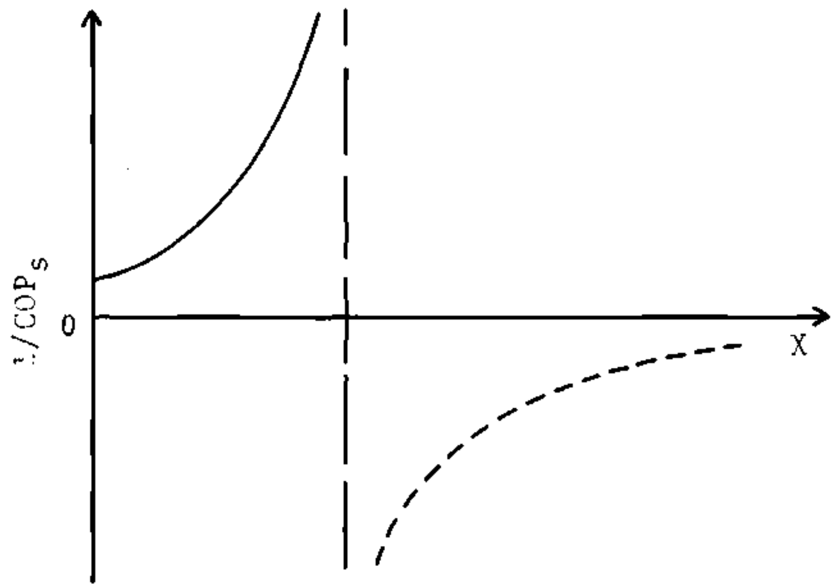

Figure 5. 1/COP$_s$ versus Depth, X, for a Fixed Volume Heat Exchanger

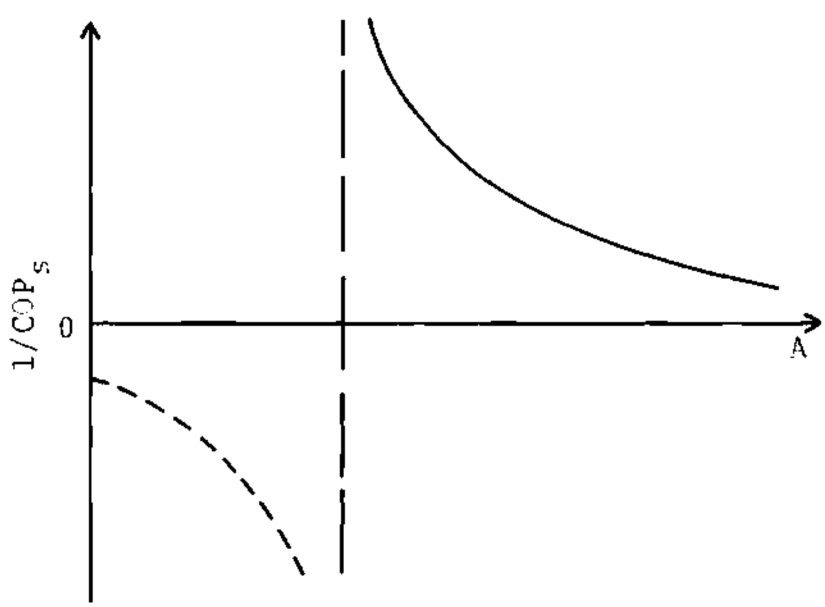

Figure 6. 1/COP$_s$ versus Frontal Area, A, for a Fixed Volume Heat Exchanger

Air Velocity Optimization

The model is used to determine the air velocity that yields the best system coefficient of performance for a fixed condenser configuration. In order to examine the system's performance over a broad range of velocities, laminar and turbulent forms of Equations (15) and (16) are developed. Details of the derivation of the expressions which follow are given in Appendix H.

Laminar Solution. For fully developed laminar flow:

$$R_e = \frac{\rho V D_H}{\mu} \qquad \text{where } D_H = 2/\eta$$

$$b = 1.0$$

$$a = 24$$

(low aspect ratio duct formed by two fins [18, page 103])

For typical values of X and η, the ratio X/D_H ranges from about 5 to 50. Thus, entrance effects are important, and $\bar{h}$, given by (5) for a duct of infinite length, is adjusted to account for these effects.

Kays [17] has correlated mean Nusselt numbers for constant wall temperature with respect to D_H/X based on the actual velocity profiles (Langhaar profiles) in the entrance region. Over the region of interest to this study, the curve given by Kays is very well approximated by the equation,

$$\overline{Nu} = \frac{\bar{h}_\ell \, D_H}{K} = 1.595 \left(\frac{Re \; Pr \; D_H}{X}\right)^{0.4} \qquad (30)$$

where $\bar{h}_\ell$ is for a duct of finite length, X. Incorporating (30), the laminar form of (16) corrected for entrance effects becomes,

$$\frac{1}{COP_s} = \frac{aX\eta^2V^2A\mu}{2E_{fc}\,\dot{Q}_e}$$

$$+ (1+\beta_e)\,\frac{(1-\frac{T_{re}}{T_1})[1-\exp(-k_L)] + \frac{\dot{Q}_e}{\rho VC_pT_1A(1-\eta t)}}{E_{com}\,\frac{T_{re}}{T_1}\,[1-\exp(-k_L)] - \frac{\dot{Q}_e}{\rho VC_pT_1A(1-\eta t)}} \tag{31}$$

where,

$$k_L = \frac{1.595(2)^{0.4}(X\eta)^{0.6}a/(1-\eta t)}{12(\frac{2\rho VPr}{\mu\eta})^{0.6}\;[1 + \frac{1-\phi}{\frac{A_t}{A_f}+\phi}] + \frac{1.595\;a\rho VC_pA_o}{2A_i\bar{h}_r}\;(\frac{2}{X\eta})^{0.4}} \tag{32}$$

<u>Turbulent Solution</u>. In fully developed turbulent flow:

$$R_e = \frac{\rho VD_H}{\mu} \qquad \text{where } D_H = 2/\eta$$

$$b = 0.2$$

$$a = 0.046$$

To correct for entrance effects, the following equation given by Kreith [19, Chapter 8] is used,

$$\bar{h}_\ell = \bar{h}[1+(\frac{D_H}{X})^{0.7}] \tag{33}$$

where $\bar{h}_\ell$ is for a duct of finite length, X. The turbulent form of (16) corrected for entrance effects becomes,

$$\frac{1}{COP_s} = \frac{aX\eta^{1.2}\ \rho^{0.8}\ V^{2.8}\ A}{(\frac{2}{\mu})^{0.2}\ E_{fc}\ \dot{Q}_e}$$

$$+ (1+\beta_e)\ \frac{(1-\frac{T_{re}}{T_1})[1-\exp(-k_T)] + \frac{\dot{Q}_e}{\rho VC_pT_1A(1-\eta t)}}{E_{com}\ \frac{T_{re}}{T_1}\ [1-\exp(-k_T)] - \frac{\dot{Q}_e}{\rho VC_pT_1A(1-\eta t)}} \tag{34}$$

where,

$$k_T = \frac{aX\eta[1+(\frac{2}{X\eta})^{0.7}]/(1-\eta t)}{(\frac{2\rho V}{\mu\eta})^{0.2}\ [1 + \frac{1-\phi}{\frac{A_t}{A_f}+\phi}] + \frac{a\rho VC_pA_o}{2A_i\ \bar{h}_r}\ [1+(\frac{2}{X\eta})^{0.7}]} \tag{35}$$

Input Constants. Table 1 gives nominal values for various quantities in the model which are assumed to be constant in the analysis that follows. The following notes apply to the indicated quantities in Table 1.

*Air properties are evaluated at a temperature of 565°R which is a reasonable mean between the fin temperature and bulk air temperature.

**The evaporator fan work rate is constant for fixed

Table 1. Nominal Values for Quantities in the Model (to be used in Equations (31)-(35))

	$T_1 = 550$	Average outdoors summer ambient (°R)
	$T_{re} = 500$	Typical value for the saturation temperature of the refrigerant in the evaporator (°R)
	$E_{com} = 0.7$	Compressor effectiveness--includes mechanical and cycle efficiencies [7, Chapter 7]
	$E_{fc} = 0.65$	Condenser fan efficiency
*	$C_p = 0.24$	Specific heat of air (Btu/lb_m-°R)
	$\rho = 0.071$	Density of air (lb_m/ft^3)
	$\mu = 1.3x10^{-5}$	Absolute viscosity of air (lb_m/ft-sec)
	$Pr = 0.72$	Prandtl number for air
**	$\beta_e = 0.05$	Ratio of evaporator fan work rate to compressor work rate
***	$\bar{h}_r = 300$	Average refrigerant heat transfer coefficient (Btu/hr-ft^2-°R)

$\dot{Q}_e$ and T_{re}, but the compressor work rate is not specified constant. Hence, β_e is not a constant. However, variation in β_e due to varying $\dot{W}_{com}$ is not that great as $\dot{W}_{com}$ changes by about 20 percent over the range of velocities considered. The range of β_c at the optimal velocities is about 0.13 to 0.06. For a well designed system β_e is expected to be less than β_c so β_e equal to 0.05 is a reasonable approximation.

***Taking $\bar{h}_r$ as a constant is not rigorously correct as it is a function of the difference between refrigerant saturation temperature and the tube wall temperature. McAdams [20, Chapter 13] gives,

$$\bar{h}_r = \frac{0.943\Omega}{(L\Delta T)^{0.25}} \tag{36}$$

where L is the tube length and Ω is a complex function involving the thermodynamic properties of the refrigerant. Evaluating $\bar{h}_r$ is a complicated problem, and since L is not specified in the model an exact analysis is impossible. Values of $\bar{h}_r$ vary over a wide range, 150-450 Btu/hr-ft^2-°R [2], so an average value was taken. The effect of taking $\bar{h}_r$ at 200 and 400 is discussed in Chapter III.

The number of tubes, their physical dimensions (length, diameter), and spacing have not been included in the model. As mentioned in Chapter I, other investigations have dealt with this aspect of optimization. For this study it is assumed that the number and spacing of tubes are more or less optimal so that typical values of fin efficiency factors and ratios of fin surface area to tube surface area may be used. Thus, the values in Table 2 have been chosen.

For smooth walled ducts the critical Reynolds number, Re, at which transition occurs is around 2300. It is common practice to ripple the fin material inducing turbulence thereby reducing the critical Reynolds number. Thus, it is assumed that transition occurs at a Reynolds number of approximately 1500. Furthermore, it is assumed that the fully turbulent solution, given by (34), is applicable in the transition zone.

Velocity Optimization Curves. The optimal velocity which produces the maximum COP_s for the system is determined for a specific heat exchanger configuration given by the three variables: fin depth, X; number of fins per inch, η; and square footage of condenser frontal area per ton of cooling, $A/\dot{Q}_e$. The following ranges were chosen to cover the possible configurations for residential A/C units.

X--2 to 6 (in)

η--6 to 15 (fins/in)

$A/\dot{Q}_e$--0.5 to 4 (ft^2/ton)

Appendix A is a compilation of the velocity optimization curves generated from expressions (31)-(35). Representative curves from Appendix A appear on the following pages to facilitate their discussion.

Figure 7 presents the two extremes of the analysis.

Table 2. Nominal Values for Heat Exchanger Geometry Factors (to be used in Equations (31)-(35))

Geometry Factor	Number of Fins/Inch			
	6	9	12	15
*A_f/A_t	15	20	25	30
*A_o/A_i	16	21	27	32
*ϕ[10,22]	0.85	0.85	0.85	0.85
t (in)	0.015	0.015	0.015	0.015

*It is assumed that as the depth, X, is varied the number of rows of tubes is varied accordingly to maintain A_f/A_t, A_o/A_i, and ϕ relatively constant.

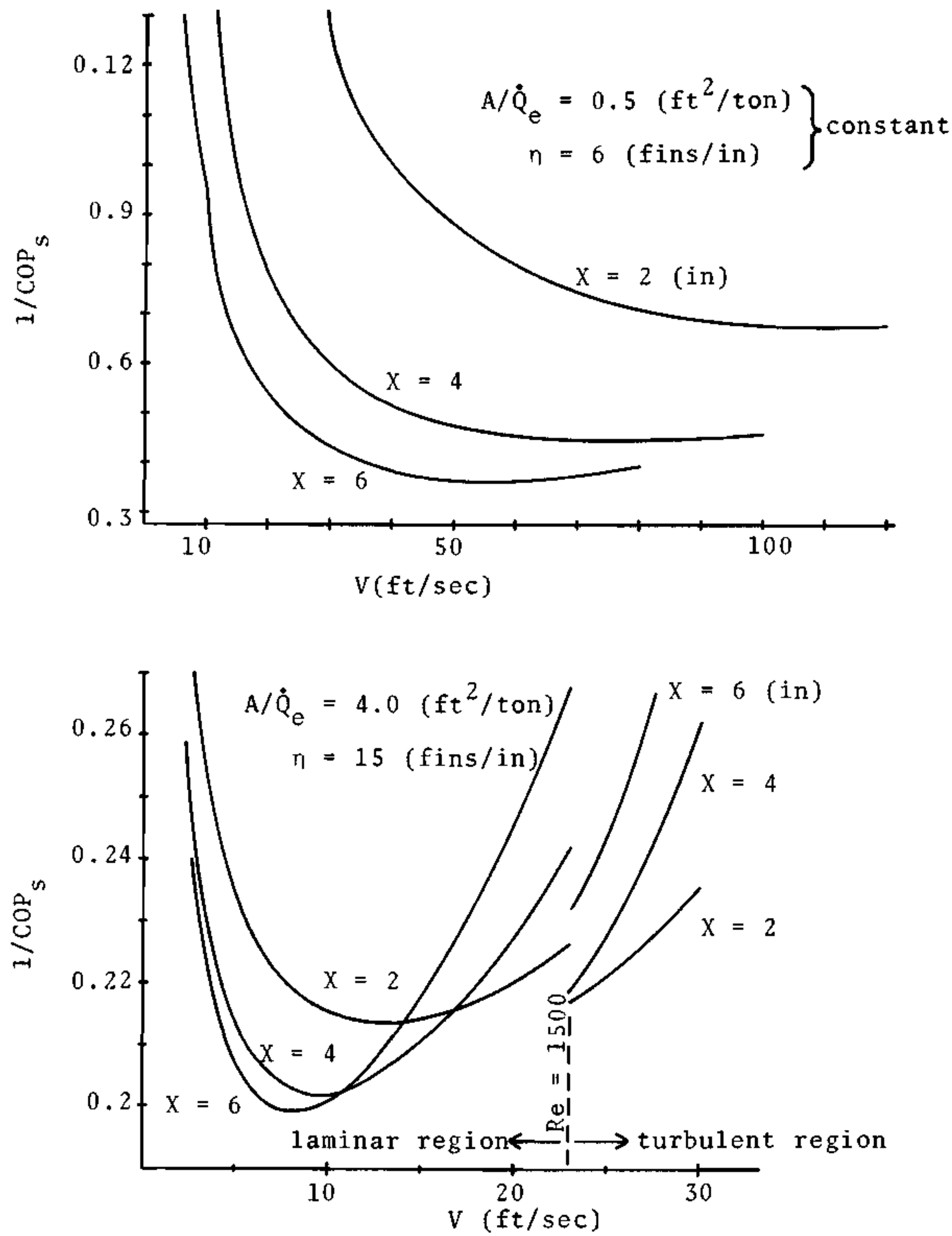

Figure 7. Representative Velocity Optimization Curves from Appendix A

The wide variation in optimal velocity is evident. It is noticed that increasing any one or any combination of the heat exchanger design variables reduces the optimal velocity and enhances system performance. The reduction in performance is also evident for operating at other than the optimal velocity. For each specific configuration there is obviously a range of velocities that offer almost equal performance. However, it is noticed that this range is increasingly restricted as the design variables increase.

Notice the sharp decrease in system performance at very low velocities. In fact, $1/COP_s \to \infty$, i.e., the system has zero efficiency, at some very small velocity. From Equation (2),

$$\dot{Q}_c = \rho VAC_p(1-\eta t)(T_2-T_1)$$

it is seen that the velocity cannot equal zero for fixed A and $\dot{Q}_c$ as this would mean an infinite temperature rise for the air which is physically impossible.

The discontinuities in the curves occur as the change is made from the laminar solution to the turbulent. Figure 8 shows a case where the optimal velocity falls on the border between laminar and turbulent flow. In this particular case the turbulent solution predicts about a 5 percent improvement in system performance over that of the laminar. Both the heat transfer rate and fan work increase in going from laminar

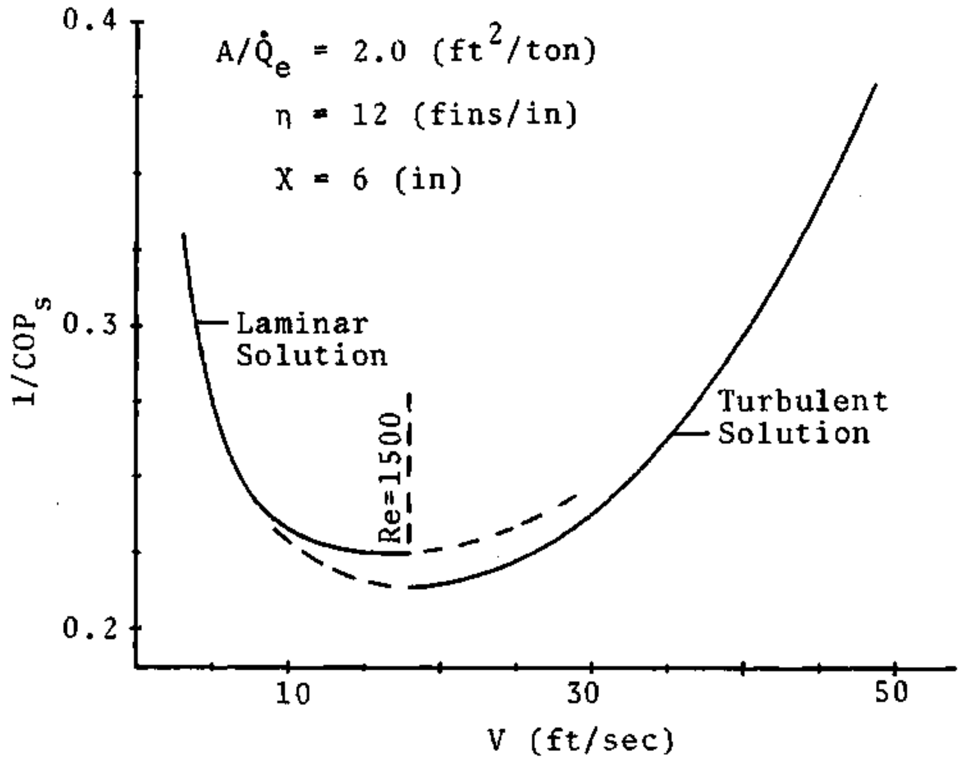

Figure 8. Velocity Optimization Curve--Transition from Laminar to Turbulent Solution

to turbulent flow. In this case the increased heat transfer more than offsets the increased fan work.

In Figure 9 the effect of fan efficiency is shown. It is noted that the fan efficiency has a very small impact on system performance at velocities up to the optimum. The optimal velocity actually increases slightly as fan efficiency improves. This is due to the manner in which fan efficiency, E_{fc}, enters expressions (31) and (34) where it is observed that E_{fc} appears only in the first term of these equations. This term is obviously associated with the fan work rate and dominates system performance at velocities above the optimum

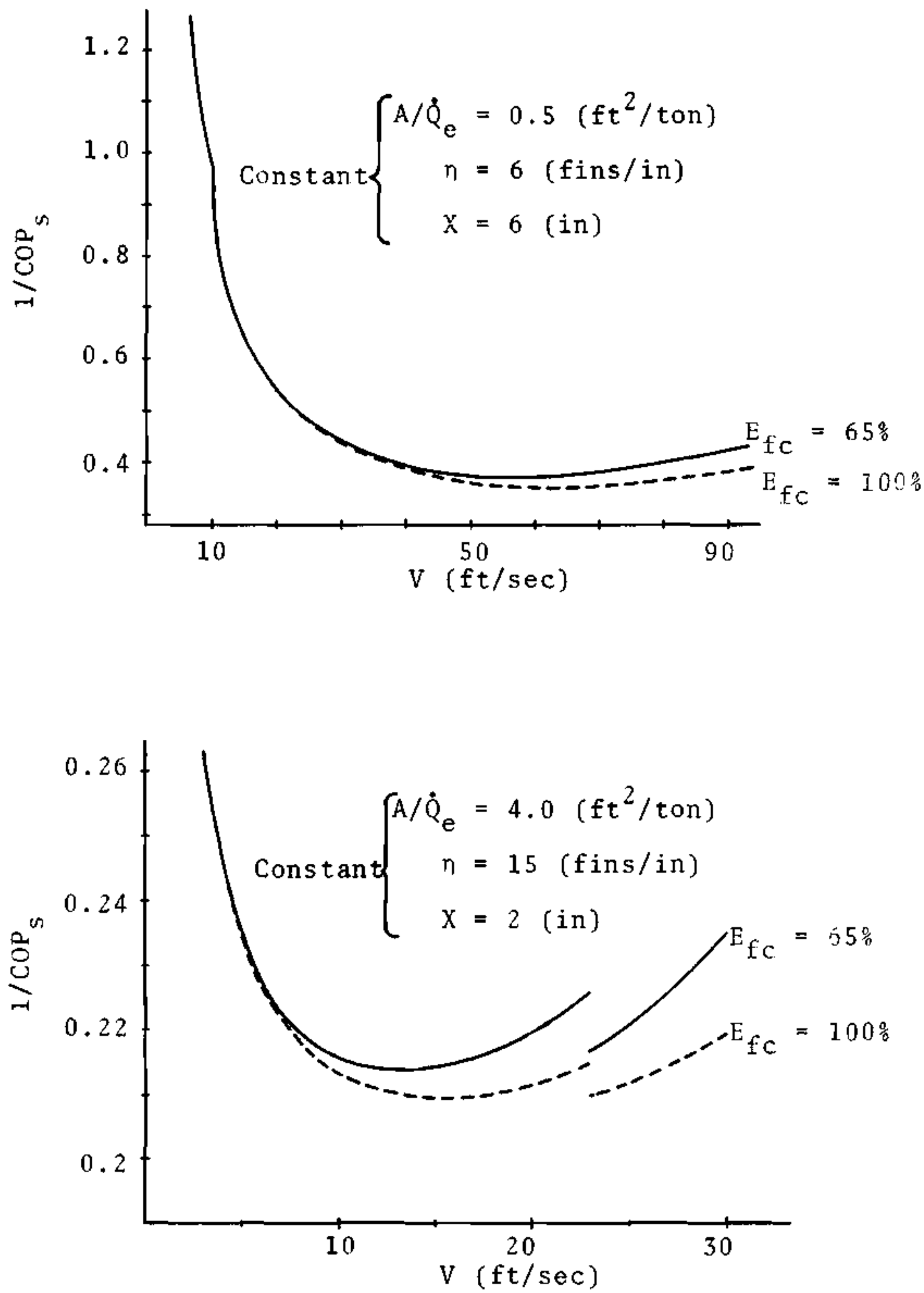

Figure 9. Effect of Condenser Fan Efficiency on System Performance

everything else being equal.

It is instructive to note the effect of compressor efficiency on system performance which is shown in Figure 10. It is evident that the compressor efficiency has a direct and marked impact on performance. However, compressor efficiency has a much smaller effect on the optimal velocity where it is observed that the optimal velocity is decreased slightly. Thus, neither fan efficiency nor compressor efficiency significantly affect the optimal air velocities predicted by the model.

The air velocities of units currently on the market generally range from about 3 ft/sec to 8 ft/sec. Depending on the particular heat exchanger design, the velocity curves indicate a substantial improvement by going to higher velocities. For instance, in Figure 8, going from a velocity of 5 ft/sec to the optimal 18 ft/sec represents a 25 percent improvement in system performance which is certainly significant. The higher fan power is more than offset by the reduction in compressor power.

The velocity optimization discussed above applies not only to the design of new A/C units but also to existing nonoptimized units. The existing unit may be retrofitted with condenser fan equipment capable of producing the optimal velocity given by the curves in Appendix A. The improvement in performance gained by optimizing the velocity will be reflected as a reduction in total electrical energy

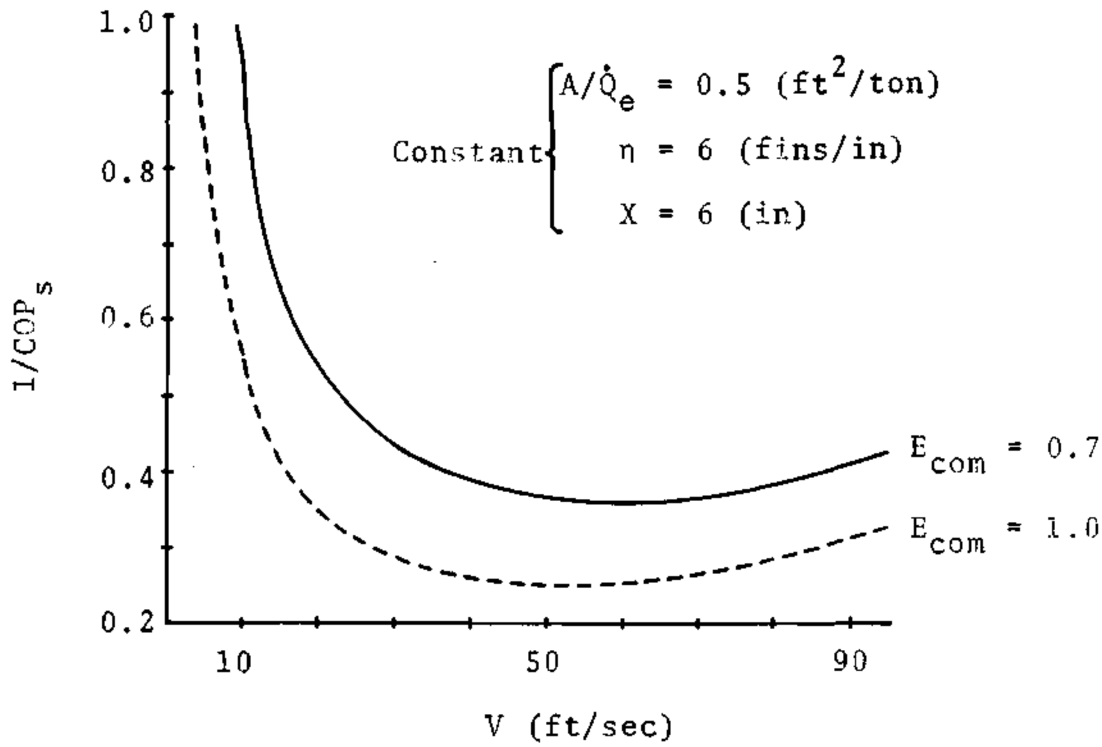

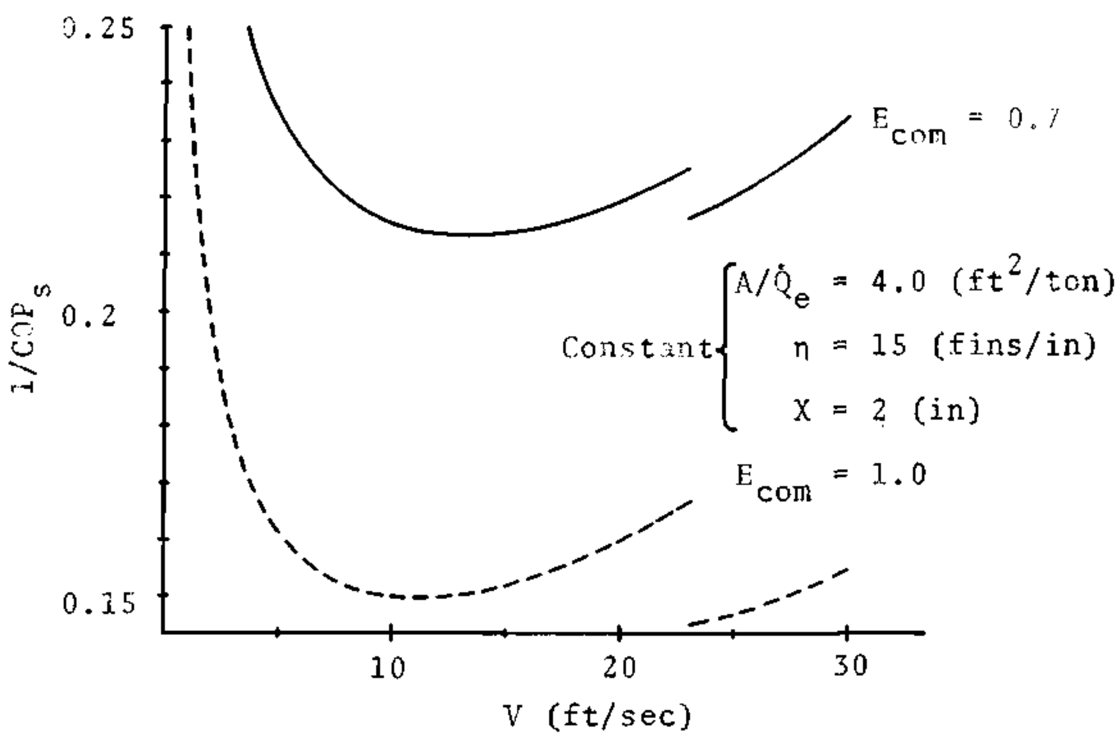

Figure 10. Effect of Compressor Efficiency on System Performance

required to operate the unit.

Increasing the condenser air velocity will affect the system balance point by increasing the heat transfer capacity of the condenser. Thus, the amount of subcooling of the refrigerant before flowing to the expansion valve will be greater. In order to prevent this, and to reduce the condenser saturation temperature, the excess refrigerant should be bled from the loop to restore the condition of having just enough subcooling to ensure that no vapor reaches the expansion valve.

The optimal velocities and their corresponding $1/COP_s$ values can be plotted versus $A/\dot{Q}_e$, as in Appendices B and C, to give the optimal velocity for any value of $A/\dot{Q}_e$ and the corresponding $1/COP_s$ value at that optimal velocity. With regard to the $1/COP_s$ (at V_{opt}) versus $A/\dot{Q}_e$ curves, several observations are worthy of note. Referring to Figure 11 it is seen that at fixed η, a doubling or tripling of $A/\dot{Q}_e$ at fixed condenser depth, X, is always more advantageous than a doubling or tripling of X at fixed $A/\dot{Q}_e$. This agrees with the idealized conclusions reached in the previous analyses. The incremental gain in performance as any one of the design variables is increased is progressively less. Thus, going from a depth of 6 inches to 8 inches would gain practically nothing in terms of performance. The same is true of going to more fins per inch than 15 or an $A/\dot{Q}_e$ greater than 4. In fact, an inspection of either equations (31) and (32) or

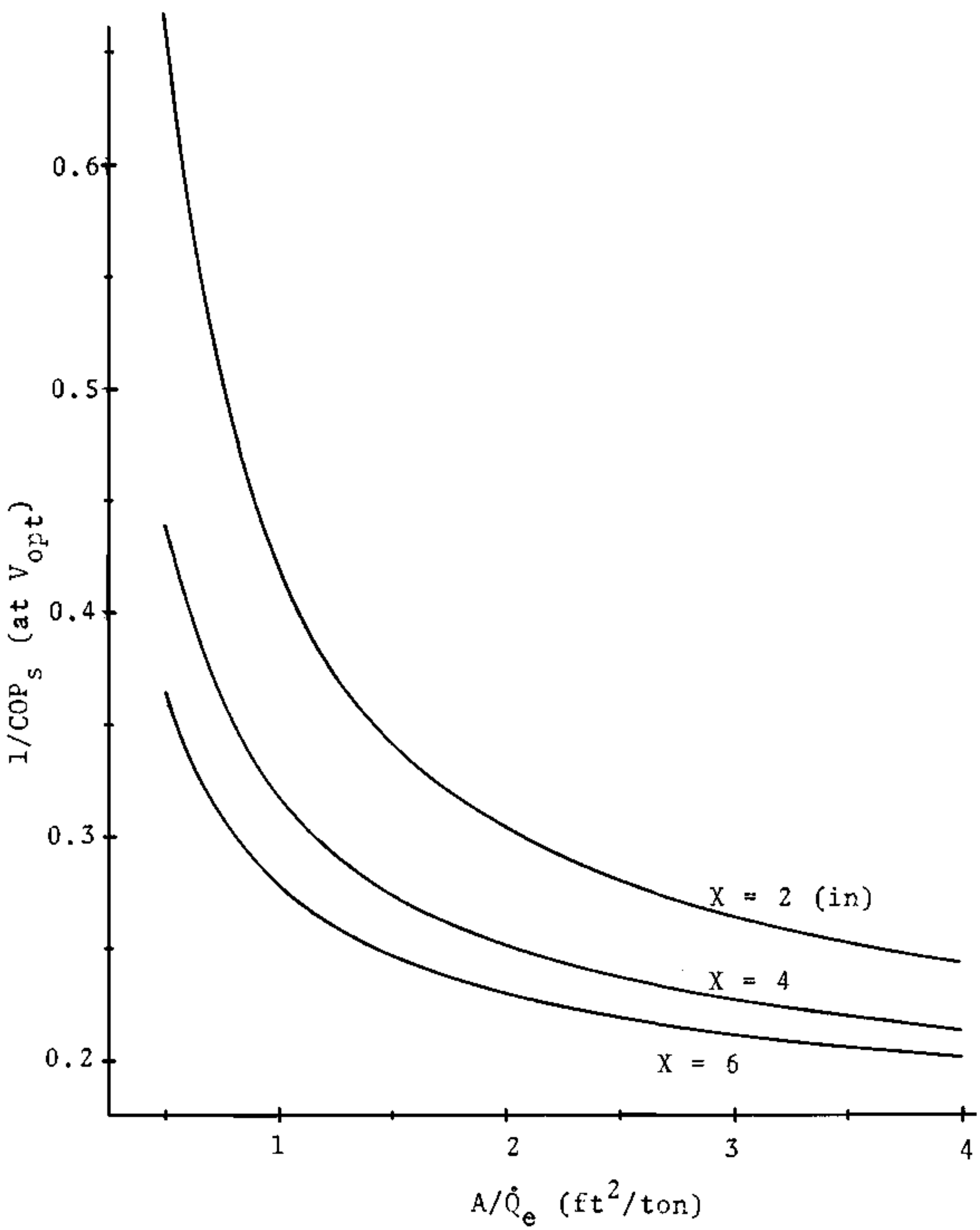

Figure 11. $1/COP_s$ (at V_{opt}) versus $A/\dot{Q}_e$ for η = 6 (fins/in)

(34) and (35) shows that increasing X to very large values, holding everything else constant, results in a decrease in system performance. In light of the previous analysis this is not surprising. Interestingly enough, the same is true of increasing the condenser frontal area, A, holding everything else constant. This result, however, does not contradict the conclusion reached for the constant-volume heat exchanger. Increasing A or X holding everything else constant means the condenser volume is becoming large. The fan work required more than offsets the effect of increased heat transfer area and system performance is reduced. It is obvious that increasing η to a large value, holding the other design variables constant, is physically impractical. Thus, the curves of Appendices A and B cover the practical range of heat exchanger design variables.

From the fundamental equations expressions can be derived to evaluate the condenser saturation temperature, T_{rc}, and the ratio of condenser fan and compressor work rates, β_c (see Appendix H). Over the range of the analysis, the saturation temperature, computed at the optimal velocity varied as follows:

$$
\begin{aligned}
T_{rc} = 697°R \text{ for } \quad & A/\dot{Q}_e = 0.5 \ (\text{ft}^2/\text{ton}) \\
& X = 2 \ (\text{in}) \\
& \eta = 6 \ (\text{fins/in})
\end{aligned}
$$

to

$$T_{rc} = 562°R \text{ for } A/\dot{Q}_e = 4.0 \text{ (ft}^2\text{/ton)}$$

$$X = 6 \text{ (in)}$$

$$\eta = 15 \text{ (fins/in)}$$

The range on β_c computed at the optimal velocity is:

$$\beta_c = 0.135 \text{ for } A/\dot{Q}_e = 0.5 \text{ (ft}^2\text{/ton)}$$

$$X = 2 \text{ (in)}$$

$$\eta = 6 \text{ (fins/in)}$$

to

$$\beta_c = 0.052 \text{ for } A/\dot{Q}_e = 4.0 \text{ (ft}^2\text{/ton)}$$

$$X = 6 \text{ (in)}$$

$$\eta = 15 \text{ (fins/in)}$$

In summary this chapter presents a model which is used to determine the most favorable operating point for a given heat exchanger configuration, cooling load, and evaporator saturation temperature. The curves in Appendices A and B provide the designer with a ready reference and guide in selecting the condenser frontal area, depth, fin spacing, and air velocity. The curves in Appendices A and B are applicable to air-cooled condensers of both residential units and larger commercial units.

CHAPTER III

ECONOMIC ANALYSIS OF AIR CONDITIONING CONDENSER COILS

In the previous chapter attention was focused only on the effect of condenser design on the air conditioner's energy consumption. In this chapter consideration is given to owning and operating costs of an air conditioning system. The economic analysis presented is predicated on the criterion of achieving the most performance at least total cost. In particular, it is desired to minimize the total annual cost of the A/C system per ton of cooling.

The Economic Model

In order to accomplish the stated objective, an economic model is developed which embodies the operating cost and owning cost. These costs are evaluated in the following sections.

Annual Operating Cost

Operating costs are those costs that result from actually operating the system. Included in operating costs are those of energy, maintenance parts and service, and materials. For residential A/C units costs for maintenance and materials are generally small and are neglected.

The annual cost of energy is a function of the electrical utility rate, the number of hours per year that the system is operated, and the efficiency of the system. It is assumed that the utility rate (¢/kw-hr) is independent of the number of operating hours, i.e., utility step rate schedules do not apply. The number of hours of operation vary widely as a function of locality and the owner's personal preference. Table 3 [4, Chapter 43] gives an indication of hours of operation for properly sized equipment for various major cities. The values in Table 3 have been substantiated by utility records.

The efficiency of the system is the coefficient of performance, COP_s, as defined in Chapter II. The annual operating cost per ton of cooling becomes,

$$C_{oper}\ (\$/\text{ton}) = \left(\frac{¢}{\text{kw-hr}}\right) \times \left(\frac{\text{hr}}{\text{yr}}\right) \times \left(\frac{1}{COP_s}\right) \qquad (37)$$

The coefficient of performance, COP_s, will fluctuate during the cooling season as the ambient temperature and cooling load vary. In this study an average ambient of 90°F and evaporator saturation temperature of 40°F have been used in the model to determine the system coefficient of performance. Thus $\frac{1}{COP_s}$ in Equation (37) is an average value for the cooling season.

Owning Cost

Owning costs include the amortized capital cost, taxes levied on property, and insurance. The latter two

Table 3. Estimated Annual Hours of Operation for Properly Sized Equipment in Typical Cities During Normal Cooling Season* [4, Chapter 43]

City	Hours
Atlanta, Georgia	750
Boston, Massachusetts	200
Chicago, Illinois	400
Cleveland, Ohio	450
Dallas, Texas	1400
Fresno, California	900
Jacksonville, Florida	1600
Minneapolis, Minnesota	350
New Orleans, Louisiana	1500
St. Louis, Missouri	1000
Washington, D. C.	800

*Based on average indoor temperature of 80°F.

costs are not considered here.

In order to evaluate the amortized capital cost, three elements must be established: (1) initial (capital) cost, (2) average useful life of the equipment, and (3) interest rate (rate of return on barely-attractive investments).

Capital Cost Analysis. Data obtained from a major manufacturer of the type of heat exchanger being dealt with here was studied. It was found that the cost (selling price to the customer) is a simple function of the heat exchanger volume, AX, for fixed fins per inch. Figure 12 shows the cost curves which are average lines fitted to a number of points plotted from the data. Appendix G shows the actual costs of condenser coils of varying volume. The curves of Figure 12 are conveniently given by the equation,

$$\text{Cost } (\$) = [1.908\ (\eta - 6) + 63.75]\ \text{Vol} + 172 \qquad (38)$$

where the Vol = AX in ft^3.

The capital cost of the remaining components of the system such as the compressor, evaporator coil, fans, etc. is taken as some number of dollars, K_1, which is considered constant. Arguments for taking K_1 constant are the following. As a fixed cooling capacity and evaporator temperature are assumed, any variation in the capital cost of the evaporator and fan as the condenser design is changed will be very small.

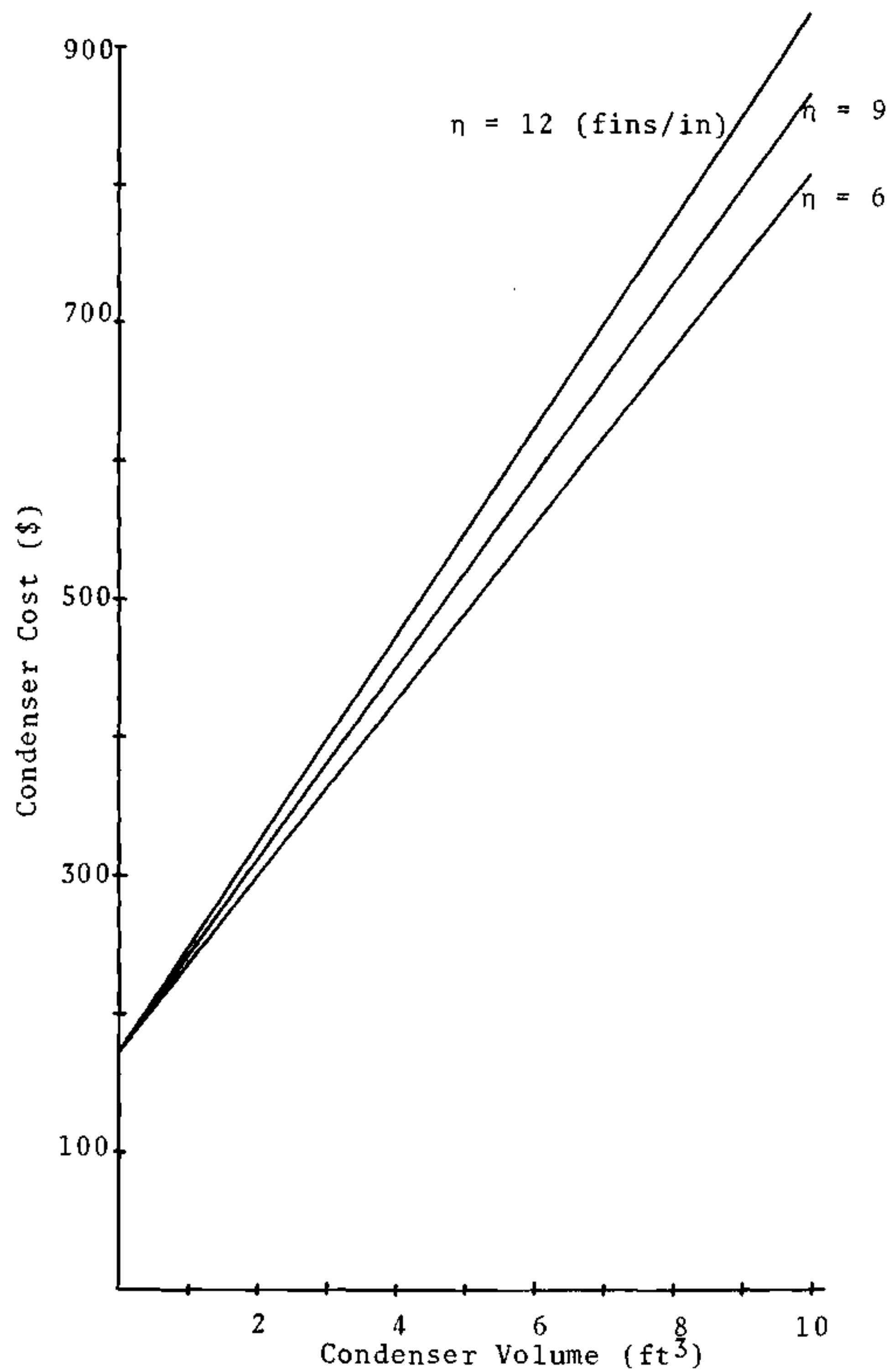

Figure 12. Capital Cost of Condensers

The compressor work rate will vary as condenser geometry is changed, but this variation is not pronounced. Hence, the change in capital cost associated with the compressor will be small compared to the cost of the condenser. Admittedly, the condenser fan work rate varies over a wide range, as indicated in Chapter II, for various condenser configurations. Thus, the capital cost for the condenser fan and motor will vary, but here again any variation is assumed small compared to condenser cost. Variation in other costs, K_2, such as erection, power installation, etc. will not be significant as condenser configuration is changed. Hence, the initial cost of the A/C system is,

$$C_{cap}\ (\$) = [1.908\ (\eta - 6) + 63.75]\ AX + 172 + K \qquad (39)$$

where $K = K_1 + K_2$ is considered fixed for a given system. Since the 172 and K are constants they can be dropped from (39) without affecting the optimization to follow.

Average Useful Life. The useful life of a piece of equipment or system is dependent on many factors such as frequency of use, policy as to repairs, climate in which it is used, etc. For the purpose of this study, an average useful life of ten years is chosen as suggested by the ASHRAE 1973 Systems Handbook [4, Chapter 44] for air conditioning systems under 5 tons capacity.

Rate of Return. Money invested in an air conditioning system must either be borrowed, obtained from equity investors, or diverted from other uses. The time value of this money lies between the rate of interest on borrowed money and the rate of return on barely-attractive investments. For the typical residential owner, an interest rate of 11 percent is taken.

In order to convert the initial cost into an equivalent uniform annual cost, it is assumed that the life of the equipment is a negative exponential random variable (N) with average life (m). Then,

$$f(N) = \frac{1}{m} e^{-t/m} \tag{40}$$

If C_{cap} dollars is spent at time (t) zero on equipment with a life given by (40), then the equivalent annual cost, $\overline{C}_{cap}$, is given by,

$$\overline{C}_{cap} = C_{cap} \left(r + \frac{1}{m}\right) \tag{41}$$

where $r = \ln (1+i)$ is the nominal continuous-compound interest rate [36].

Economic Optimization

The total annual cost is given by,

$$C_T = C_{oper} + \overline{C}_{cap} \tag{42}$$

The operating cost, C_{oper}, is by Equation (37),

$$C_{oper}\ (\$/\text{ton}) = (\frac{¢}{\text{kw-hr}}) \times (\frac{\text{hr}}{\text{yr}}) \times (\frac{1}{COP_s})$$

where $1/COP_s$, given by Equations (31)-(35), is a function of the following variables,

$$1/COP_s = f(V, A/\dot{Q}_e, X, \eta)$$

After dropping the constants appearing in Equation (39) and normalizing the result per ton of cooling, the amortized cost per ton becomes,

$$\overline{C}_{cap}\ (\$/\text{ton}) = [\ln(1+i) + \frac{1}{m}]\{[1.908(\eta-6)+63.75]\ \frac{AX}{\dot{Q}_e}\} \tag{43}$$

Equation (43) is a function of the following,

$$\overline{C}_{cap} = g(A/\dot{Q}_e, X, \eta)$$

Thus total annual cost is functionally dependent on,

$$C_T = f_1\ (\frac{¢}{\text{kw-hr}}, \frac{\text{hr}}{\text{yr}}, V, \frac{A}{\dot{Q}_e}, X, \eta) + g(A/\dot{Q}_e, X, \eta) \tag{44}$$

It is clear from (44) that the amortized capital cost is independent of the air velocity. Thus C_T is minimized with respect to velocity by using the value of $\frac{1}{COP_s}$ (at V_{opt}), derived in the previous chapter, in the operating cost term. The expression for total annual cost becomes,

$$C_T\ (\$/\text{ton}) = \left(\frac{¢}{\text{kw-hr}}\right) \times \left(\frac{\text{hr}}{\text{yr}}\right) \times \left(\frac{1}{COP_s}\ (\text{at } V_{opt})\right)$$

$$+ \left[\ln\ (1+i) + \frac{1}{m}\right]\left\{[1.908\ (\eta-6) + 63.75]\ \frac{AX}{\dot{Q}_e}\right\} \qquad (45)$$

where $\frac{1}{COP_s}$ (at V_{opt}) and its corresponding $A/\dot{Q}_e$, X, and η given by the saddle points of the curves in Appendix A (or the data in Appendix C); m equals 10 years; and i equals 11 percent.

With the use of Equation (45) the curves of Appendix D are generated where C_T is plotted versus $A/\dot{Q}_e$ for a number of combinations of hours of operation per year and electricity rates. The hours of operation and electrical rates have been combined. For instance, $1.5\text{x}10^3$ (¢/kw-yr) is equivalent to 500 $(\frac{\text{hr}}{\text{yr}})$ at 3 $(\frac{¢}{\text{kw-hr}})$ or 750 $(\frac{\text{hr}}{\text{yr}})$ at 2 $(\frac{¢}{\text{kw-hr}})$ etc.

From the curves in Appendix D, the optimal (least cost) heat exchanger configuration is the one with least depth, the greatest number of fins per inch, and $A/\dot{Q}_e$ given by the curve. Again, this fact agrees with the "ideal" conclusions cited in Chapter II. However, the least depth configuration is the optimum only if there is no restriction placed on $A/\dot{Q}_e$. If the constraint is imposed that $A/\dot{Q}_e$

equals one, then it is noticed that the four or six inch deep configuration is optimal depending on hours of operation and electric rate. It is interesting that the minimal costs for the various depths at a given η, hours of operation, and electrical rate, are within a few dollars of each other over the entire range of the analysis. This fact gives the designer a large number of combinations of exchanger configurations that are practically equally cost effective. The curves also show the penalty for a nonoptimum configuration. As energy costs increase the optimal $A/\dot{Q}_e$ for fixed X and η definitely shifts to a higher value. Depending on the magnitude of energy cost increase, the customer is justified in going to a more capital cost intensive system.

Figures 13 through 18 show the effect of various values of the refrigerant-film heat transfer coefficient, $\bar{h}_r$, on the C_T versus $A/\dot{Q}_e$ curves. When $\bar{h}_r$ is reduced from 300 to 200 (Btu/ft^2-hr-°R), the effect is to shift the curves upward and to the right so that the optimal value for $A/\dot{Q}_e$ is increased by about 15-20 percent for $1.5\text{x}10^3$ (¢/kw-yr). A decrease in $\bar{h}_r$ results in a greater refrigerant-film resistance (Equation 4) so the trend in the curves is what would be expected. The shift becomes more pronounced as hours of operation and energy cost increase so that at $1.35\text{x}10^4$ (¢/kw-yr) the optimal $A/\dot{Q}_e$ is increased by about 30-35 percent.

Increasing $\bar{h}_r$ from 300 to 400 (Btu/ft^2-hr-°R) has the

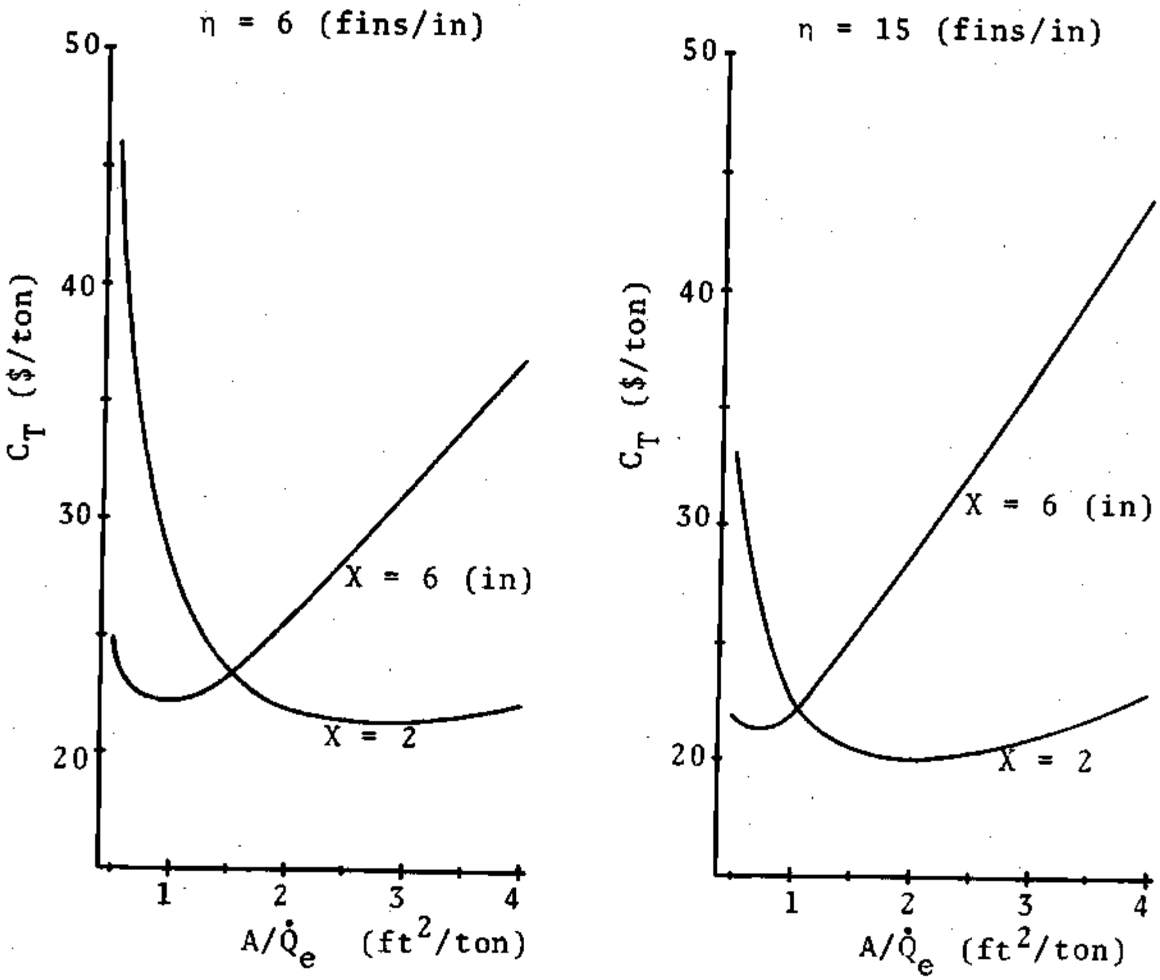

Figure 13. Effect of Refrigerant Heat Transfer Coefficient, $\bar{h}_r$, on Total Annual Cost and Condenser Design for 1.5×10^3 (¢/kw-yr); $\bar{h}_r$ = 200 (Btu/ft^2-hr-°R)

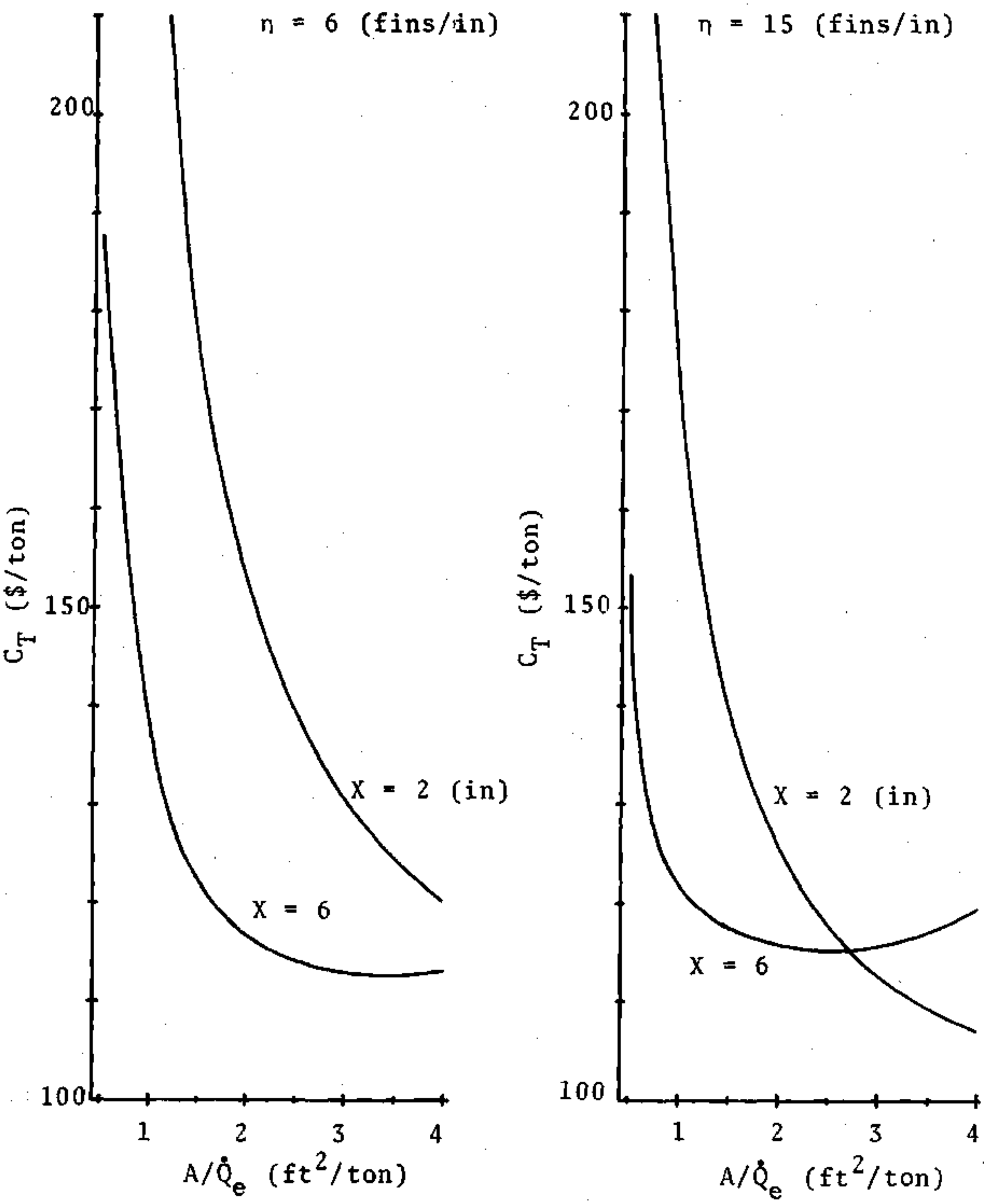

Figure 14. Effect of Refrigerant Heat Transfer Coefficient, $\bar{h}_r$, on Total Annual Cost and Condenser Design for $1.35x10^4$ (¢/kw-yr); $\bar{h}_r$ = 200 (Btu/ft^2-hr-°R)

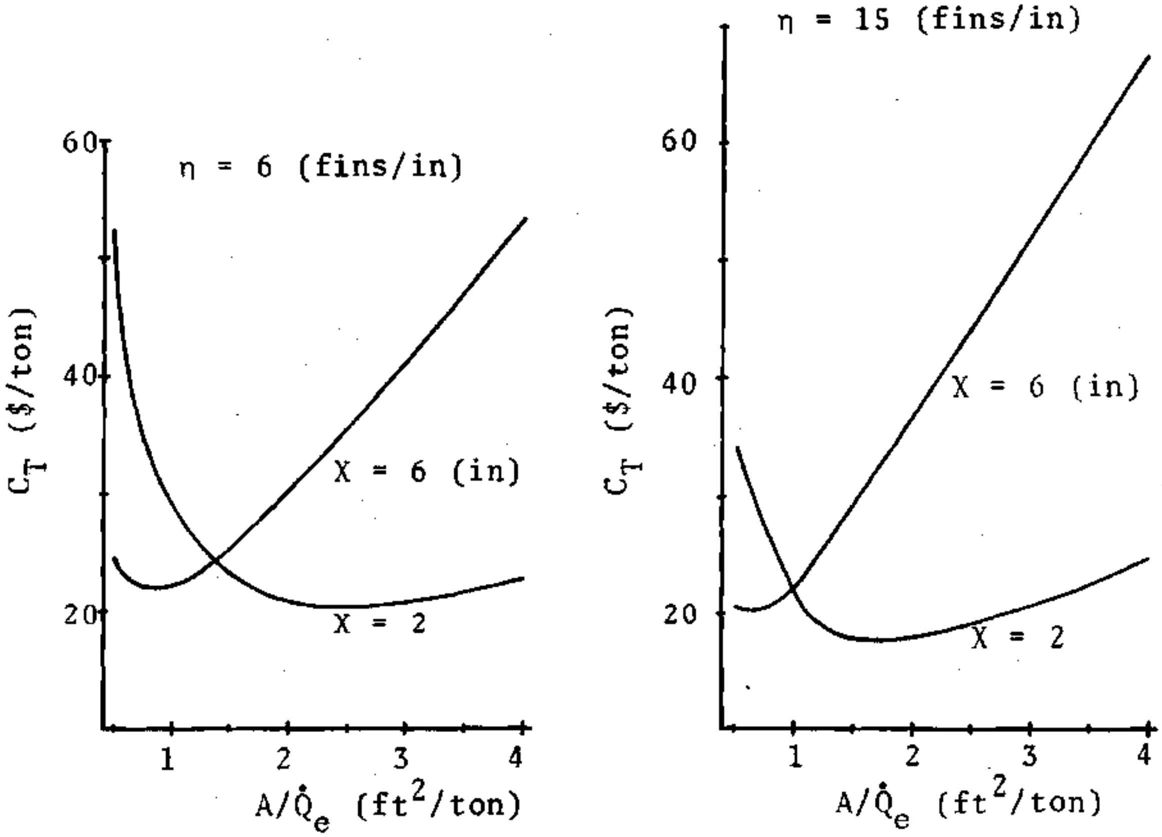

Figure 15. Effect of Refrigerant Heat Transfer Coefficient, $\bar{h}_r$, on Total Annual Cost and Condenser Design for 1.5×10^3 (¢/kw-yr); $\bar{h}_r$ = 300 (Btu/ft^2-hr-°R)

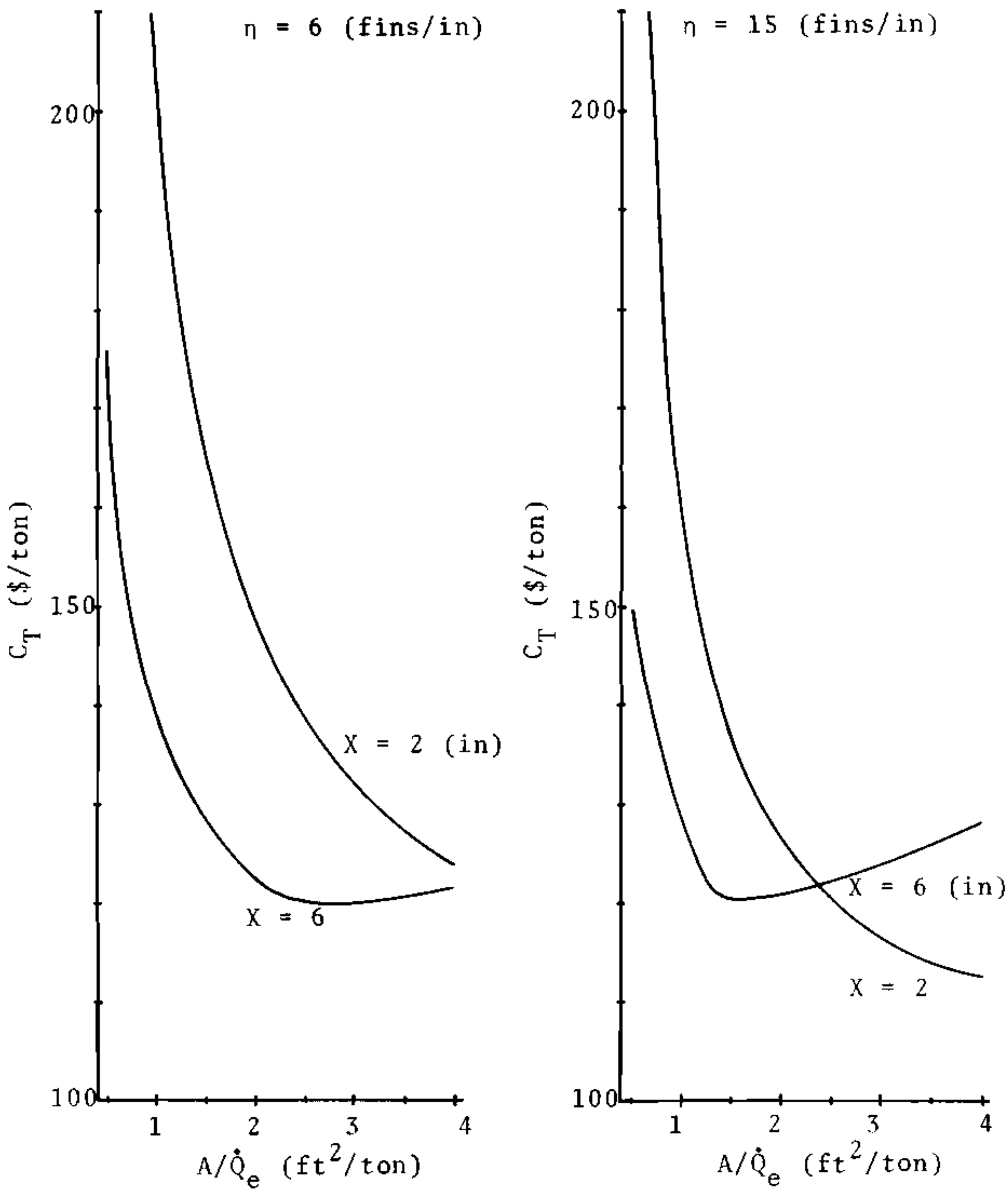

Figure 16. Effect of Refrigerant Heat Transfer Coefficient, $\bar{h}_r$, on Total Annual Cost and Condenser Design for 1.35×10^4 (¢/kw-yr); $\bar{h}_r$ = 300 (Btu/ft^2-hr-°R)

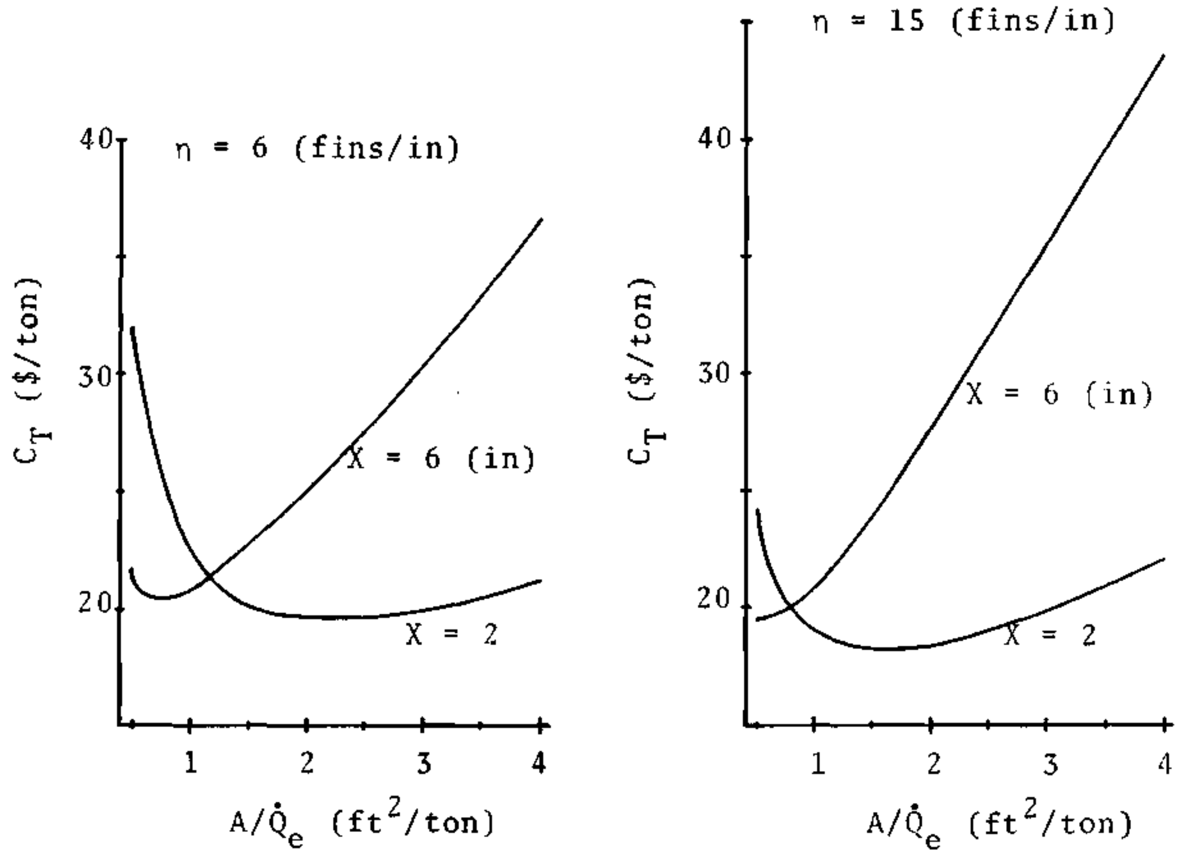

Figure 17. Effect of Refrigerant Heat Transfer Coefficient, $\bar{h}_r$ on Total Annual Cost and Condenser Design for 1.5×10^3 (¢/kw-yr); $\bar{h}_r$ = 400 (Btu/ft^2-hr-°R)

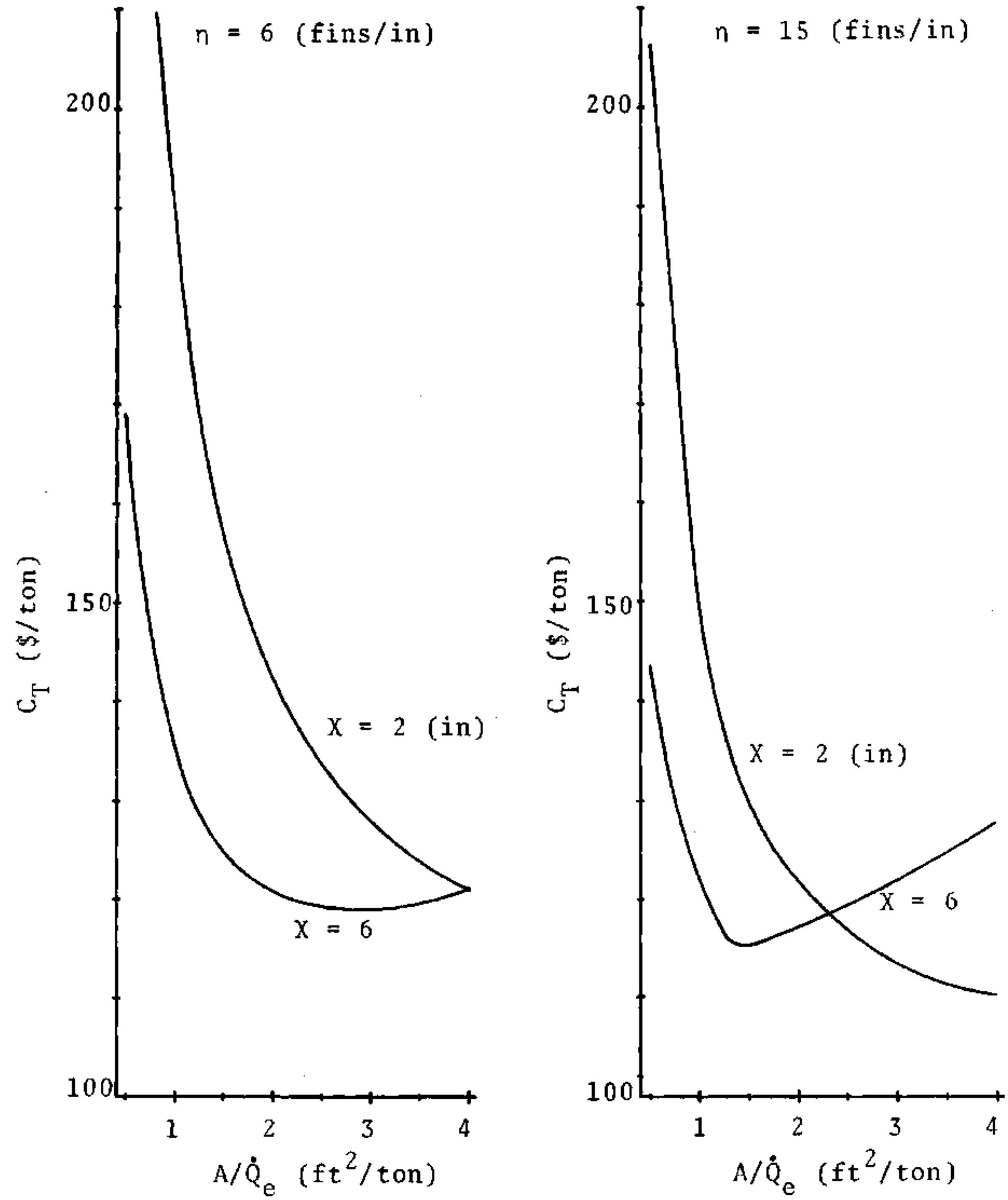

Figure 18. Effect of Refrigerant Heat Transfer Coefficient, $\bar{h}_r$, on Total Annual Cost and Condenser Design for 1.35×10^4 (¢/kw-yr); $\bar{h}_r$ = 400 (Btu/ft^2-hr-°R)

reverse effect. However, the shift is much less than for the previous case. The optimal $A/\dot{Q}_e$ being about 5-10 percent less over the entire range of hours of operation and energy cost.

The minimal cost configurations indicated by the curves in Appendix D can be plotted as shown in Figure 19. These curves, compiled in Appendix E, are extremely useful in that fixing any two of the heat exchanger design variables the optimal value of the third can be found. The designer generally will know the hours of operation per year and appropriate utility rate applicable to the system he wishes to design. He then enters the appropriate set of curves in Appendix E and chooses any two design variables at random or consistent with constraints that might apply. Having determined a minimal cost configuration from these curves, the designer enters the curves of Appendices B and C to determine the corresponding $1/COP_s$ value and optimal operating velocity. In this way the entire least cost condenser design and operating characteristics are found from the design curves. Equations (31), (34), and (37) may then be used to study how the operating cost varies at velocities other than the optimum. Appendix F shows how operating cost varies with velocity for the minimal cost configurations of Appendix E. Table 4 shows operating cost per ton for several cases selected from Appendix F. The reduction in operating cost varies from about 10 percent to 150 percent depending upon

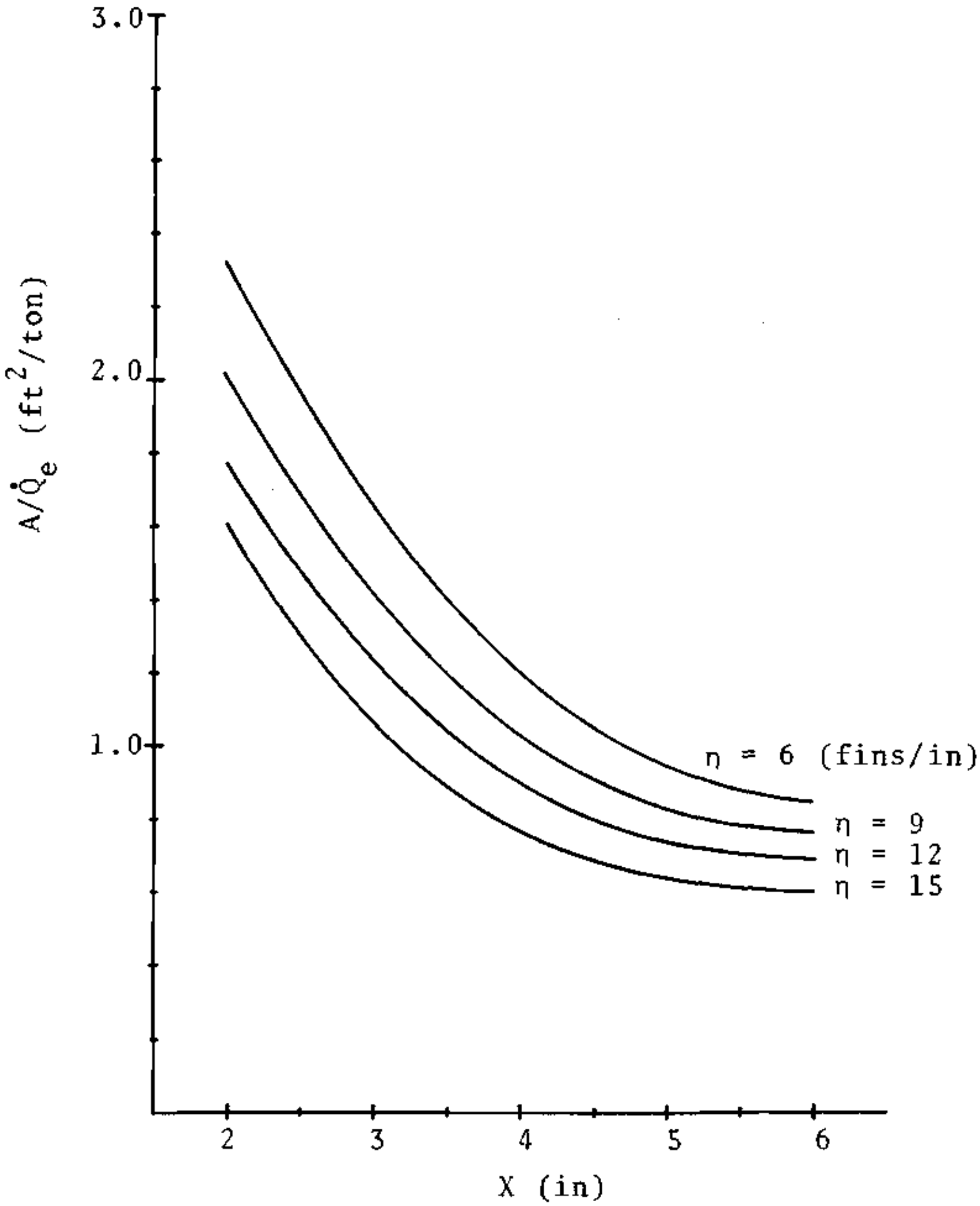

Figure 19. Optimal Heat Exchanger Design Curves for 1.5×10^3 (¢/kw-yr)

Table 4. Annual Operating Cost at Varying Air Velocities for the Optimal Condenser Configurations*

1.5×10^3 (¢/kw-yr), $\eta = 6$ (fins/in)					
$X = 2$ (in), $A/\dot{Q}_{e_{opt}} = 2.3$		$X = 4$ (in), $A/\dot{Q}_{e_{opt}} = 1.2$		$X = 6$ (in), $A/\dot{Q}_{e_{opt}} = 0.85$	
V	C_{oper}	V	C_{oper}	V	C_{oper}
5	25.68	5	33.21	5	38.80
10	24.91	10	26.88	10	27.26
20	17.90	20	18.70	20	18.27
42 opt	15.16	43 opt	15.71	43 opt	15.45
9.0×10^3 (¢/kw-yr), $\eta = 15$ (fins/in)					
$X = 2$ (in), $A/\dot{Q}_{e_{opt}} = 4.0$		$X = 4$ (in), $A/\dot{Q}_{e_{opt}} = 2.4$		$X = 6$ (in), $A/\dot{Q}_{e_{opt}} = 1.1$	
V	C_{oper}	V	C_{oper}	V	C_{oper}
5	74.22	5	81.19	5	117.00
7	70.52	7	75.18	10	90.26
10	68.23	10	71.43	15	83.37
13 opt	67.68	13.2 opt	70.10	20 opt	76.89

Units: $A/\dot{Q}_{e_{opt}}$ (ft^2/ton); V (ft/sec); C_{oper} (\$/ton)

*Data selected from Appendix F.

the condenser configuration. A velocity of 5 ft/sec is typical of units currently on the market.

After the condenser configuration and velocity have been determined, the designer selects the other components of the system-compressor, evaporator coil, fans, expansion device, etc. The selection of components must be such that the system is balanced at the desired operating conditions.

If the design calls for a rather high air velocity, the designer may need to consider the level of noise associated with a higher velocity. The noise level is in large part dependent on the type of fan, number of blades, fan RPM, and pressure drop, etc. The sound level admissible at the source will vary with the individual situation. It is dependent on the directivity factors of propagation, listening areas near the equipment, the paths by which noise travels from source to listening area, etc. [4, Chapter 35; 14]. Expense incurred in the control of noise, such as for acoustical enclosures, would increase the capital cost of the system.

CHAPTER IV

CONCLUSIONS AND RECOMMENDATIONS

This study develops a methodology for determining the minimal cost condenser for an air conditioning system. This is accomplished by finding the condenser configuration and its corresponding operating air velocity which minimize the system's capital and operating costs. It should be noted that the results obtained in this work are essentially the same as that of minimizing the cost of a heat transfer unit, a technique familiar to many involved in the design of heat transfer equipment [30, Chapter 2].

Figure 20 will aid the reader in grasping the essential features of the optimization undertaken in this study. Total annual cost, C_T (\$/ton), which includes the operating cost of the A/C system and incremental capital cost of the condenser is plotted as a function of the air velocity, V (ft/sec), through the condenser and the condenser frontal area per ton, $A/\dot{Q}_e$ (ft^2/ton). The surface shown is for a fixed condenser depth, X (in), a fixed number of fins per inch, η (fins/in), and fixed electrical energy cost-consumption factor (¢/kw-yr = ¢/kw-hr•hr/yr). Figure 20 is representative of the surfaces that result as any one of the above parameters is changed. These surfaces result from

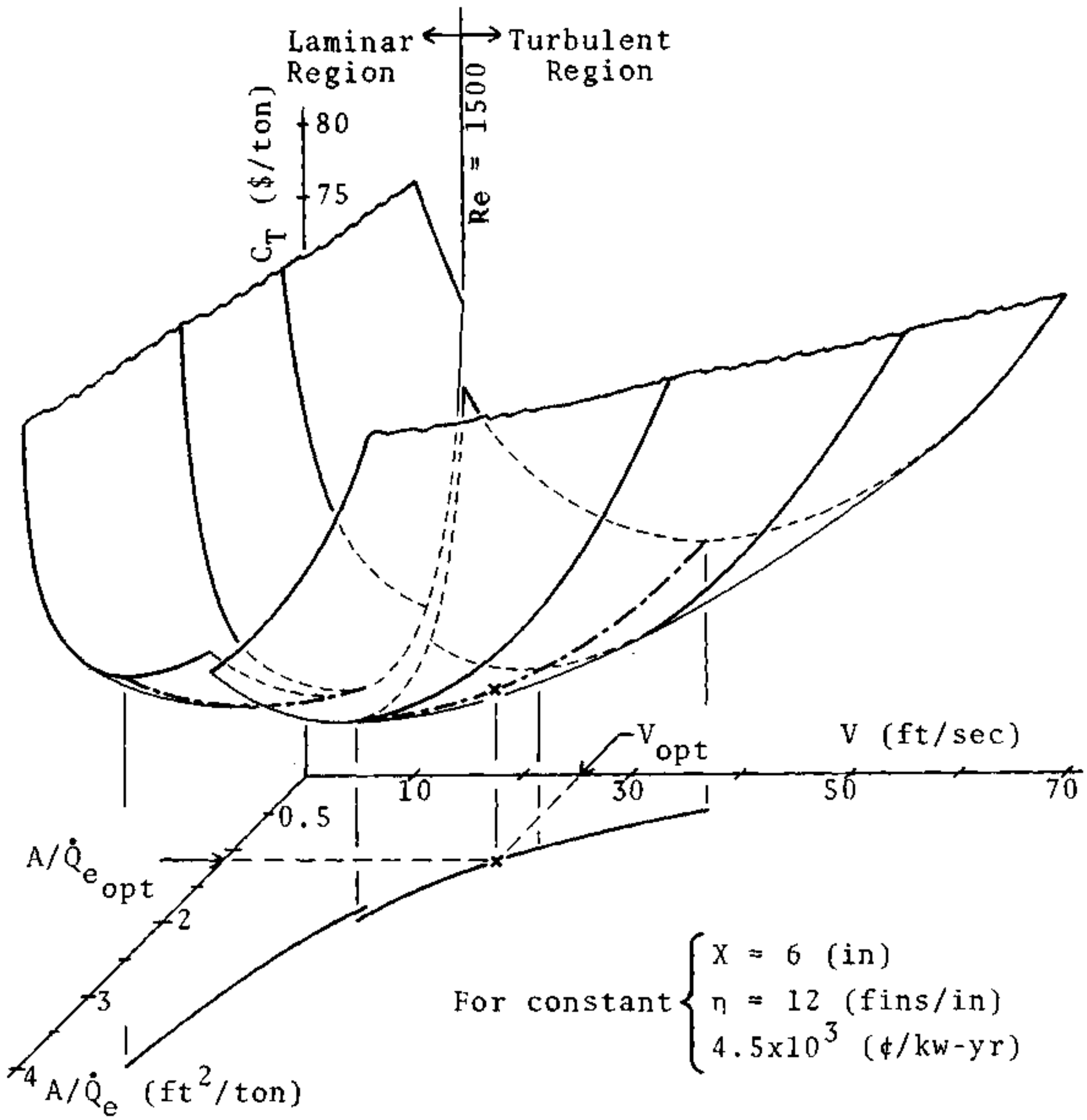

Note: The laminar region is computed from Equation (45) with $1/COP_s$ evaluated by Equations (31) and (32). The turbulent region is computed from Equation (45) with $1/COP_s$ evaluated by Equations (34) and (35). Tables 1 and 2 give nominal values (taken as constants) for various quantities appearing in Equations (31)-(35).

Figure 20. Representative 3-Dimensional Surface for Total Annual Cost as a Function of Air Velocity and Condenser Frontal Area

the use of the equations and tables as explained in the note of Figure 20.

The analysis indicates two areas for potential improvement in the cost associated with typical residential air conditioning units. The first area for potential savings to the owner lies in the selection of an optimal configuration for the condenser, i.e., selecting the optimal $A/\dot{Q}_e$ for given X, η, and energy cost-consumption rate as shown in Figure 20. The curves in Appendix D, which are slices along the saddle lines of "troughs" similar to that of Figure 20, show the optimal $A/\dot{Q}_e$ for a number of different values of X, η, and energy consumption. At each energy consumption-cost rate the condenser configuration with least depth, X = 2 (in), and the greatest number of fins, η = 15 (fins/in), gives the minimal cost configuration if no restriction is placed on $A/\dot{Q}_e$. However, it is noted that a condenser with depth greater than two inches with its corresponding optimal $A/\dot{Q}_e$ is nearly as cost-effective. From Appendix D it is clear the penalty incurred for operating an "undersized" condenser is substantial for high annual hours of operation and energy cost. In selecting a new system, an $A/\dot{Q}_e$ somewhat greater than the indicated optimum should probably be chosen because, over the life span (assumed 10 years in this study) of the equipment, energy costs are likely to increase.

Since a number of condenser configurations have nearly the same cost-effectiveness as mentioned above for a given energy cost and annual hours of operation, the optimal solutions in Appendix D give rise to the curves of Appendix E which define all combinations of minimal cost condenser configurations. These curves, while giving the designer latitude in choosing a configuration, ensure the selection of a near optimal condenser design.

The second area of potential saving is that of operating at an air velocity which ensures as low an operating cost as possible. From Figure 20 and a consideration of the derivation of the curves in Appendix E it is clear that it is possible to optimize the system with respect to condenser configuration but then incur a penalty by not operating at the optimal velocity. Numerous curves for optimizing velocity for various configurations are given in Appendix A. These curves are slices, at constant $A/\dot{Q}_e$, through surfaces similar to that of Figure 20. Since each condenser configuration has a unique optimal velocity, the optimal velocities may be plotted versus $A/\dot{Q}_e$ for fixed X and η as in Appendix B. These curves are similar to the one shown in the $A/\dot{Q}_e$-V plane of Figure 20.

Appendix F has been prepared to show how the annual operating cost increases when systems are operated at other than the optimal velocity. The figures indicate that increasing air velocity from 5 ft/sec, which is a common value for currently available units, to the optimal velocity produces savings ranging from 10 percent to 150 percent depending on the particular configuration.

Air velocity optimization applies not only to the design of new units but also to existing A/C units. An unoptimized unit can be retrofitted with condenser fan equipment capable of producing the desired optimal velocity for that specific configuration. Adjustment should be made to the amount of refrigerant in the system to prevent excess subcooling in the condenser produced by the increased heat transfer rate.

To show the practical usefulness of this study's results, the data in Table 5 has been compiled. Optimal condensers (configurations and operating characteristics) are defined for various geographical locations in the United States. Given the annual hours of operation and cost of electrical energy, the designer is able to select the optimal condenser and compute costs associated with its operation. The source from which each quantity is derived is explained in the note accompanying Table 5.

Notice the correlation among the parameters as the energy cost and annual hours of operation vary. For instance, in Boston with a low energy consumption-cost factor, 9.4×10^2 (¢/kw-yr), the optimal solution specifies a system with low overall efficiency (high $1/COP_s$), low $A/\dot{Q}_e$ (low capital investment), and a high air velocity. At the other end of the spectrum in Dallas with a high energy consumption-cost

Table 5. Optimal Condensers for Various Geographical Locations

City	$\frac{hr}{yr}$	$\frac{¢}{kw\text{-}hr}$	X	η	$\frac{A}{\dot{Q}_e}$	V	$\frac{1}{COP_s}$	β_c	C_{oper}	C_T
Atlanta	750	2.66	2	15	1.86	23.5	0.261	0.68	18.31	23.44
Boston	200	4.7	2	15	1.26	34	0.3	0.80	9.92	13.39
Cleveland	400	3.8	2	15	1.61	29.5	0.275	0.72	14.70	19.14
Dallas	1400	2.84	2	15	2.79	17	0.233	0.58	32.57	40.26
Minneapolis	350	3.57	2	15	1.45	31	0.283	0.76	12.43	16.43
St. Louis	1000	3.03	2	15	2.4	19	0.242	0.62	25.78	32.39
Washington, D. C.	800	4.05	2	15	2.5	18.5	0.239	0.61	27.23	34.12

Units: X (in); η (fins/in); $A/\dot{Q}_e$ (ft^2/ton); V (ft/sec); C_{oper} and C_T (annual $/ton)

Note: Hr/yr taken from Table 3.
¢/kw-hr--June 1974 rates for 500 kw-hr/month [21].
With no constraint placed on $A/\dot{Q}_e$ X = 2 and η = 15 give minimal cost--Appendix D.
$A/\dot{Q}_e$ found in Appendix E.
V found in Appendix B.
$1/COP_s$ found in Appendix C.
β_c computed from Equation (31H) Appendix H.
C_{oper} computed from Equation (37).
C_T computed from Equation (45).

factor, 3.976×10^3 (¢/kw-yr), the optimum is a system with high overall efficiency (low $1/COP_s$), a high $A/\dot{Q}_e$ (large capital investment), and low air velocity. Based on earlier observations, it is noted that other combinations of X, η, and $A/\dot{Q}_e$, as given by Appendix E, would give nearly the same cost-effectiveness as the configurations proposed in Table 5.

Several existing A/C units, typical of units currently on the market, are compared with the optimal units of Table 5 to determine what improvement in total cost is possible. Figures 21 and 22 give the velocity optimization curves, as predicted by the model, for two existing units. In each case the units are operating at too low an air velocity. The improvement in system coefficient of performance by increasing velocity to the optimal value is readily apparent. For the Lennox unit in Figure 21 an 18.6 percent improvement is indicated while for the York unit, Figure 22, a 25 percent increase in system coefficient of performance is possible.

In Table 6 the existing units are compared to the optimal solutions of Table 5. Costs based on the unit's actual air velocity and the indicated optimum are shown. From the figures it is clear that system efficiency becomes increasingly important as the combination of annual hours of operation and energy cost increases. Of major significance is the fact that optimizing the existing units with respect to velocity alone leads to total annual costs, C_T (\$/ton), which compare most favorably with those of the optimal units.

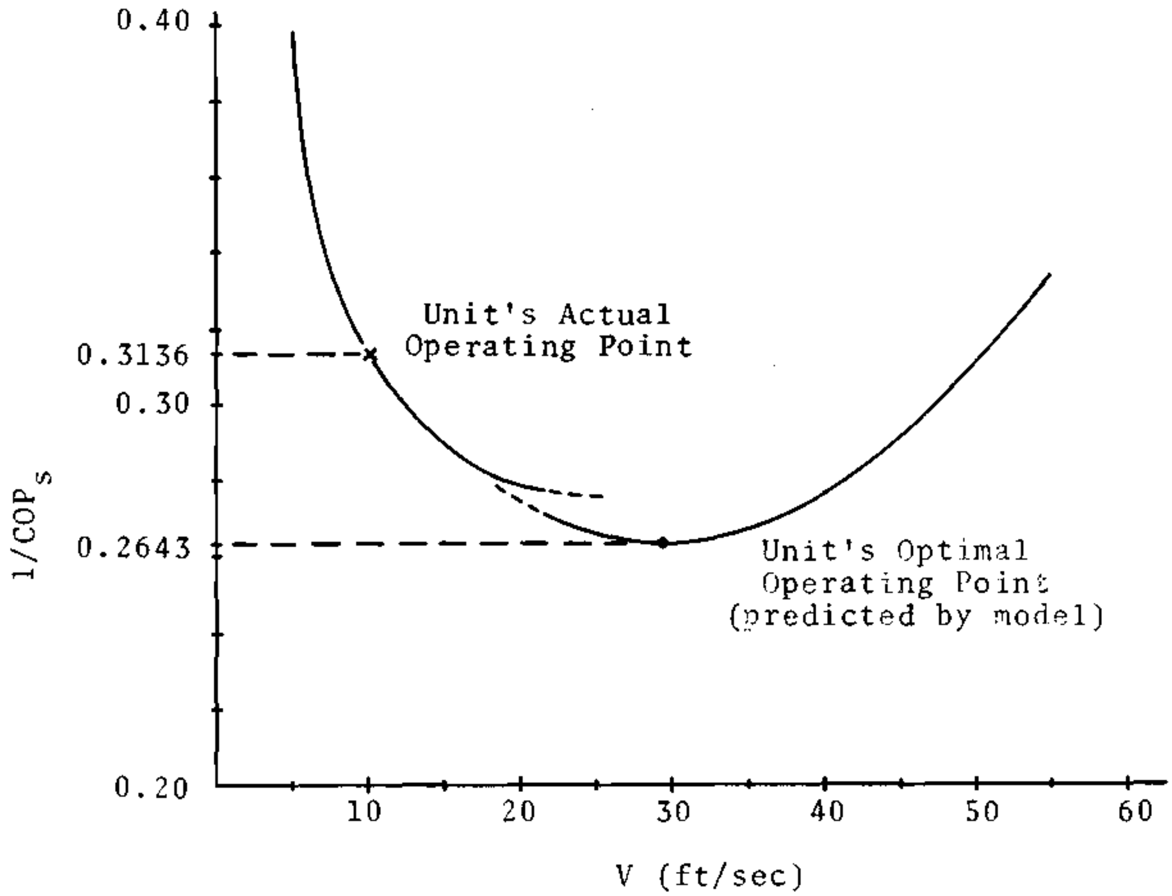

Note: The curve above is generated by the use of Equations (31)-(35) with $A/\dot{Q}_e$, X, and η given in the specifications below and values from Tables 1 and 2.

Specifications for Lennox unit:
Model HS8-411-1FFA
$X = 3$ (in); $\eta = 14$ (fins/in);
$A = 4$ (ft^2); $\dot{Q}_e = 3$ (ton);
$V = 10$ (ft/sec)

Figure 21. Velocity Optimization Curve for Lennox Unit

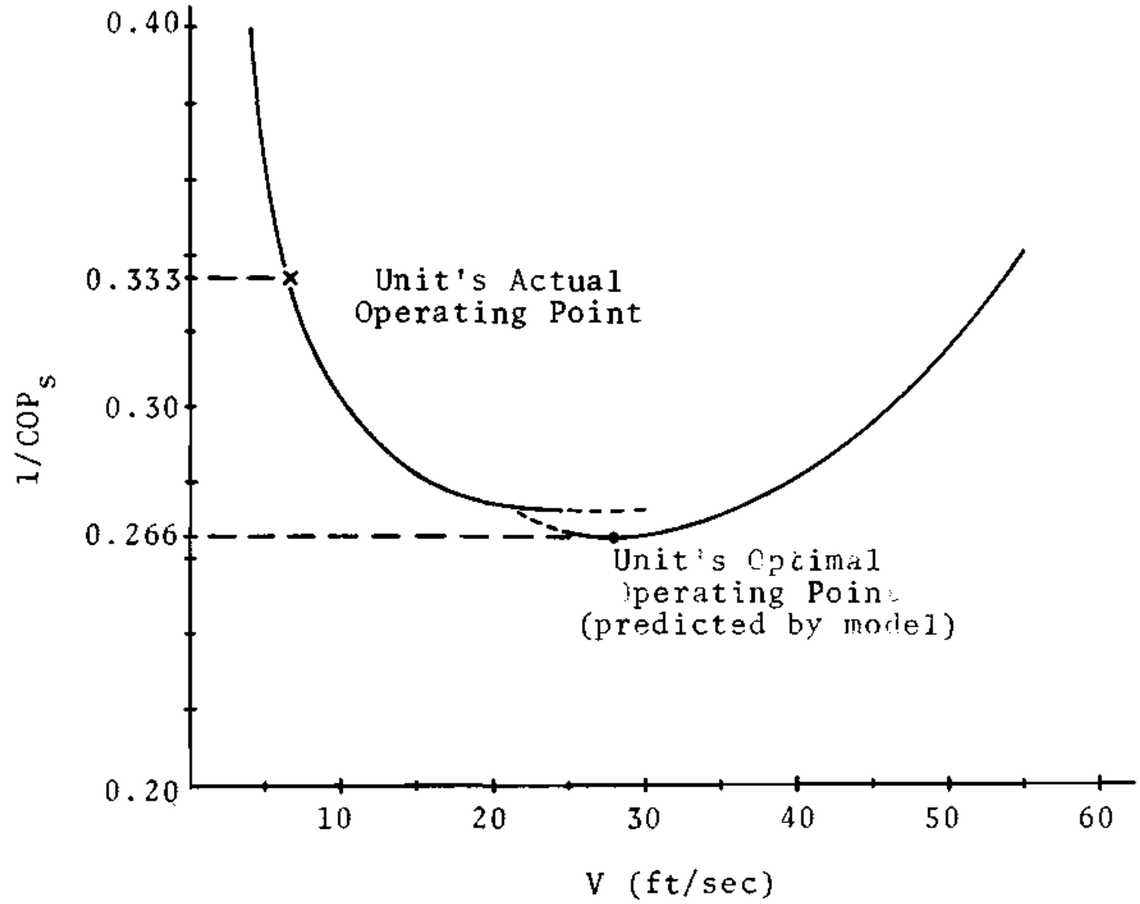

Note: The curve above is generated by the use of Equations (31)-(35) with $A/\dot{Q}_e$, X, and η given in the specifications below and values from Tables 1 and 2.

Specifications for York Unit:
Model CL36
$X = 2.2$ (in); $\eta = 16$ (fins/in);
$A = 5.6$ (ft^2); $\dot{Q}_e = 3.5$ (tons);
$V = 6.6$ (ft/sec)

Figure 22. Velocity Optimization Curve for York Unit

Table 6. Comparison of the Optimal Units with Typical Existing Units

			Lennox Model HS8-411-1FFA				York-Model CL-36			
	Optimal Units Table 5		Unoptimized (V = 10.2)		Optimized* (V_{opt} = 29)		Unoptimized (V = 6.6)		Optimized* (V_{opt} = 28)	
City	C_{oper}	C_T	C_{oper}	C_T	C_{oper}	C_T	C_{oper}	C_T	C_{oper}	C_T
Atlanta	18.31	23.44	22.00	27.38	18.54	23.92	23.53	28.50	18.68	23.65
Boston	9.92	13.39	10.37	15.75	8.74	14.11	11.09	16.05	8.80	13.77
Cleveland	14.70	19.14	16.76	22.14	14.13	19.51	17.93	22.90	14.23	19.20
Dallas	32.57	40.26	43.84	49.22	36.95	42.33	46.90	51.87	37.23	42.20
Minneapolis	12.43	16.43	13.78	19.16	11.61	16.99	14.74	19.71	11.70	16.67
St. Louis	25.78	32.39	33.41	38.80	28.16	33.54	35.74	40.71	28.37	33.34
Washington, D.C.	27.23	34.12	35.73	41.11	30.11	35.49	38.22	43.19	30.34	35.30

Units: V (ft/sec); C_{oper} and C_T (annual $/ton)

*See Figures 21 and 22 for specifications of Lennox and York units. Units are optimized with respect to air velocity only as shown in Figures 21 and 22.

What this suggests is that, given a condenser configuration that is within reason, i.e., a reasonable $A/\dot{Q}_e$, the key parameter is the air velocity and its effect on the system's operating cost. Optimizing the condenser configuration results in much smaller savings. This is borne out by the curves in Appendix D where it is seen that $A/\dot{Q}_e$ can vary rather widely in the region of the optimal $A/\dot{Q}_e$ without having much effect on total annual cost.

As mentioned earlier, air velocities for currently available units typically range from 3 to 8 ft/sec. The results of this study indicate significantly higher velocities are in order. The reduction in operating cost due to higher velocities is very significant. Suppose that an average 10 percent reduction in operating cost is achievable for residential air conditioning. Based on the figures stated in the Introduction, this reduction would amount to a savings of about $1.3 billion/year for the nation as a whole.

The direct benefit to the owner of reducing annual cost is evident. Other less obvious benefits are also involved. Decreasing the electrical consumption, lowers the summer peak load demand on the power generating facilities. This is significant in that the utilities must design their plants with enough reserve capacity to satisfy peak demand periods. Lowering peak demand would allow the utility to increase the load factor and thus supply more energy with the same generating equipment. This would reduce the utilities capital requirements and yield lower energy costs.

This analysis has by no means solved the complete problem. Improvements to the existing model would allow more factors to be taken into account. Specific areas of improvement would be: (1) the capability to evaluate the refrigerant heat transfer coefficient, $\bar{h}_r$, more precisely; (2) including the tube diameter, spacing, and length; (3) accounting for the pressure drop in the tubes; (4) a more precise description of the compressor; and (5) evaluation of those costs and variations in cost neglected in the economic analysis. As the results of this study indicate that significantly higher air velocities ought to be used in A/C units, experimental verification of the $1/COP_s$ expressions as given by Equations (31)-(35) should be undertaken.

A logical extension to the present analysis would involve an evaluation of the evaporator in order to optimize its function. The ideal would be a computer study, accompanied by experimental verification, describing the dynamics of the entire system so that the most cost effective combination of components could be determined.

This study is an example of a class of energy related problems the analysis of which becomes increasingly important as energy costs rise. The rather simple yet effective methodology used here recommends itself to other related problems. It is incumbent upon the engineering community to address itself to such problems.

APPENDICES

APPENDIX A

VELOCITY OPTIMIZATION CURVES FOR VARIOUS CONDENSER CONFIGURATIONS

Note: The discontinuities in the velocity optimization curves occur where the change is made from the laminar solution, Equations (31) and (32), to the turbulent solution, Equations (34) and (35). The transition from laminar to turbulent flow is assumed to occur at a Reynolds number of 1500. Tables 1 and 2 (Chapter II) give nominal values for quantities in the equations mentioned above.

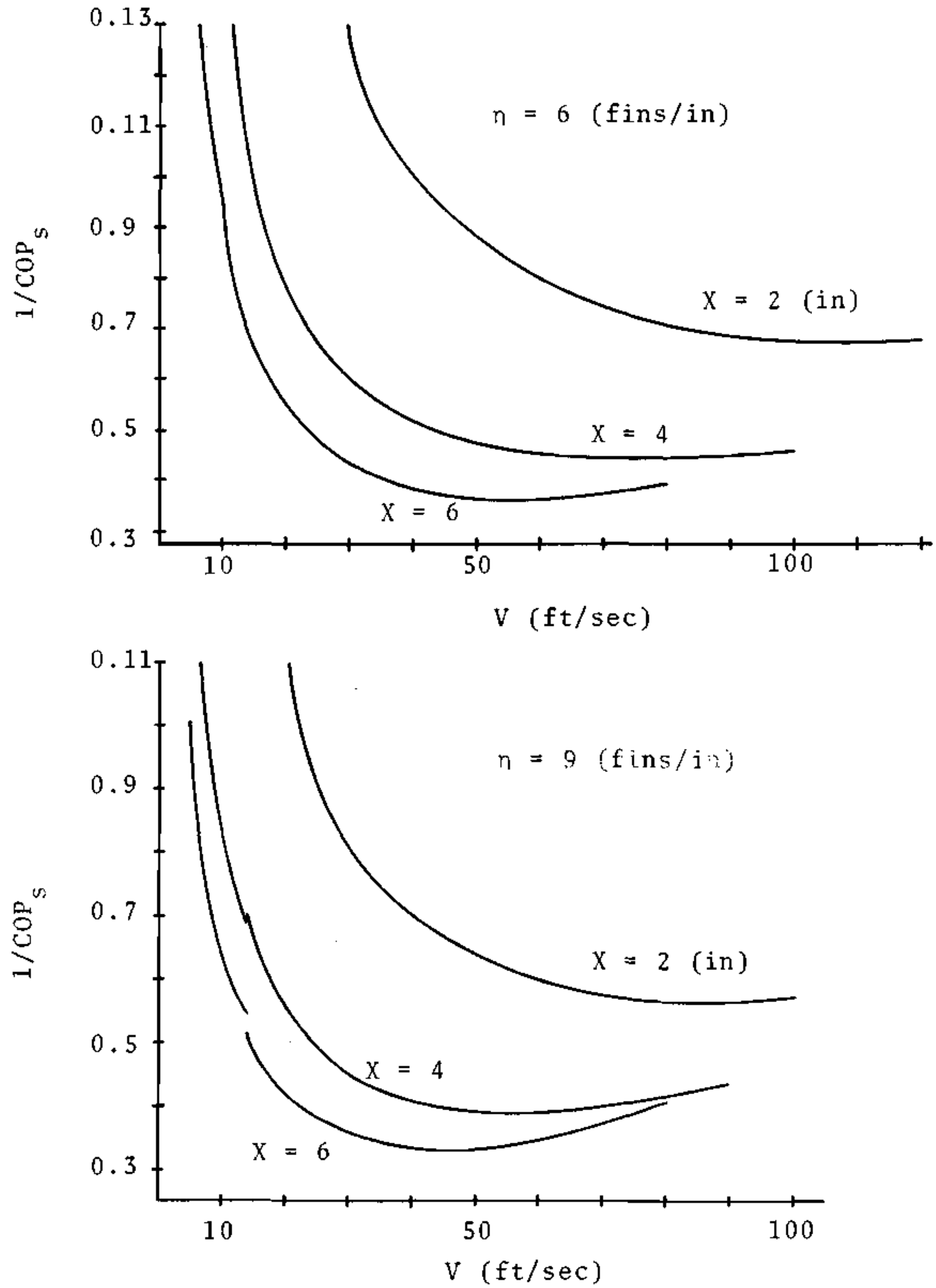

Figure 23. Velocity Optimization Curves for $A/\dot{Q}_e = 0.5$ (ft^2/ton); $\eta = 6$ and 9 (fins/in)

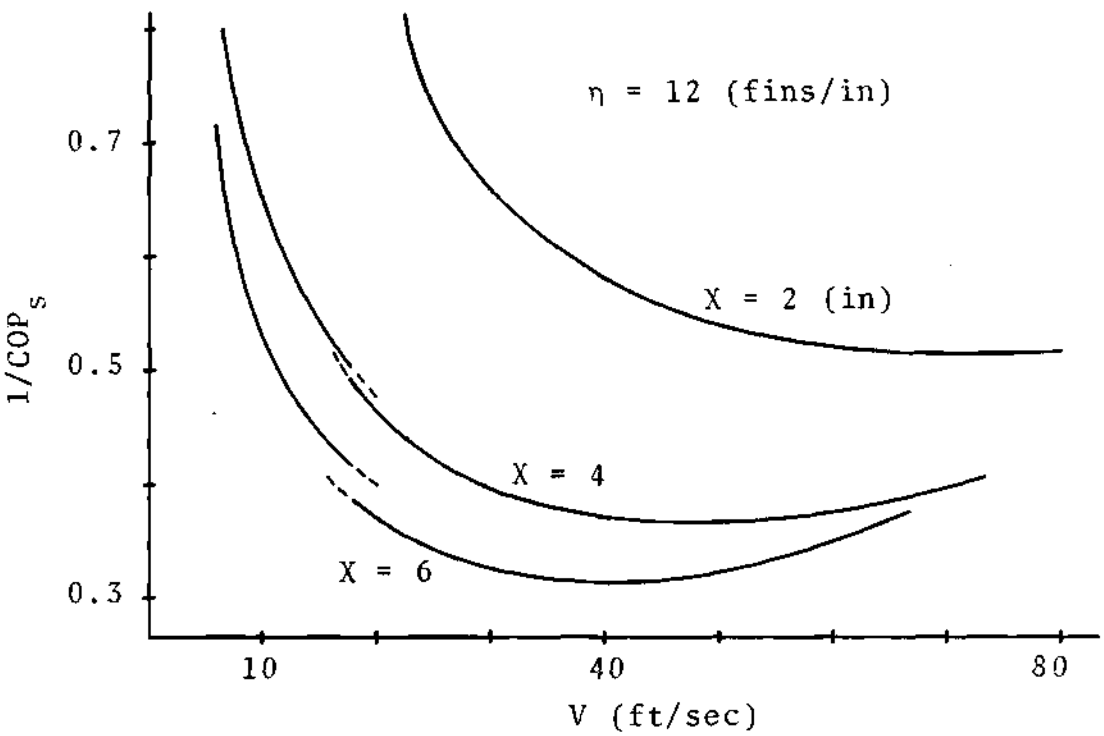

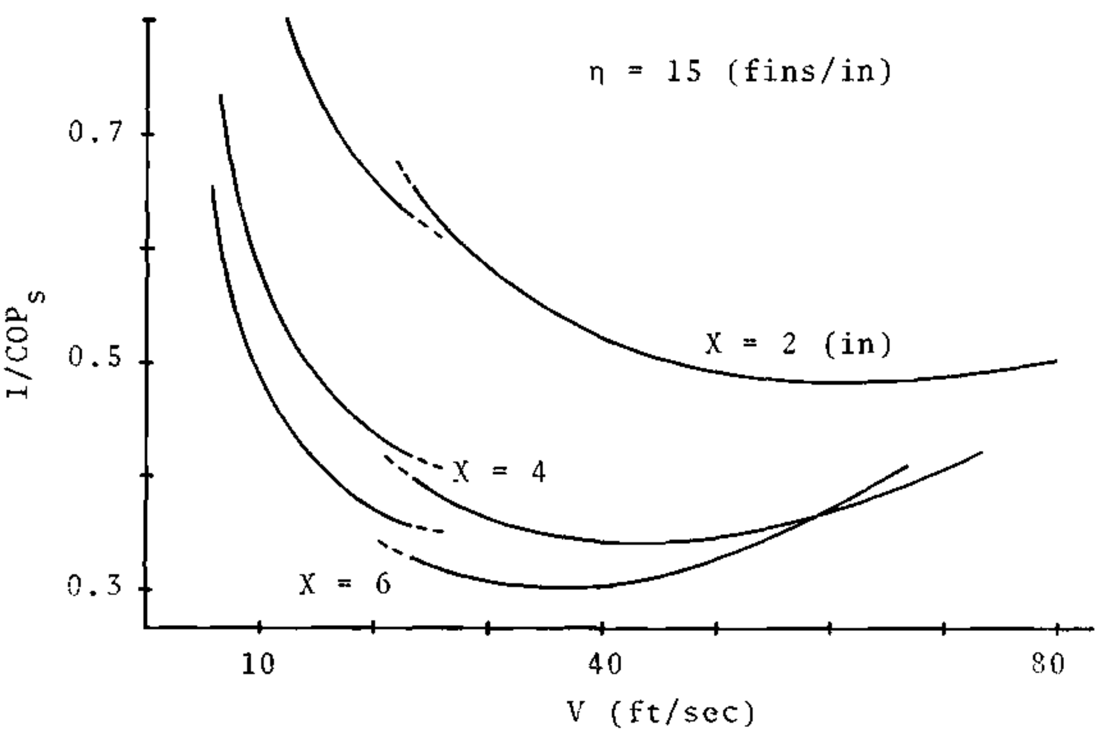

Figure 24. Velocity Optimization Curves for $A/\dot{Q}_e = 0.5$ (ft^2/ton); $\eta = 12$ and 15 (fins/in)

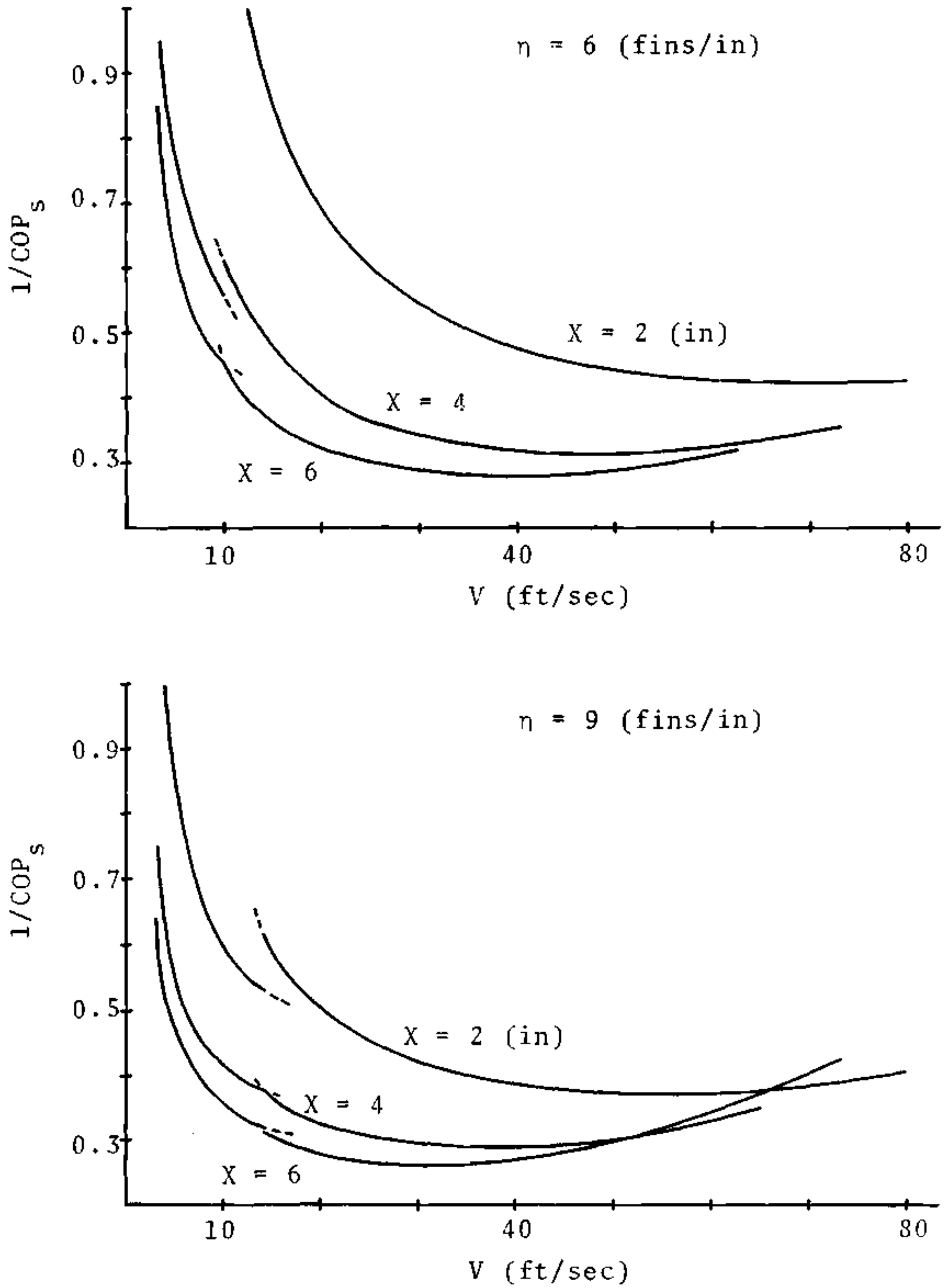

Figure 25. Velocity Optimization Curves for $A/\dot{Q}_e = 1.0$ (ft^2/ton); η = 6 and 9 (fins/in)

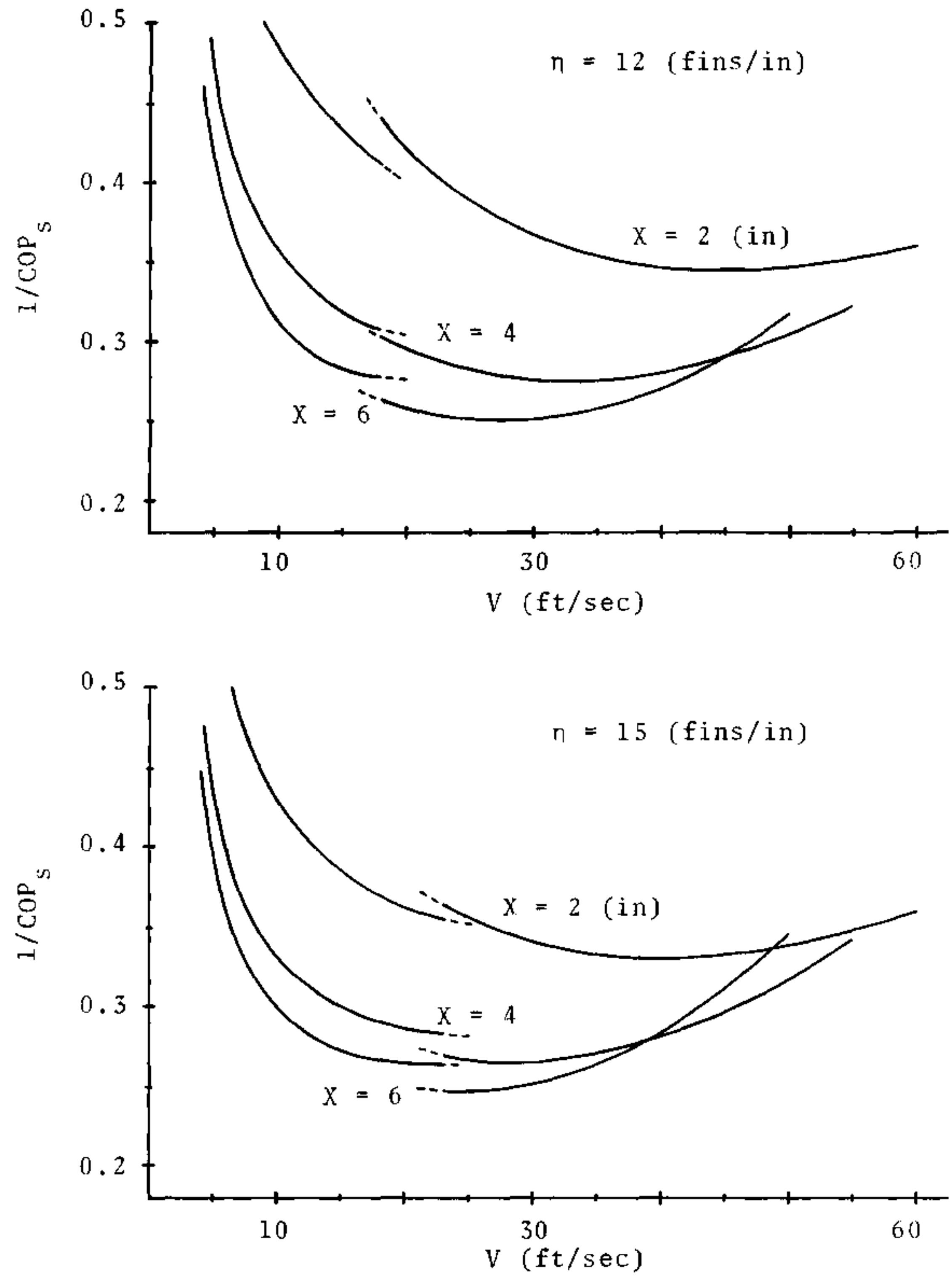

Figure 26. Velocity Optimization Curves for $A/\dot{Q}_e = 1.0$ (ft^2/ton); η = 12 and 15 (fins/in)

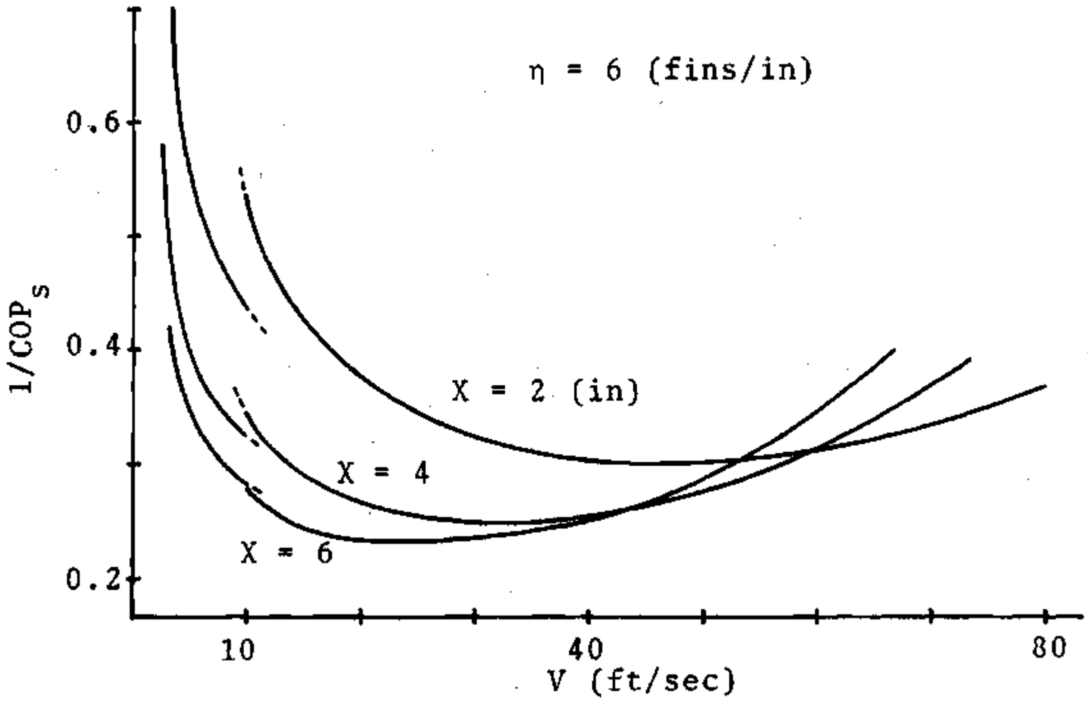

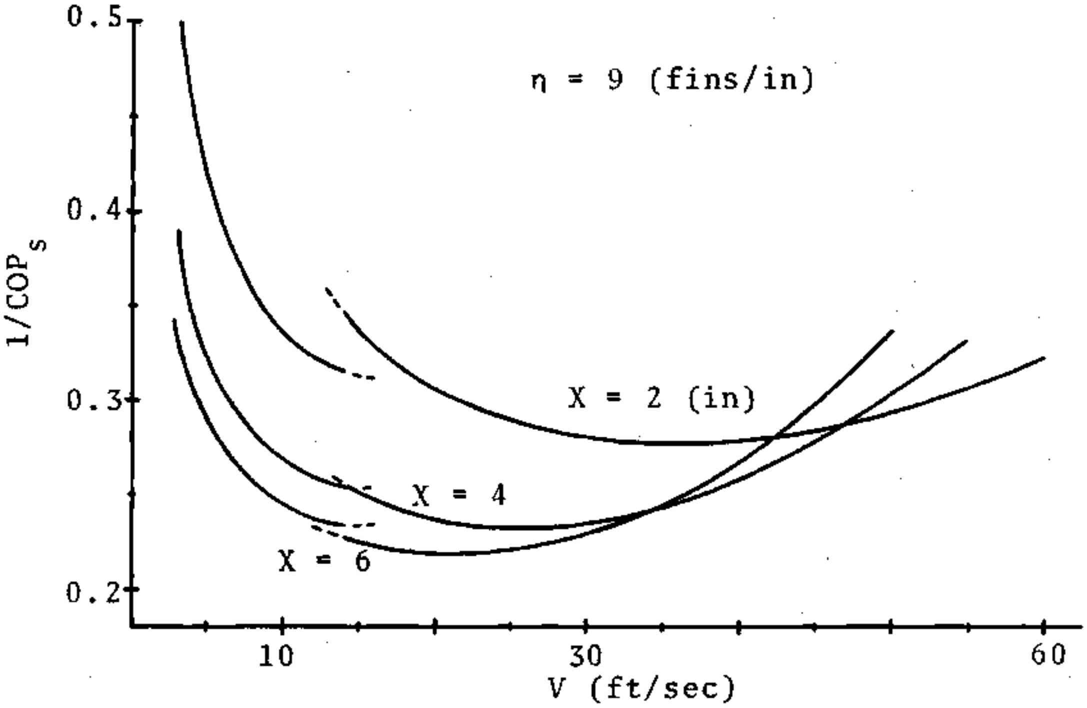

Figure 27. Velocity Optimization Curves for $A/\dot{Q}_e = 2.0$ (ft^2/ton); $\eta = 6$ and 9 (fins/in)

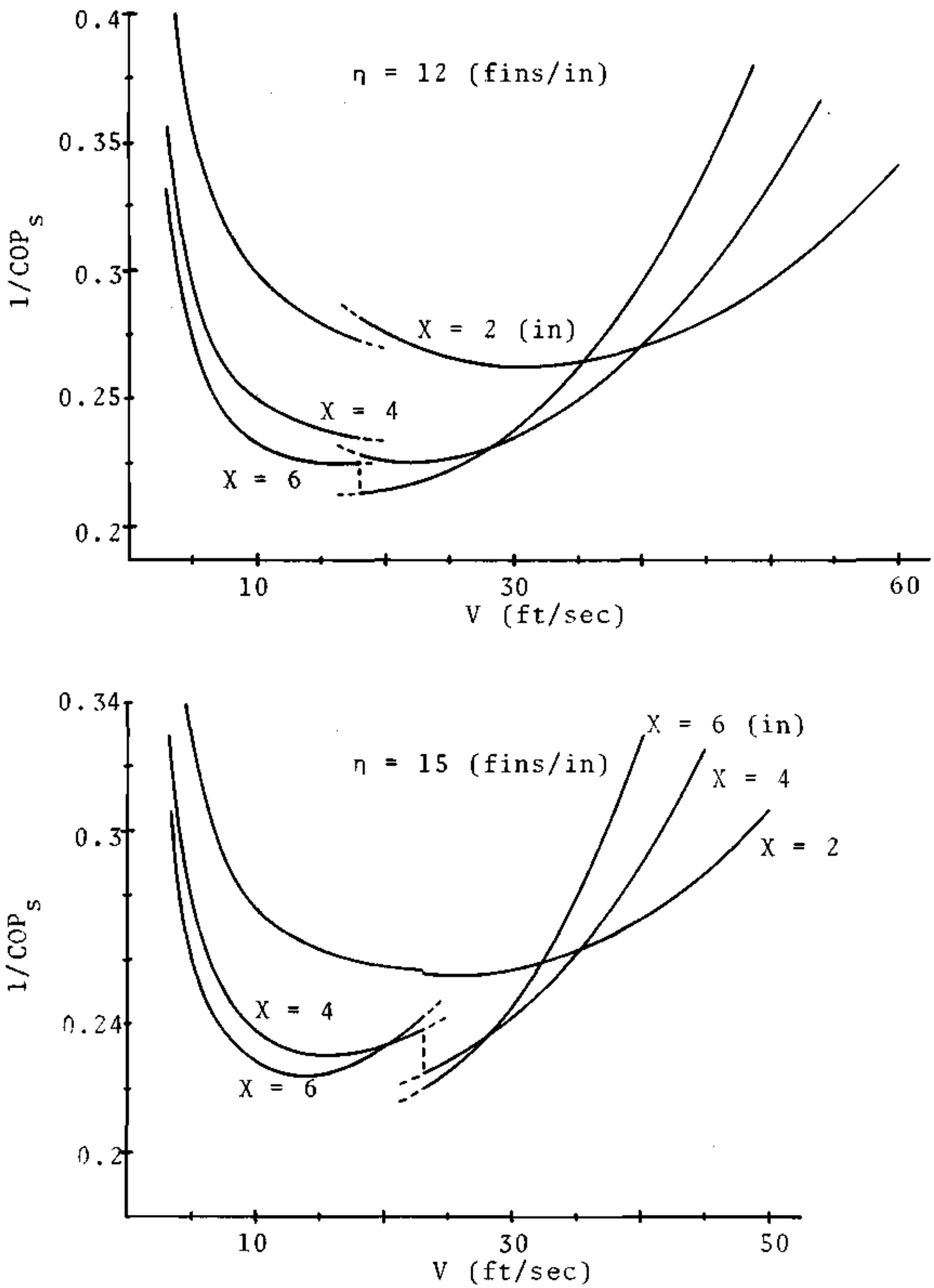

Figure 28. Velocity Optimization Curves for $A/\dot{Q}_e = 2.0$ (ft^2/ton); η = 12 and 15 (fins/in)

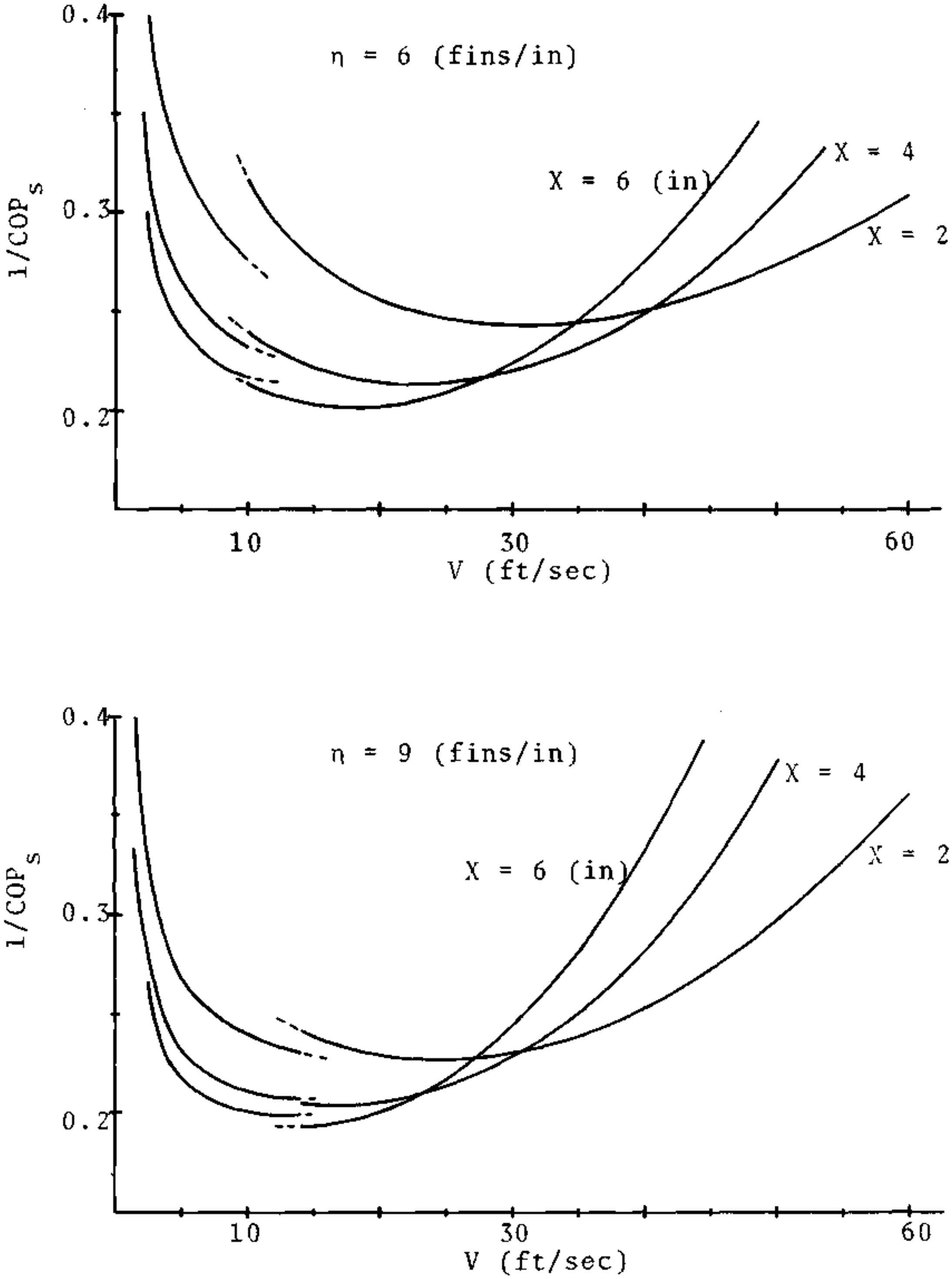

Figure 29. Velocity Optimization Curves for $A/\dot{Q}_e = 4.0$ (ft^2/ton); η = 6 and 9 (fins/in)

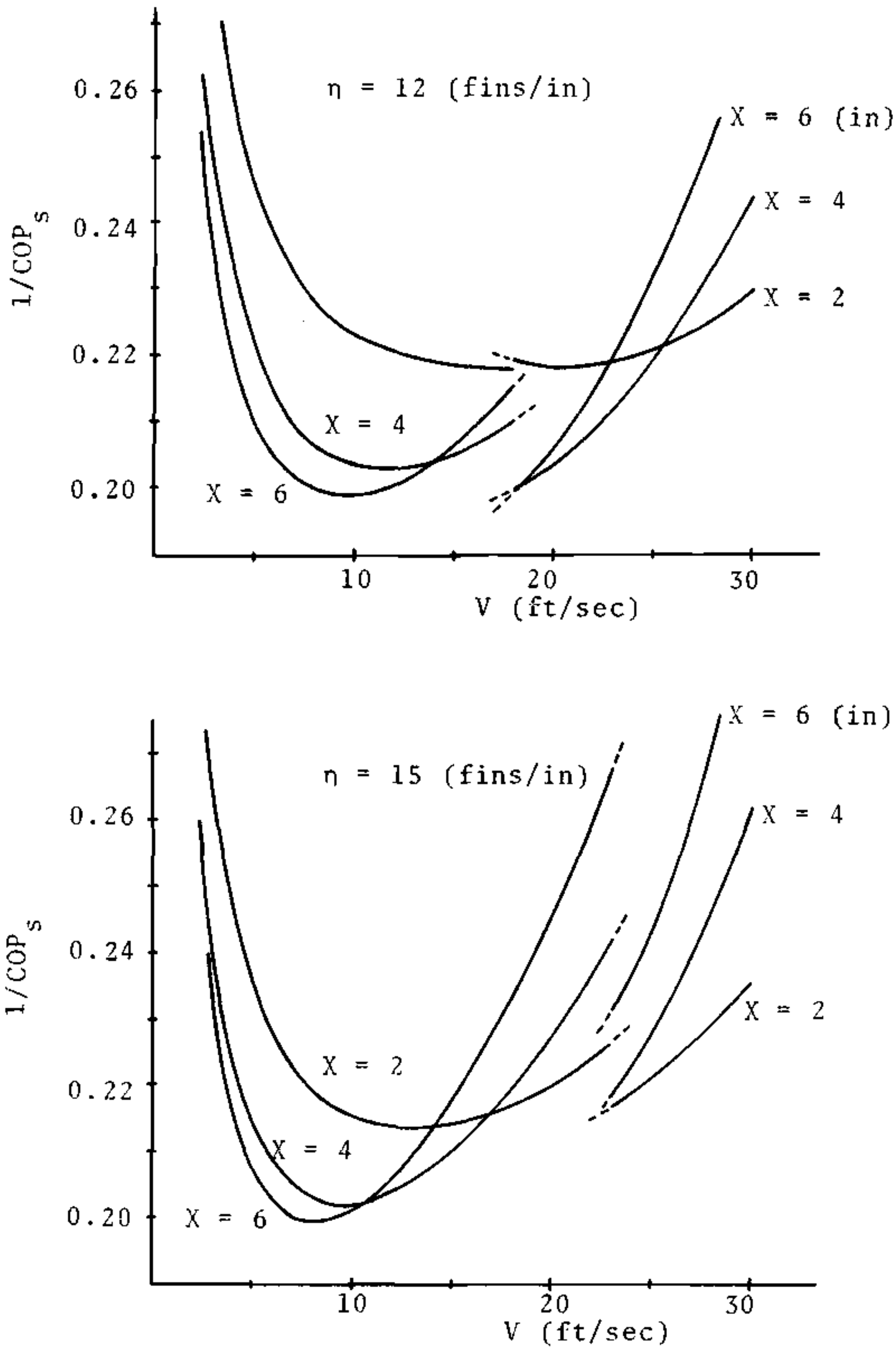

Figure 30. Velocity Optimization Curves for $A/\dot{Q}_e = 4.0$ (ft^2/ton); $\eta = 12$ and 15 (fins/in)

APPENDIX B

OPTIMAL VELOCITY CURVES

Note: The following curves are generated by plotting the air velocities, V (ft/sec), given by the saddle points of the curves in Appendix A for a fixed number of fins, η (fins/in), and condenser depth, X (in).

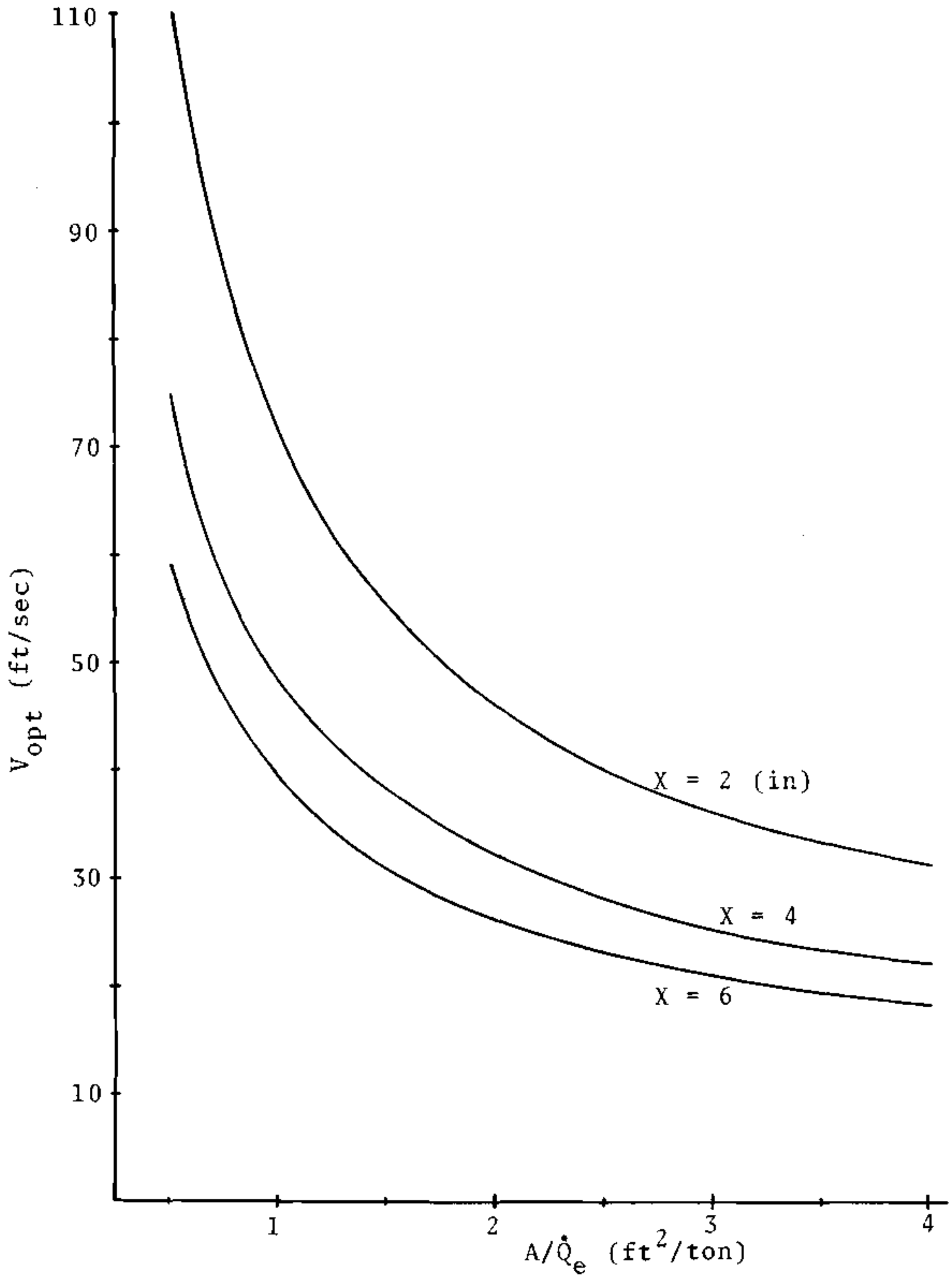

Figure 31. Optimal Velocity versus $A/\dot{Q}_e$ for η = 6 (fins/in)

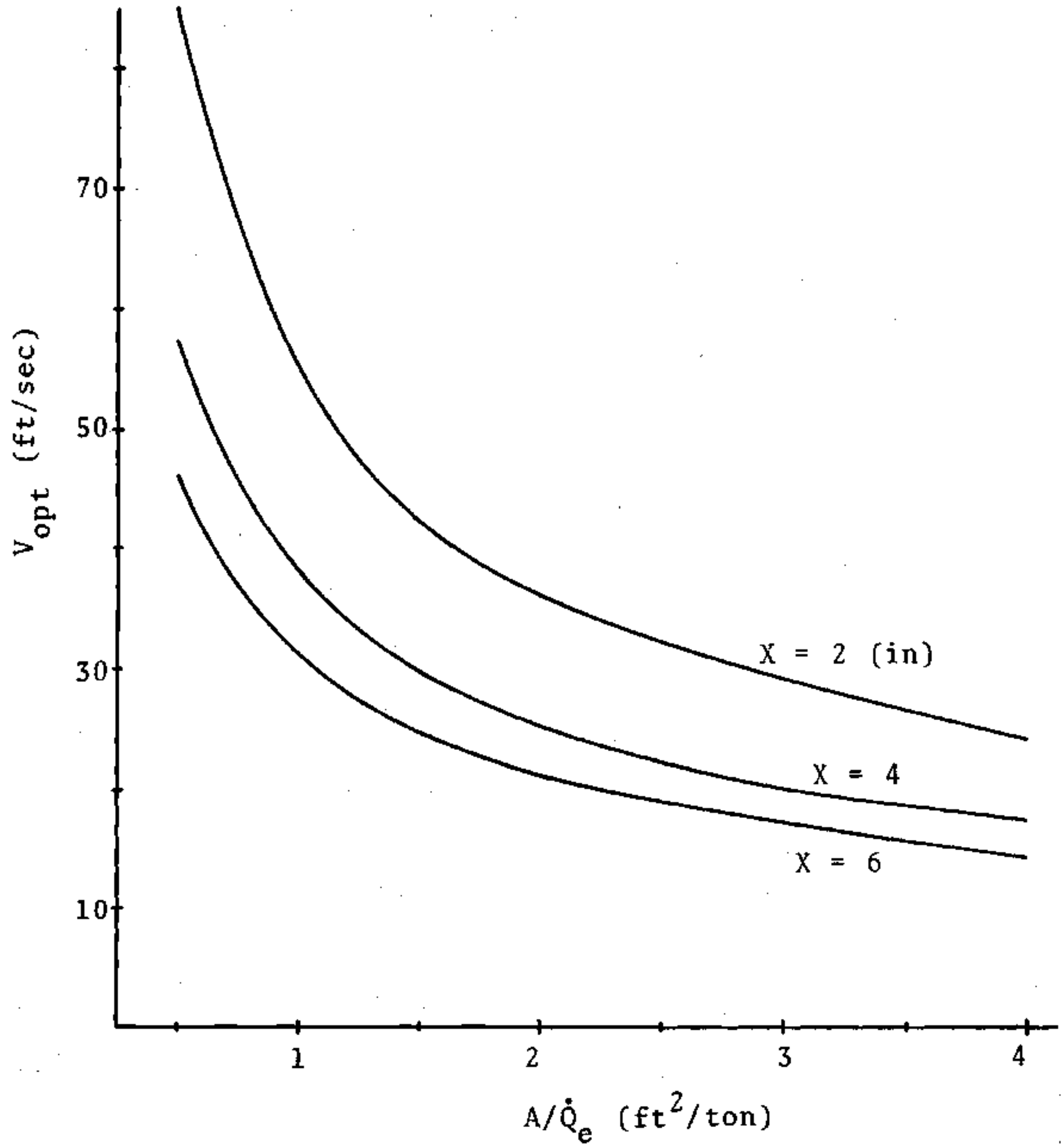

Figure 32. Optimal Velocity versus $A/\dot{Q}_e$ for $\eta = 9$ (fins/in)

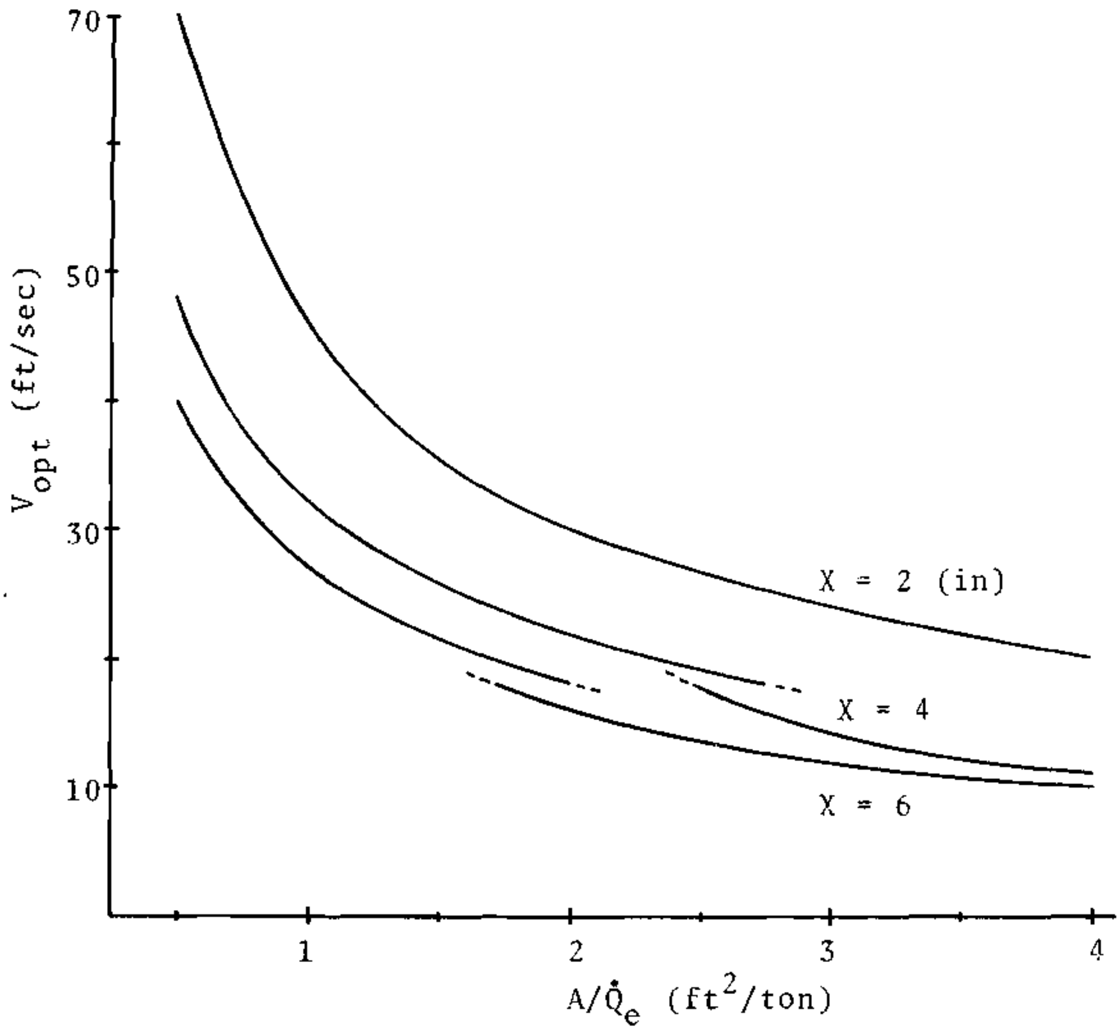

Note: The breaks in the curves occur at a Reynolds number of 1500 where the change is made from the laminar to turbulent solution.

Figure 33. Optimal Velocity versus $A/\dot{Q}_e$ for η = 12 (fins/in)

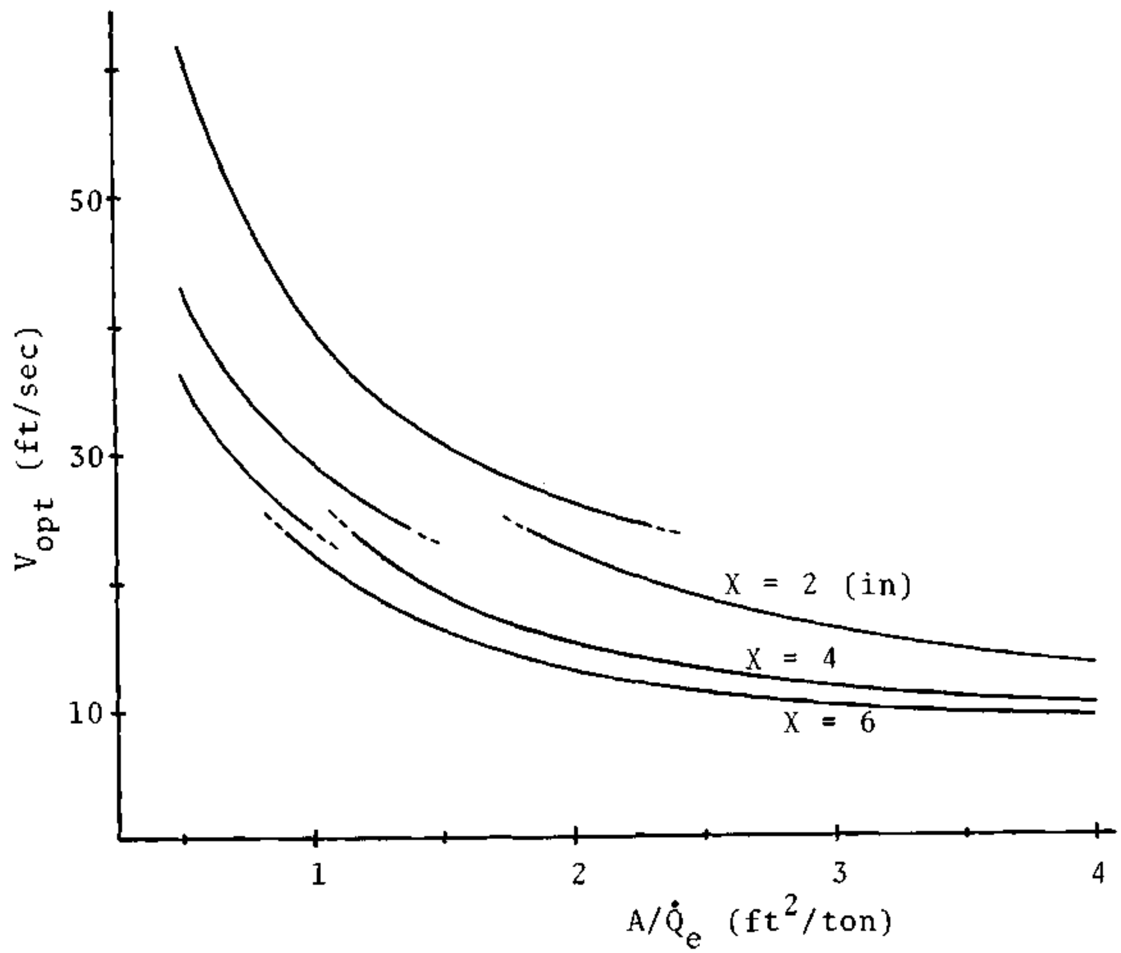

Note: The breaks in the curves occur at a Reynolds number of 1500 where the change is made from the laminar to turbulent solution.

Figure 34. Optimal Velocity versus $A/\dot{Q}_e$ for η = 15 (fins/in)

APPENDIX C

SYSTEM COEFFICIENT OF PERFORMANCE AT THE OPTIMAL VELOCITY

Note: The following curves are generated by plotting the system coefficient of performance, $1/COP_s$, given by the saddle points of the curves in Appendix A for a fixed number of fins, η (fins/in), and condenser depth, X (in).

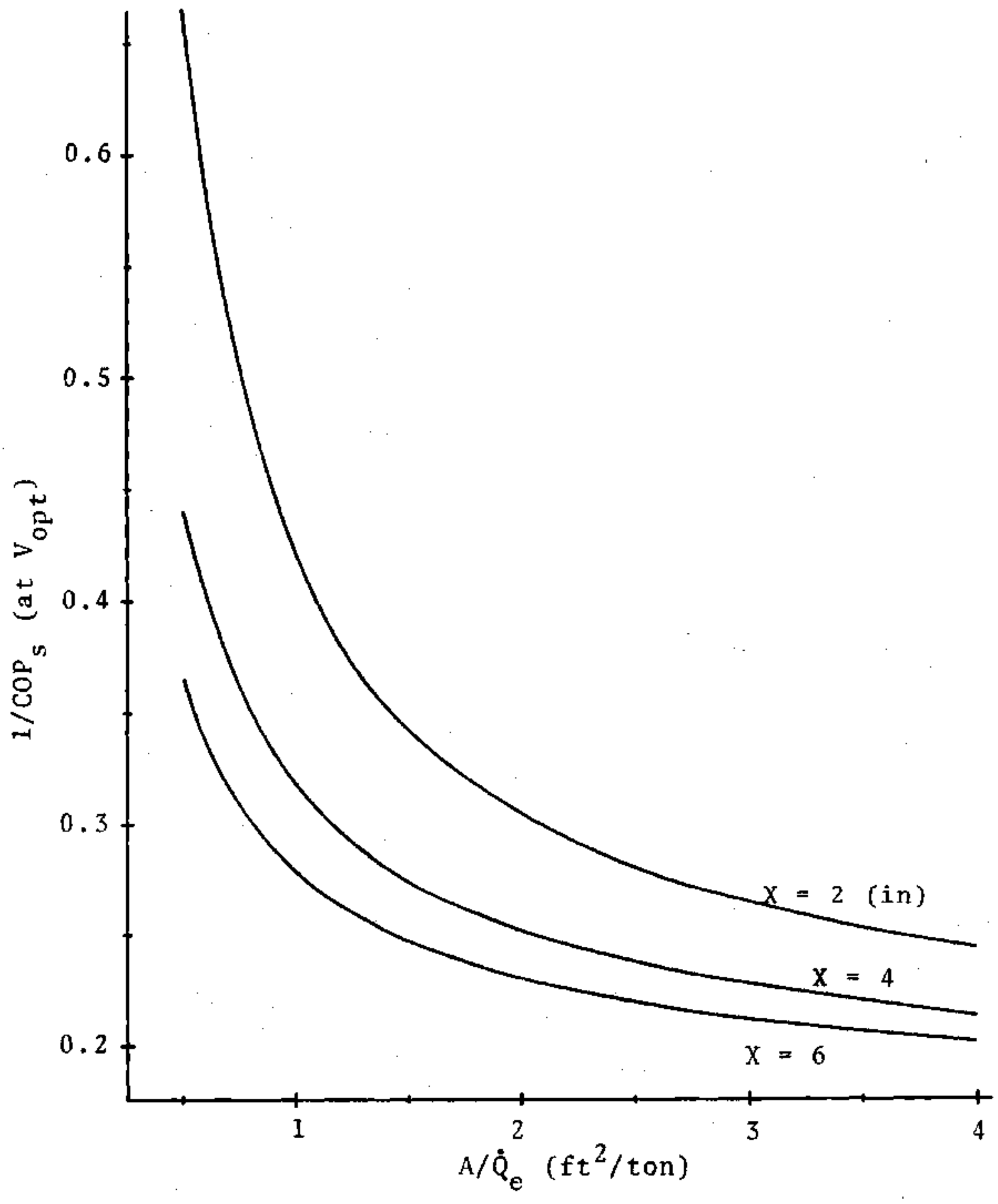

Figure 35. System Coefficient of Performance at V_{opt} versus $A/\dot{Q}_e$ for η = 6 (fins/in)

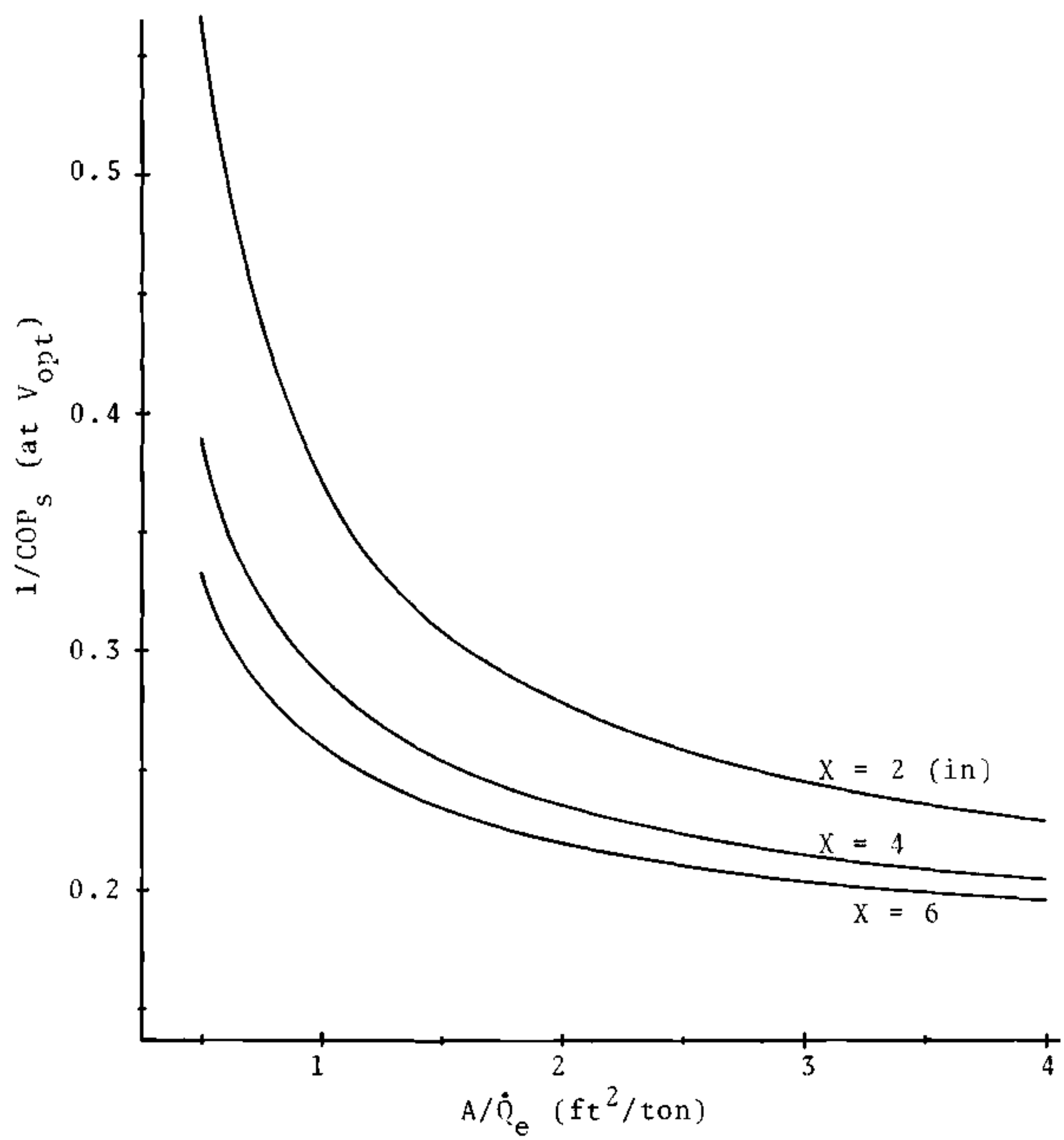

Figure 36. System Coefficient of Performance at V_{opt} versus $A/\dot{Q}_e$ for η = 9 (fins/in)

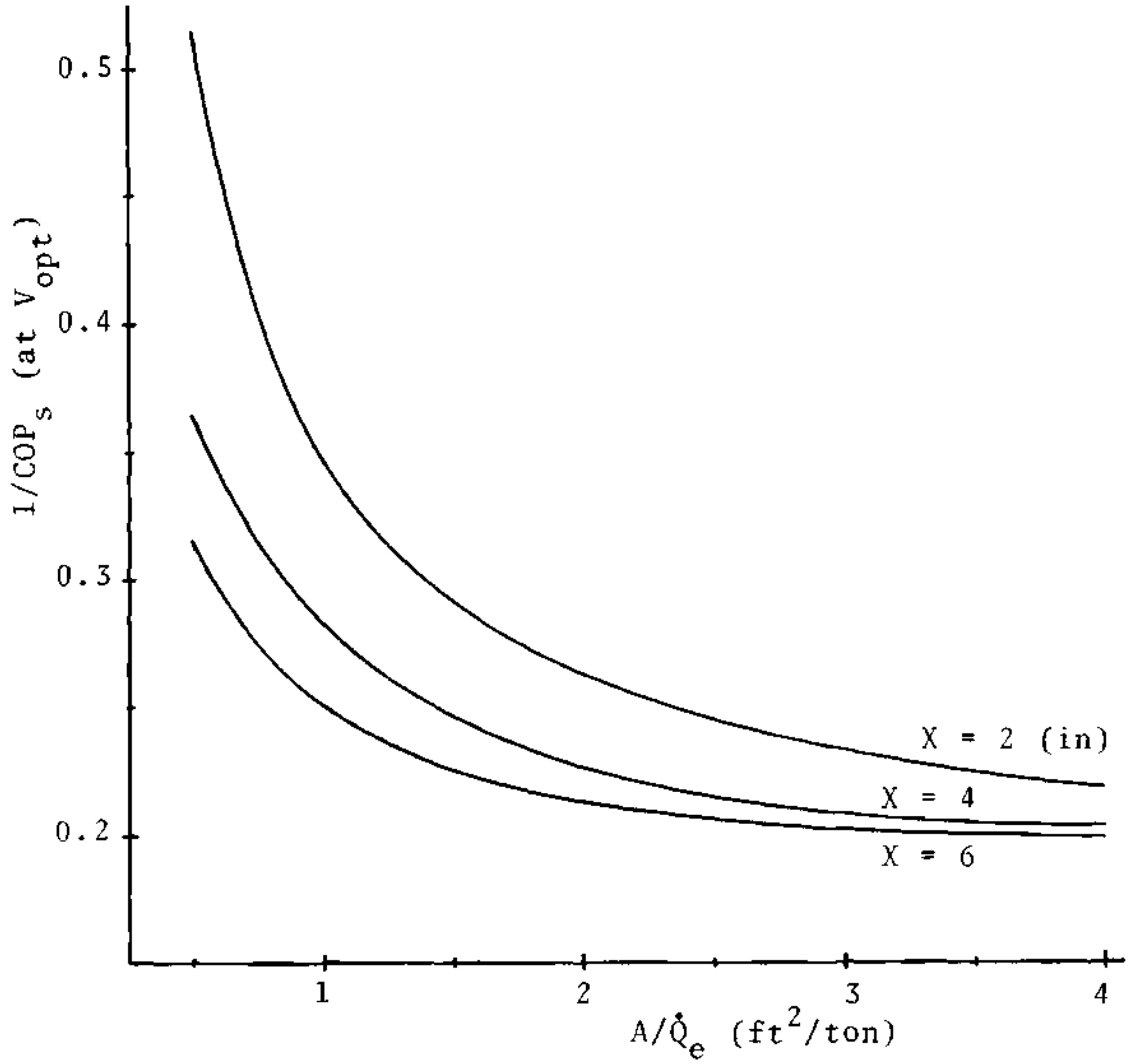

Figure 37. System Coefficient of Performance at V_{opt} versus $A/\dot{Q}_e$ for $\eta = 12$ (fins/in)

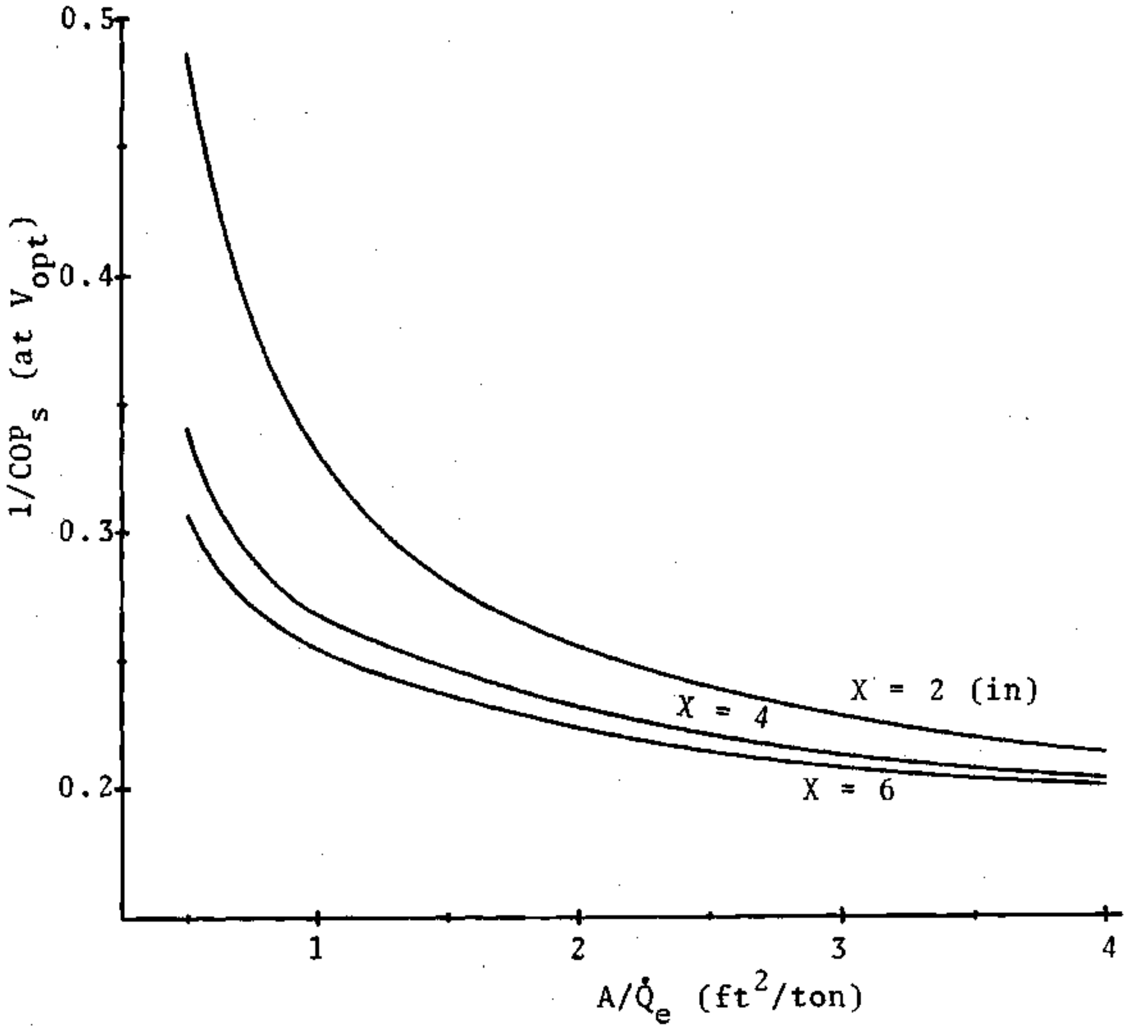

Figure 38. System Coefficient of Performance at V_{opt} versus $A/\dot{Q}_e$ for η = 15 (fins/in)

APPENDIX D

TOTAL ANNUAL COST FOR VARYING ANNUAL HOURS OF OPERATION AND ENERGY COSTS

Note: Total annual cost, C_T, is the sum of the operating cost at V_{opt} and the amortized incremental cost of the condenser coil all on a per ton basis. The annual hours of operation and energy cost have been combined. Thus, $1.5x10^3$ (¢/kw-yr) equals 500 (hr/yr) at 3 (¢/kw-hr) or 750 (hr/yr) at 2 (¢/kw-hr), etc. These curves result from the use of Equation (45) and (31)-(35) with Tables 1 and 2.

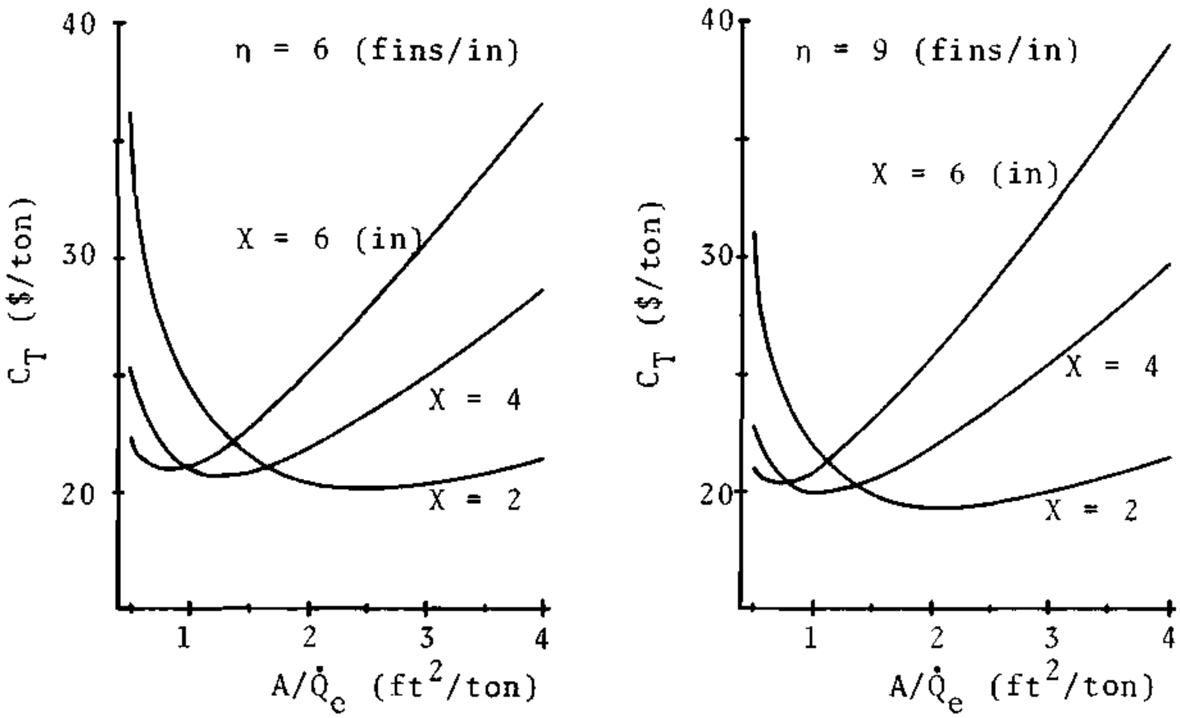

Figure 39. Total Annual Cost versus $A/\dot{Q}_e$ for 1.5×10^3 (¢/kw-yr); η = 6 and 9 (fins/in)

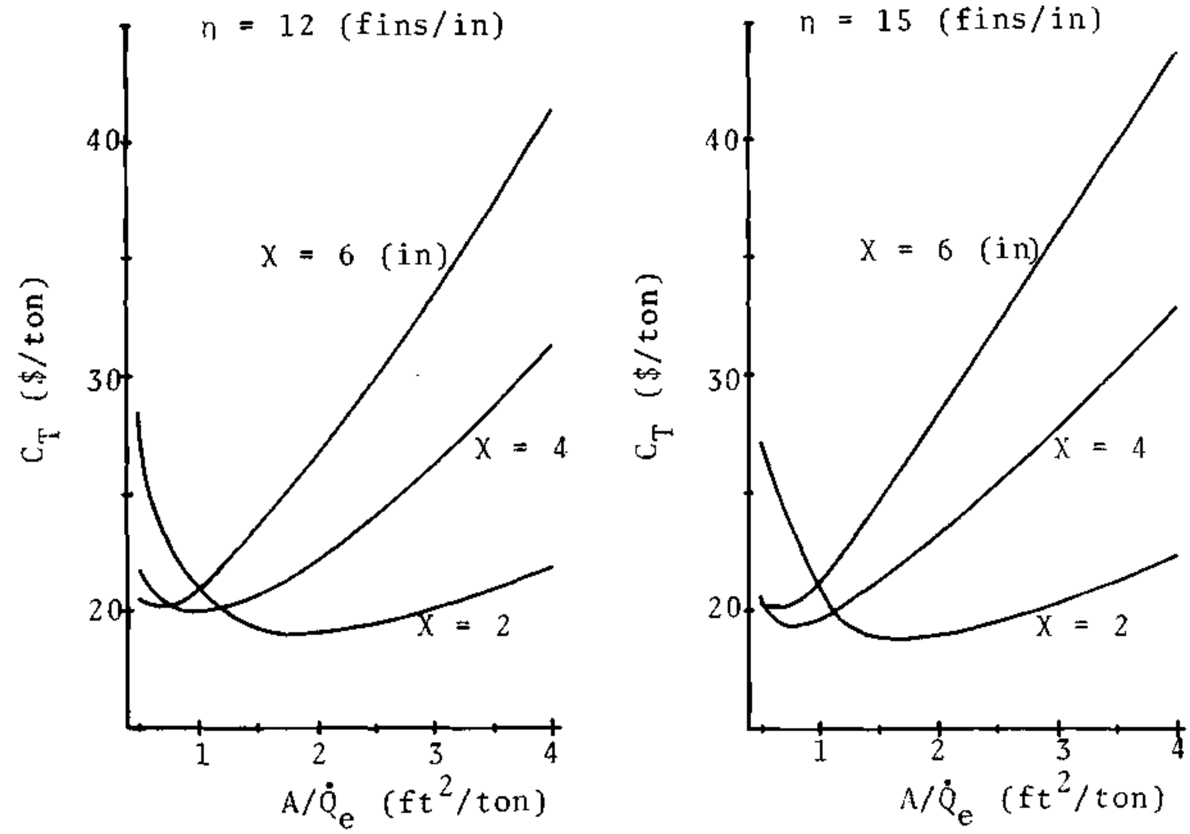

Figure 40. Total Annual Cost versus $A/\dot{Q}_e$ for 1.5×10^3 (¢/kw-yr); η = 12 and 15 (fins/in)

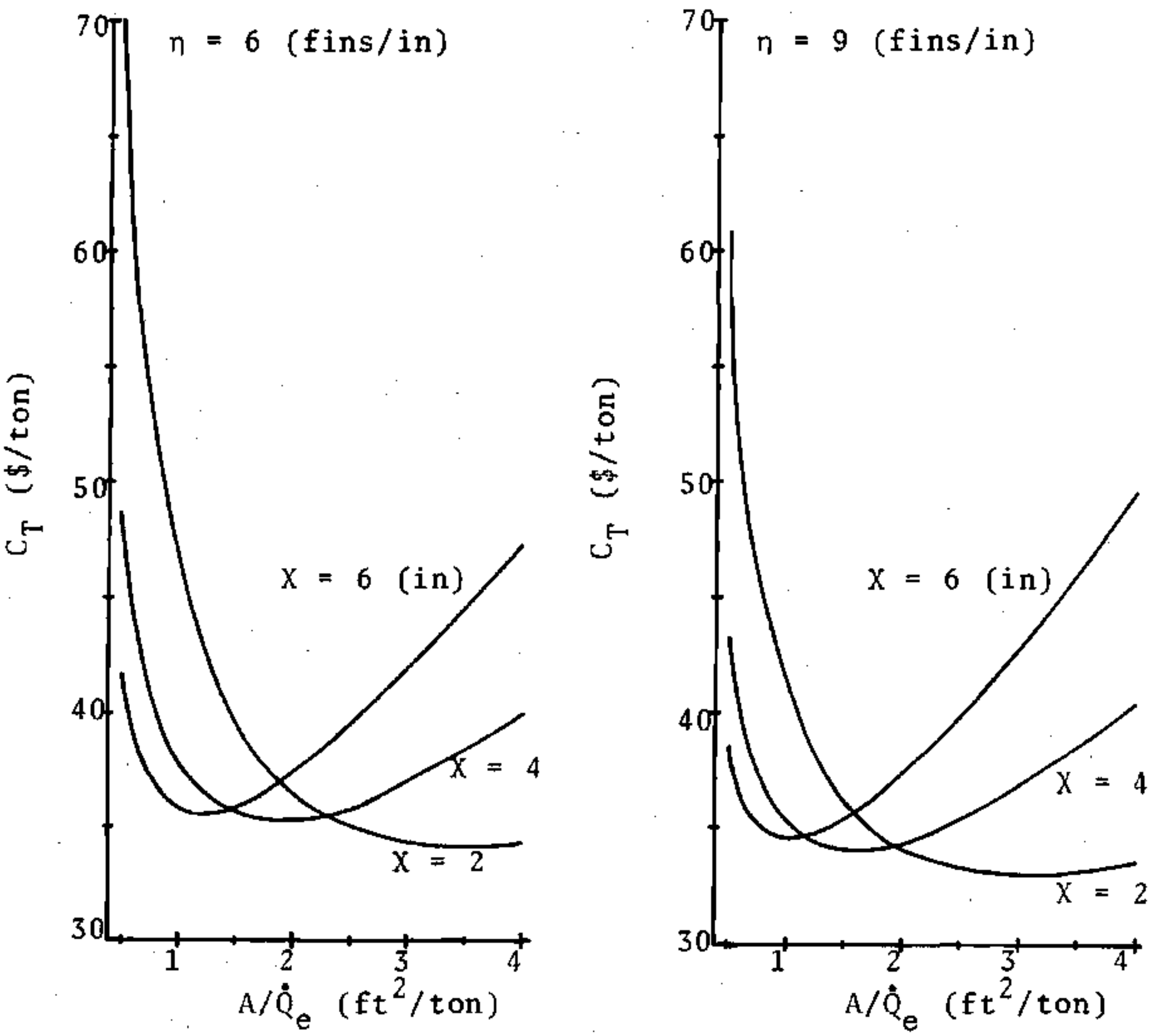

Figure 41. Total Annual Cost versus $A/\dot{Q}_e$ for 3.0×10^3 (¢/kw-yr); η = 6 and 9 (fins/in)

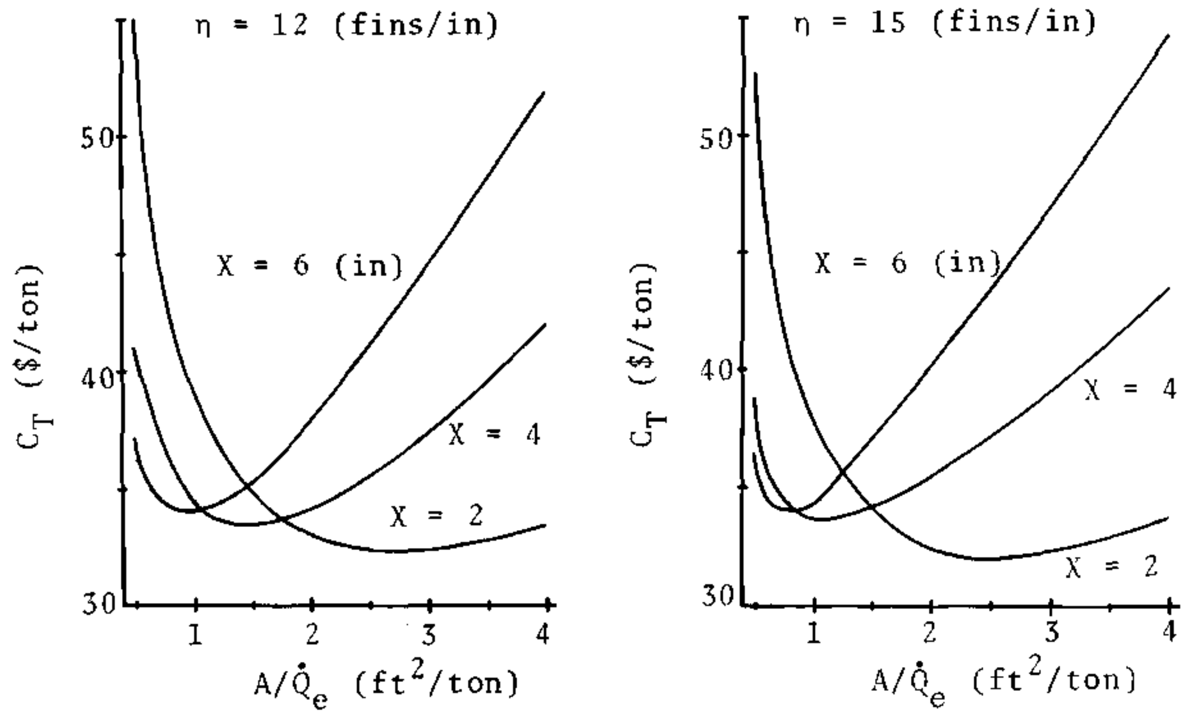

Figure 42. Total Annual Cost versus A/$\dot{Q}_e$ for 3.0×10^3 (¢/kw-yr); η = 12 and 15 (fins/in)

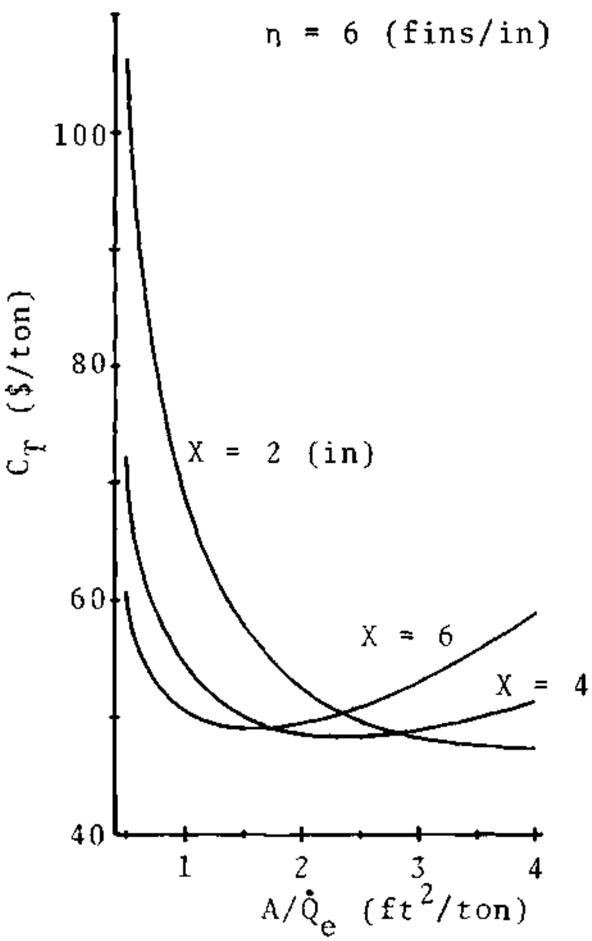

Figure 43. Total Annual Cost versus $A/\dot{Q}_e$ for $4.5\text{x}10^3$ (¢/kw-yr); η = 6 and 9 (fins/in)

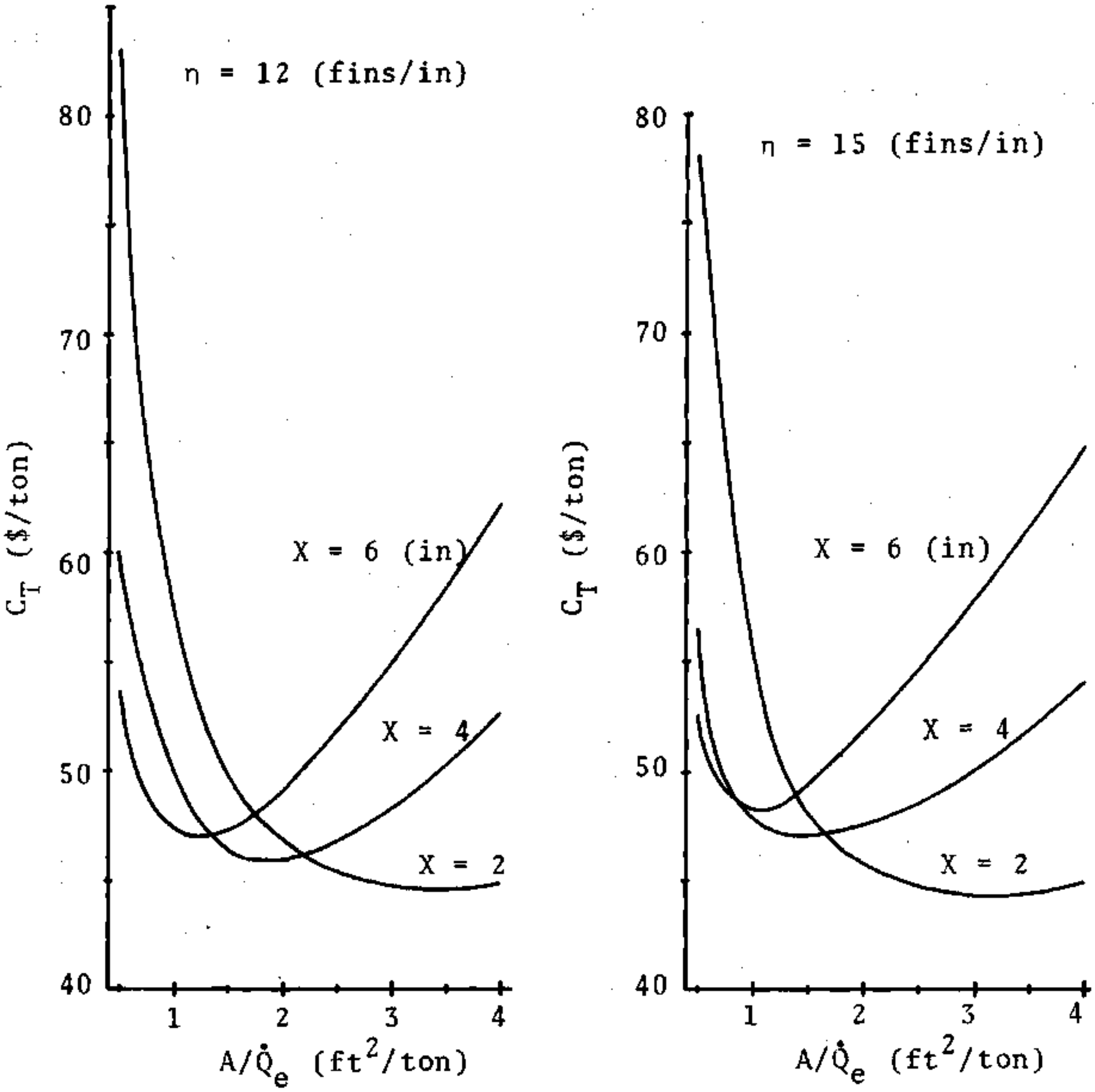

Figure 44. Total Annual Cost versus $A/\dot{Q}_e$ for 4.5×10^3 (¢/kw-yr); η = 12 and 15 (fins/in)

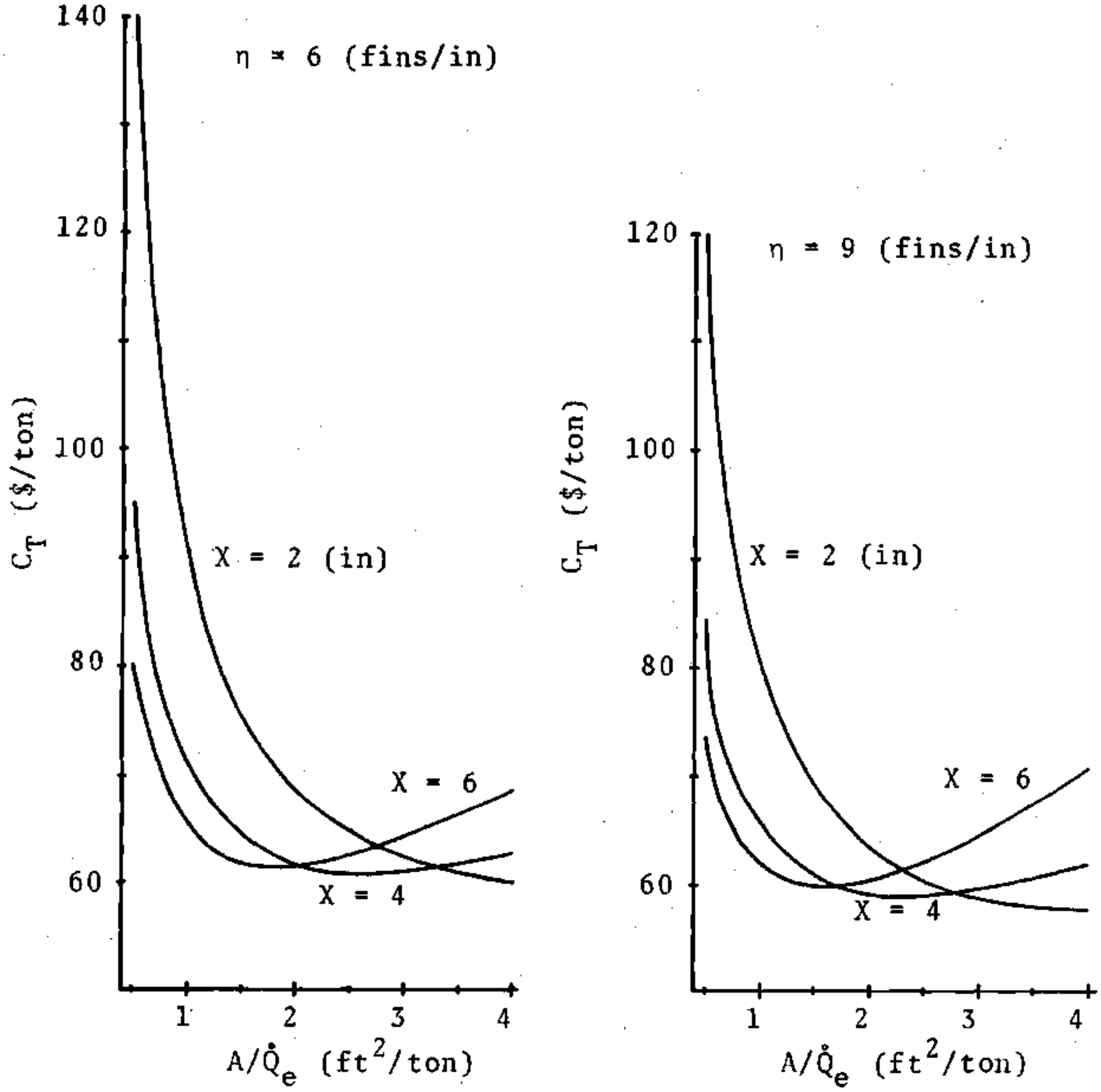

Figure 45. Total Annual Cost versus $A/\dot{Q}_e$ for 6.0×10^3 (¢/kw-yr); η = 6 and 9 (fins/in)

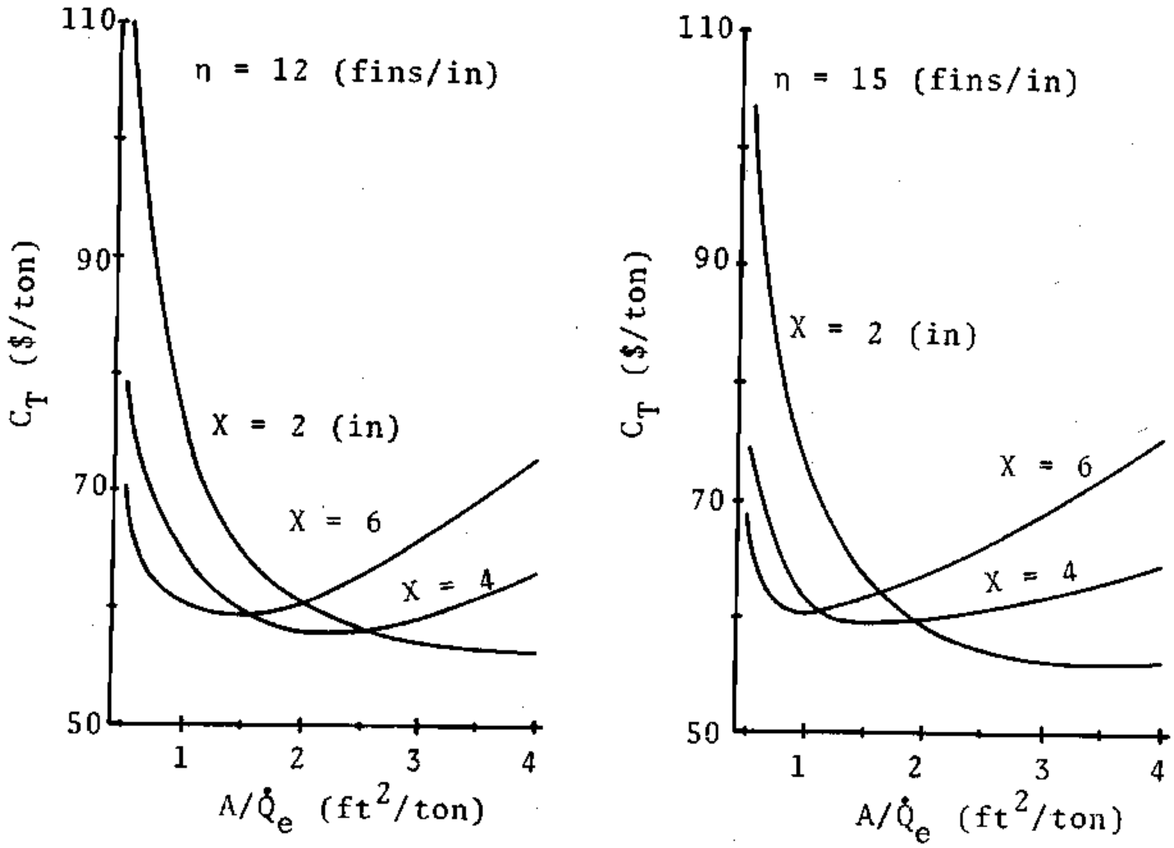

Figure 46. Total Annual Cost versus $A/\dot{Q}_e$ for 6.0×10^3 (¢/kw-yr); η = 12 and 15 (fins/in)

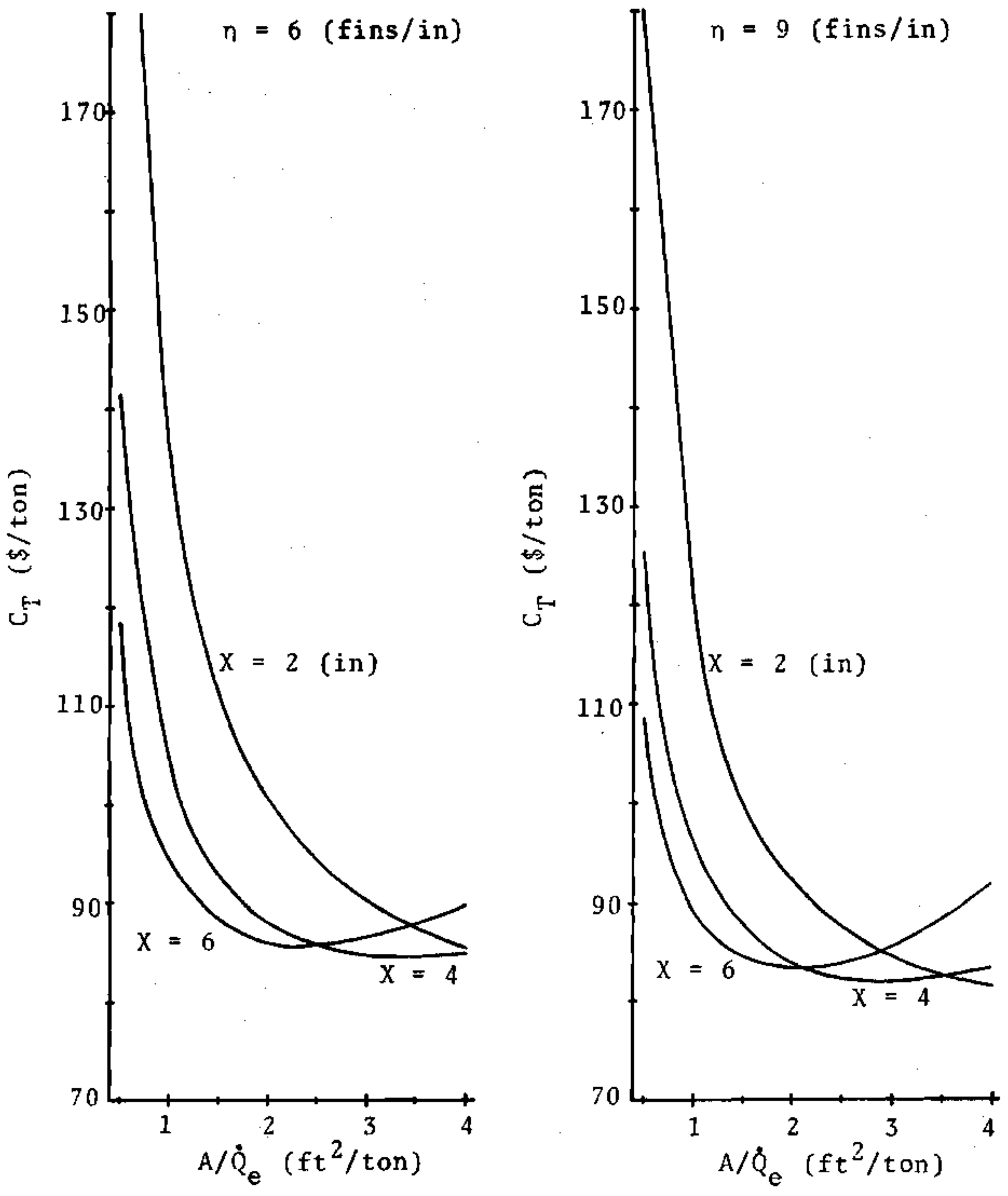

Figure 47. Total Annual Cost versus $A/\dot{Q}_e$ for 9.0×10^3 (¢/kw-yr); η = 6 and 9 (fins/in)

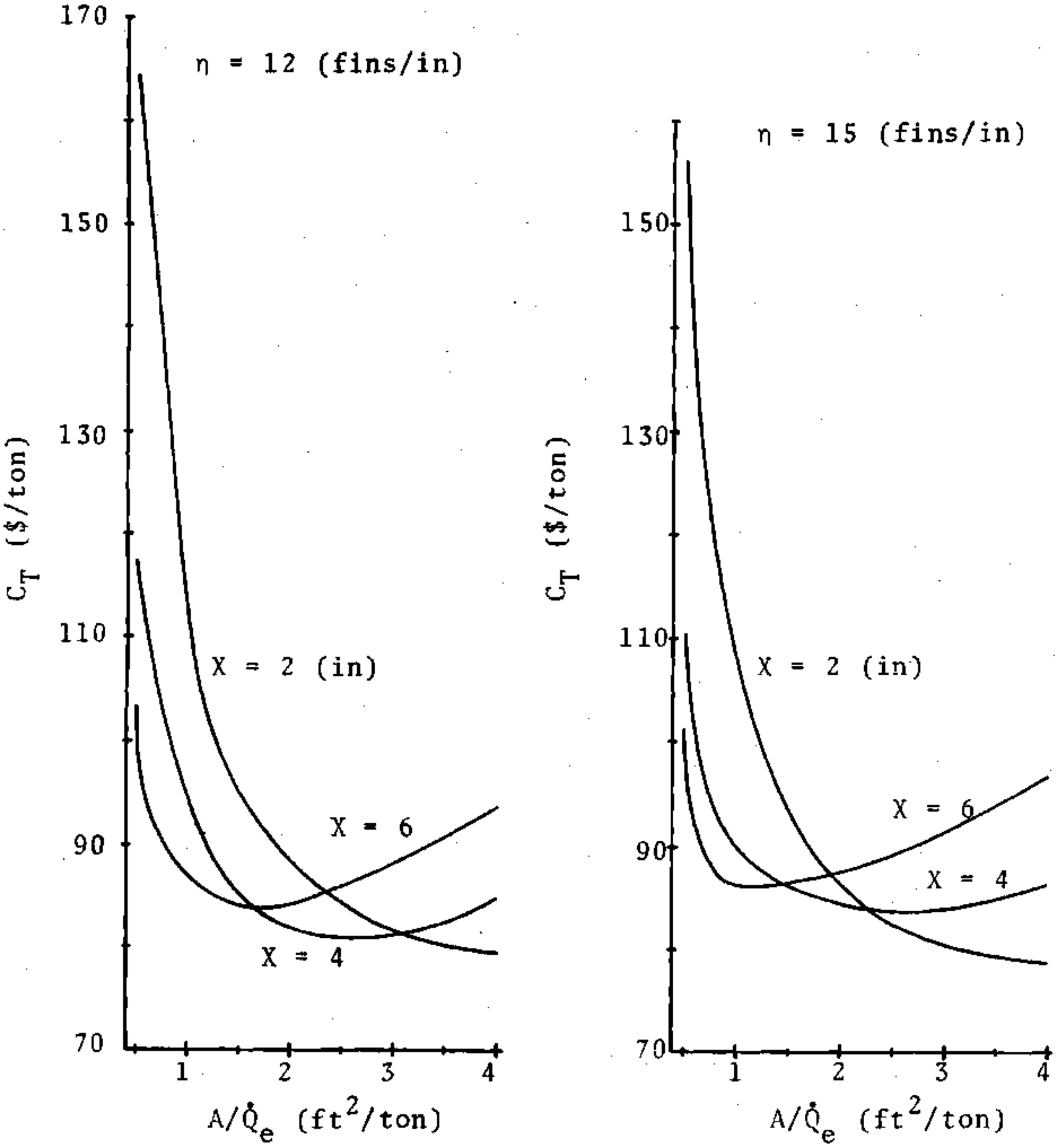

Figure 48. Total Annual Cost versus $A/\dot{Q}_e$ for 9.0×10^3 (¢/kw-yr); η = 12 and 15 (fins/in)

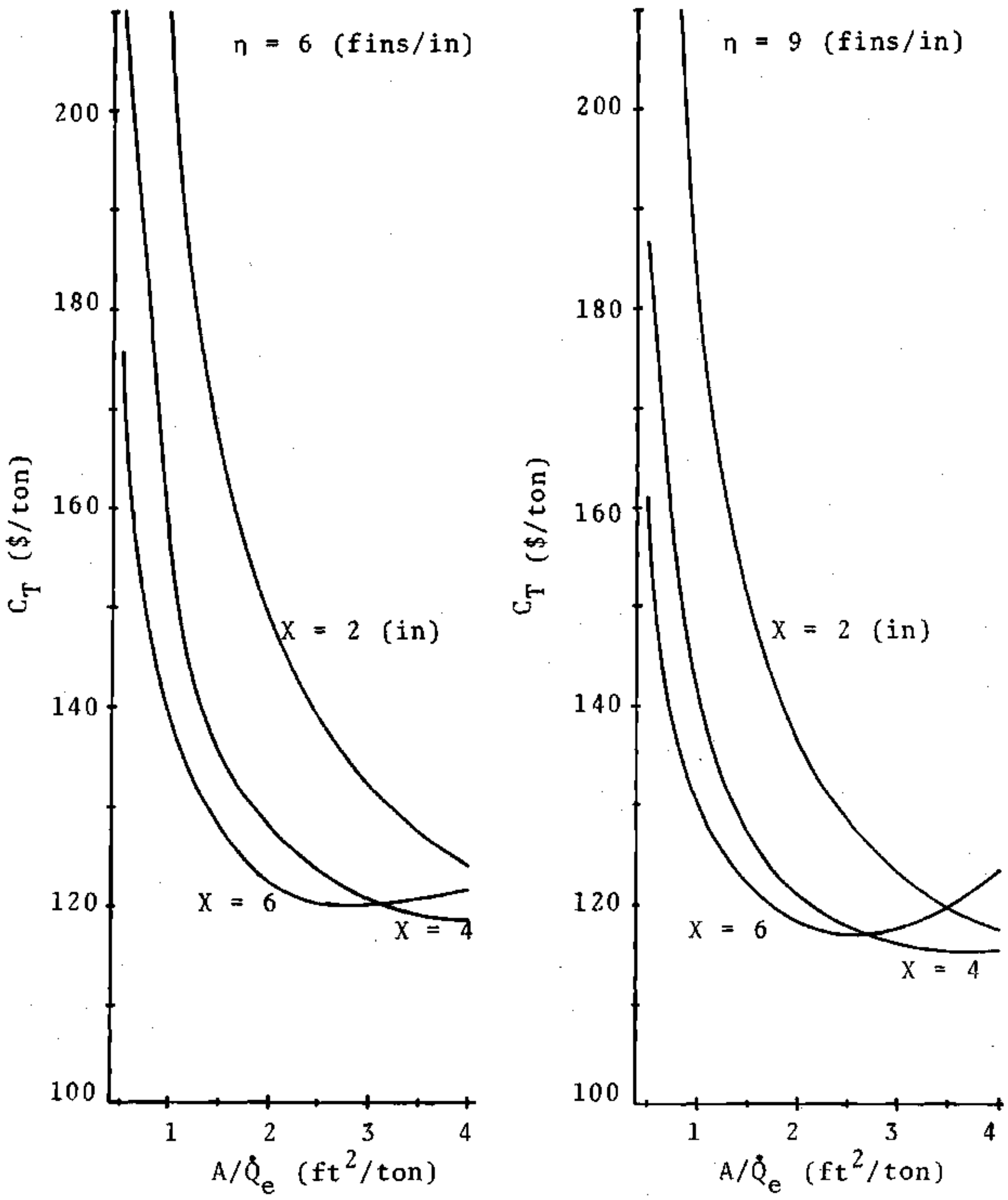

Figure 49. Total Annual Cost versus $A/\dot{Q}_e$ for 1.35×10^4 (¢/kw-yr); η = 6 and 9 (fins/in)

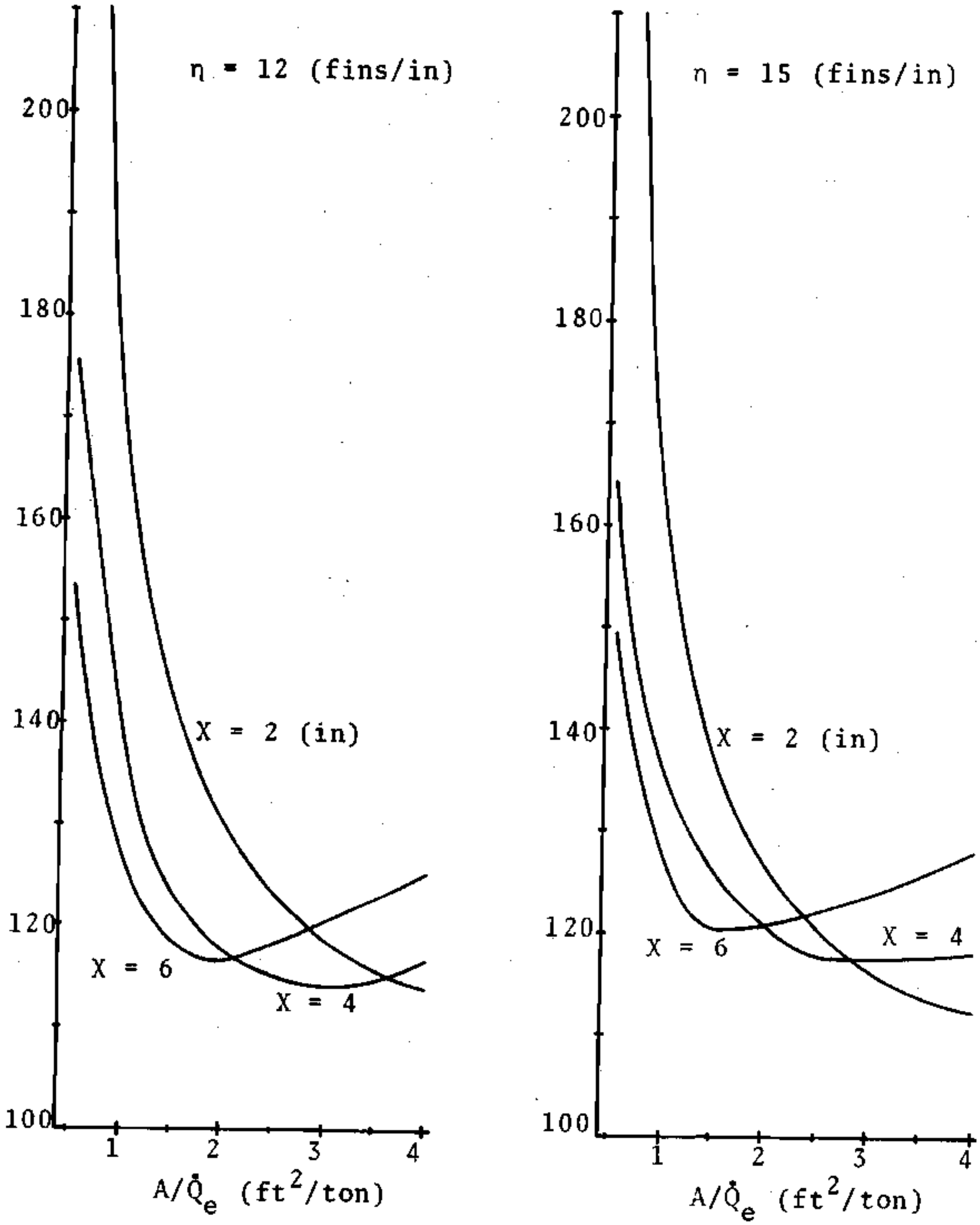

Figure 50. Total Annual Cost versus A/$\dot{Q}_e$ for 1.35×10^4 (¢/kw-yr); η = 12 and 15 (fins/in)

APPENDIX E

OPTIMAL CONDENSER DESIGN CURVES FOR VARYING ANNUAL HOURS OF OPERATION AND ENERGY COST

Note: The optimal design is that which minimizes total annual cost. The hours of operation per year and energy cost have been combined. Thus, 1.5×10^3 (¢/kw-yr) equals 500 (hr/yr) at 3 (¢/kw-hr) or 750 (hr/yr) at 2 (¢/kw-hr), etc.

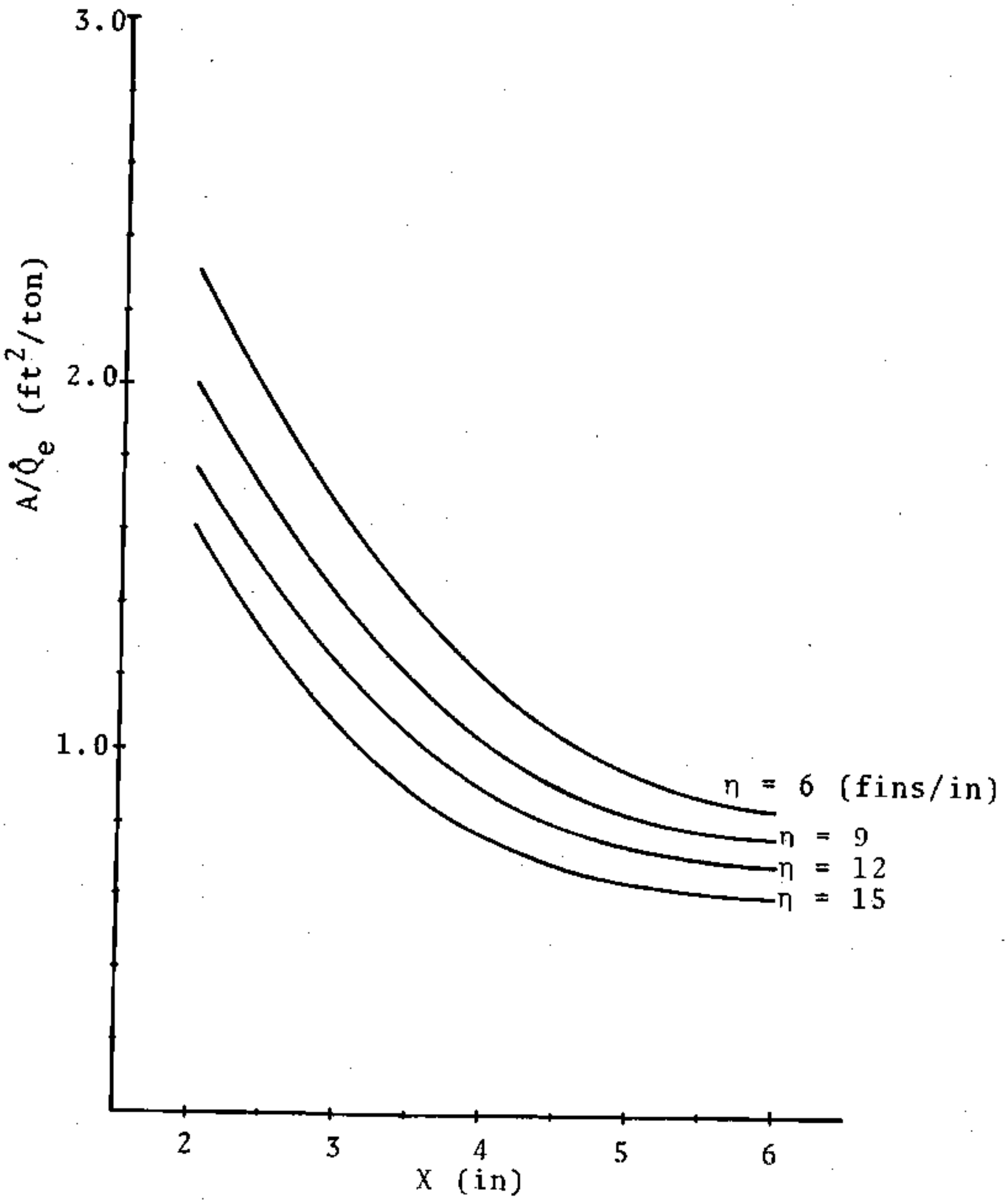

Figure 51. Optimal Condenser Design Curves for 1.5×10^3 (¢/kw-yr)

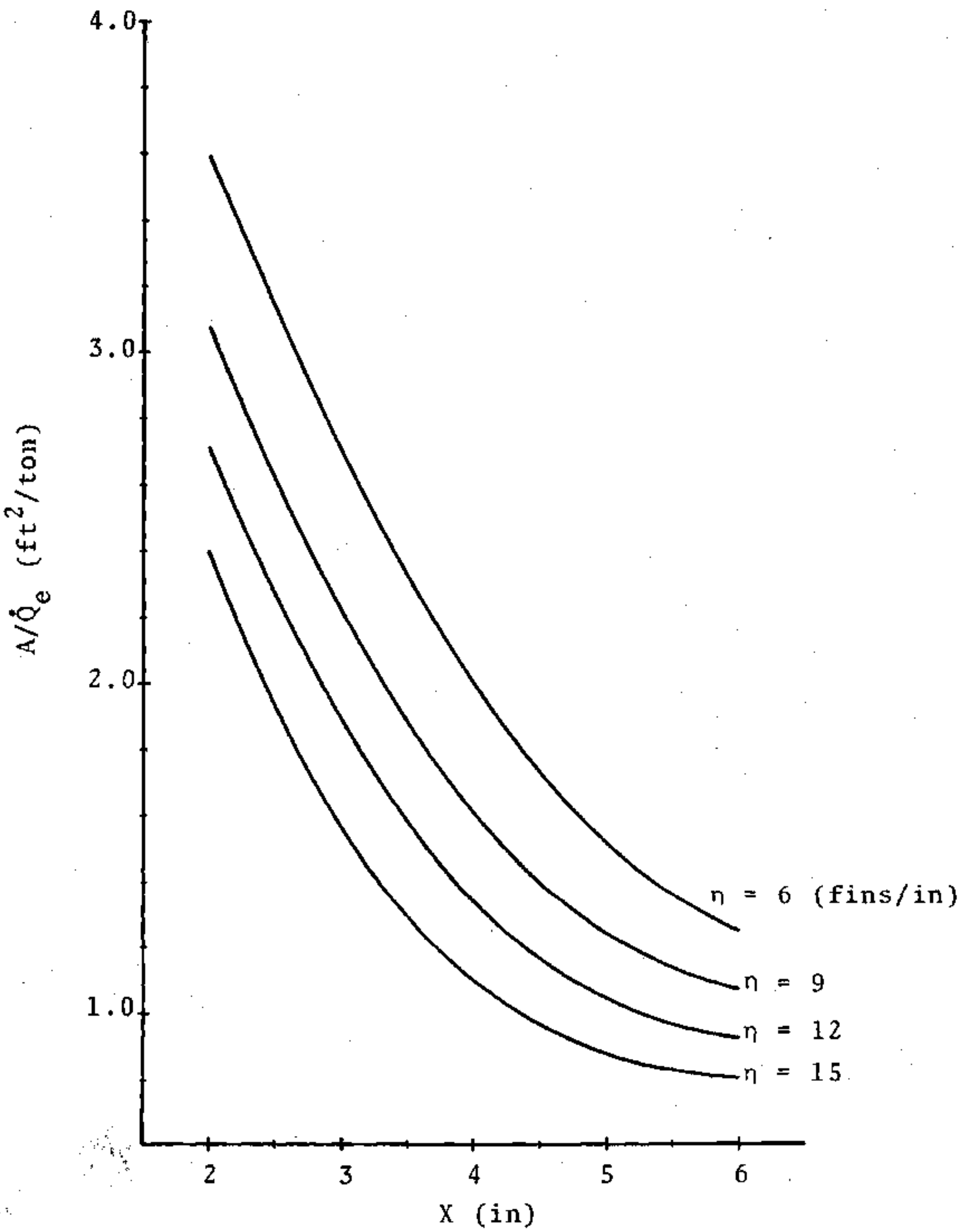

Figure 52. Optimal Condenser Design Curves for 3.0×10^3 (¢/kw-yr)

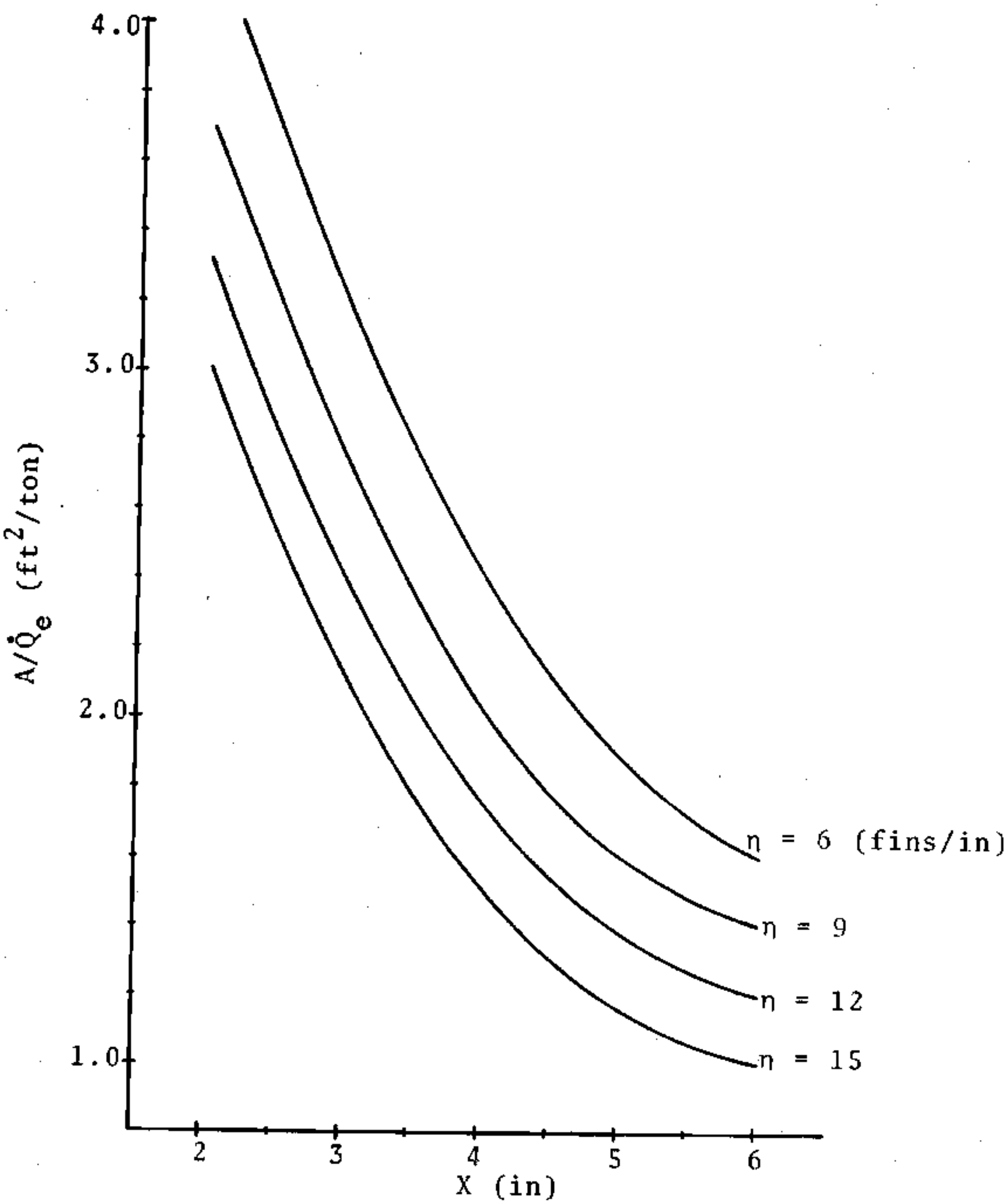

Figure 53. Optimal Condenser Design Curves for 4.5×10^3 (¢/kw-yr)

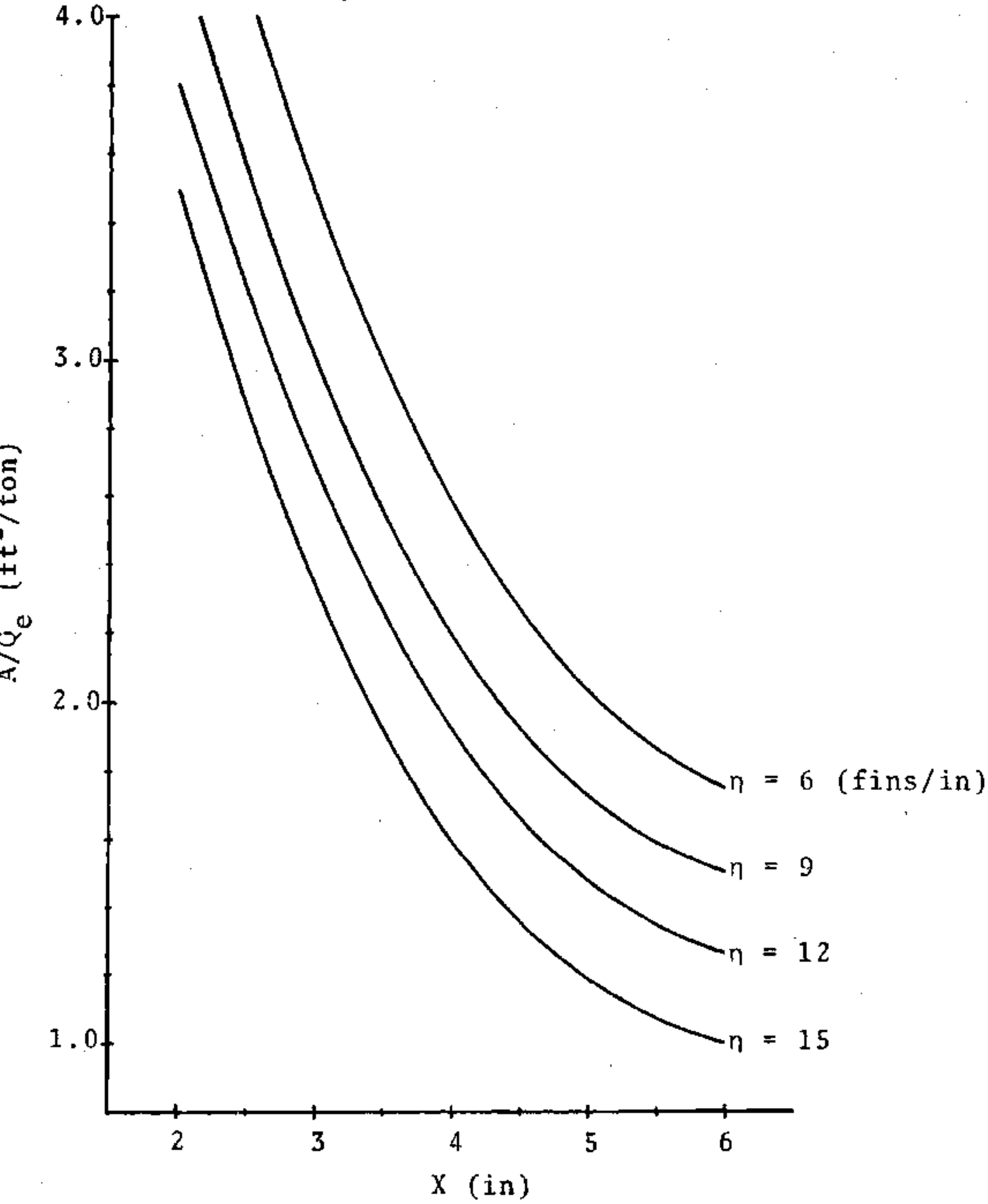

Figure 54. Optimal Condenser Design Curves for 6.0×10^3 (¢/kw-yr)

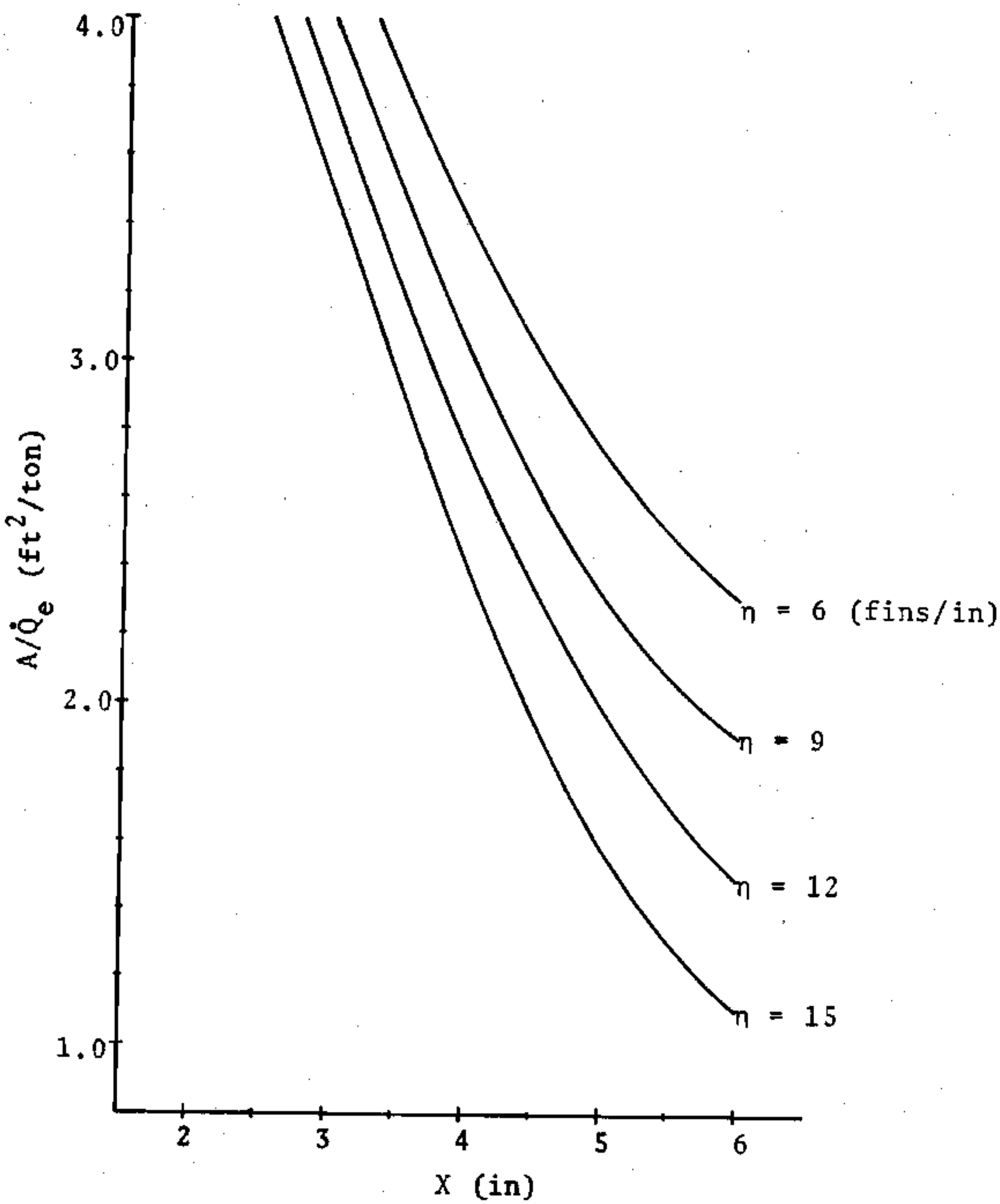

Figure 55. Optimal Condenser Design Curves for 9.0×10^3 (¢/kw-yr)

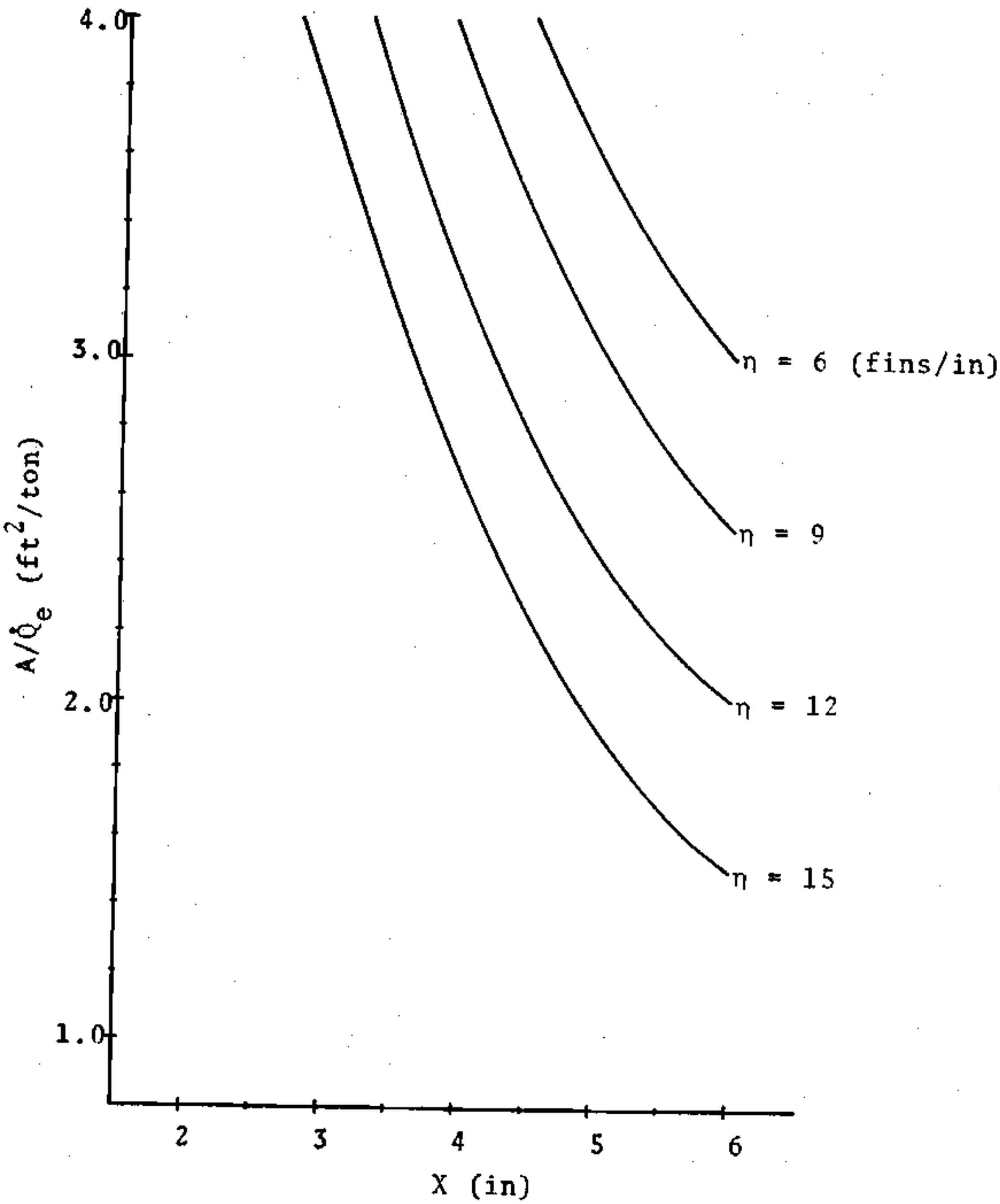

Figure 56. Optimal Condenser Design Curves for 1.35×10^4 (¢/kw-yr)

APPENDIX F

ANNUAL OPERATING COST OF THE OPTIMAL CONDENSER CONFIGURATIONS FOR VARYING AIR VELOCITIES

Note: All configurations with an $A/\dot{Q}_e$ opt greater than 4.0, as predicted by the curves of Appendix D, have been computed at $A/\dot{Q}_e$ equal to 4.0 in the following tables and are indicated by an asterisk. The savings gained in using an $A/\dot{Q}_e$ greater than 4.0 are small.

Table 7. Annual Operating Cost for $1.5x10^3$ (¢/kw-yr)

η = 6 (fins/in)					
X = 2 (in) $A/\dot{Q}_{e_{opt}}$ = 2.3		X = 4 (in) $A/\dot{Q}_{e_{opt}}$ = 1.2		X = 6 (in) $A/\dot{Q}_{e_{opt}}$ = 0.85	
V	C_{oper}	V	C_{oper}	V	C_{oper}
5	25.68	5	33.21	5	38.80
10	24.91	10	26.88	10	27.26
20	17.90	20	18.70	20	18.67
42 opt	15.16	43 opt	15.71	43 opt	15.45
η = 9					
X = 2 $A/\dot{Q}_{e_{opt}}$ = 2.0		X = 4 $A/\dot{Q}_{e_{opt}}$ = 1.02		X = 6 $A/\dot{Q}_{e_{opt}}$ = 0.75	
V	C_{oper}	V	C_{oper}	V	C_{oper}
5	21.75	5	28.54	5	32.44
10	17.85	10	21.46	10	23.06
20	16.13	20	17.02	20	16.88
36 opt	14.65	37.5 opt	15.12	36.8 opt	15.06
η = 12					
X = 2 $A/\dot{Q}_{e_{opt}}$ = 1.75		X = 4 $A/\dot{Q}_{e_{opt}}$ = 0.9		X = 6 $A/\dot{Q}_{e_{opt}}$ = 0.69	
V	C_{oper}	V	C_{oper}	V	C_{oper}
5	20.67	5	27.36	5	30.49
10	16.99	10	20.32	10	21.34
18	15.31	18	17.34	18	17.73
32.5 opt	14.50	34 opt	15.42	33.5 opt	14.86
η = 15					
X = 2 $A/\dot{Q}_{e_{opt}}$ = 1.6		X = 4 $A/\dot{Q}_{e_{opt}}$ = 0.75		X = 6 $A/\dot{Q}_{e_{opt}}$ = 0.6	
V	C_{oper}	V	C_{oper}	V	C_{oper}
5	20.15	5	22.21	5	32.84
10	16.51	10	21.23	10	21.90
20	14.85	20	17.51	20	17.53
29.5 opt	14.39	34.5 opt	15.19	32.5 opt	15.19

Units: $A/\dot{Q}_{e_{opt}}$ (ft^2/ton); V (ft/sec); C_{oper} (\$/ton)

Table 8. Annual Operating Cost for 3.0×10^3 (¢/kw-yr)

η = 6 (fins/in)					
X = 2 (in) $A/\dot{Q}_{e_{opt}}$ = 3.5		X = 4 (in) $A/\dot{Q}_{e_{opt}}$ = 2.0		X = 6 (in) $A/\dot{Q}_{e_{opt}}$ = 1.25	
V	C_{oper}	V	C_{oper}	V	C_{oper}
5	37.25	5	42.01	5	52.18
10	36.33	10	36.24	10	39.84
20	28.66	20	28.55	20	29.99
32 opt	26.73	32 opt	26.49	34 opt	27.43
η = 9					
X = 2 $A/\dot{Q}_{e_{opt}}$ = 3.08		X = 4 $A/\dot{Q}_{e_{opt}}$ = 1.7		X = 6 $A/\dot{Q}_{e_{opt}}$ = 1.07	
V	C_{oper}	V	C_{oper}	V	C_{oper}
5	32.54	5	35.49	5	46.65
10	28.17	10	29.33	10	35.75
20	26.42	20	26.63	20	28.25
28.5 opt	25.56	27.5 opt	25.89	30 opt	26.90
η = 12					
X = 2 $A/\dot{Q}_{e_{opt}}$ = 2.75		X = 4 $A/\dot{Q}_{e_{opt}}$ = 1.35		X = 6 $A/\dot{Q}_{e_{opt}}$ = 0.92	
V	C_{oper}	V	C_{oper}	V	C_{oper}
5	31.00	5	39.39	5	39.88
10	26.99	10	31.52	10	35.08
15	25.74	15	29.06	15	31.51
25 opt	25.11	27.5 opt	26.76	28.5 opt	27.02
η = 15					
X = 2 $A/\dot{Q}_{e_{opt}}$ = 2.4		X = 4 $A/\dot{Q}_{e_{opt}}$ = 1.1		X = 6 $A/\dot{Q}_{e_{opt}}$ = 0.8	
V	C_{oper}	V	C_{oper}	V	C_{oper}
5	31.22	5	42.78	5	49.94
10	27.03	10	33.05	10	35.89
15	25.87	20	29.13	20	30.46
19 opt	25.44	27.5 opt	27.54	27.5 opt	28.12

Units: $A/\dot{Q}_{e_{opt}}$ (ft^2/ton); V (ft/sec); C_{oper} (\$/ton)

Table 9. Annual Operating Cost for 4.5×10^3 (¢/kw-yr)

$\eta = 6$ (fins/in)					
X = 2 (in) *$A/\dot{Q}_{e_{opt}}$ = 4.0		X = 4 (in) $A/\dot{Q}_{e_{opt}}$ = 2.4		X = 6 (in) $A/\dot{Q}_{e_{opt}}$ = 1.6	
V	C_{oper}	V	C_{oper}	V	C_{oper}
5	51.15	5	57.13	5	65.57
10	50.15	10	50.38	10	52.54
20	40.43	20	41.56	20	42.05
31 opt	38.45	28.5 opt	39.54	30 opt	40.18
$\eta = 9$					
X = 2 $A/\dot{Q}_{e_{opt}}$ = 3.7		X = 4 $A/\dot{Q}_{e_{opt}}$ = 2.02		X = 6 $A/\dot{Q}_{e_{opt}}$ = 1.4	
V	C_{oper}	V	C_{oper}	V	C_{oper}
5	44.18	5	50.72	5	57.20
10	39.01	10	42.57	10	45.93
20	37.16	20	37.59	20	38.23
25.5 opt	36.64	25 opt	37.06	25.5 opt	37.74
$\eta = 12$					
X = 2 $A/\dot{Q}_{e_{opt}}$ = 3.3		X = 4 $A/\dot{Q}_{e_{opt}}$ = 1.76		X = 6 $A/\dot{Q}_{e_{opt}}$ = 1.2	
V	C_{oper}	V	C_{oper}	V	C_{oper}
5	42.38	5	49.78	5	57.66
10	37.66	10	41.53	10	45.38
15	36.34	15	39.13	15	41.82
23.6 opt	36.05	23.6 opt	36.88	24.5 opt	37.71
$\eta = 15$					
X = 2 $A/\dot{Q}_{e_{opt}}$ = 3.0		X = 4 $A/\dot{Q}_{e_{opt}}$ = 1.5		X = 6 $A/\dot{Q}_{e_{opt}}$ = 1.0	
V	C_{oper}	V	C_{oper}	V	C_{oper}
5	41.84	5	51.89	5	62.65
10	37.22	10	42.38	10	47.37
16 opt	36.00	15	39.90	15	43.29
		19 opt	38.24	22 opt	40.03

Units: $A/\dot{Q}_{e_{opt}}$ (ft^2/ton); V (ft/sec); C_{oper} ($/ton)

Table 10. Annual Operating Cost for 6.0×10^3 (¢/kw-yr)

$\eta = 6$ (fins/in)					
X = 2 (in) *$A/\dot{Q}_{e_{opt}} = 4.0$		X = 4 (in) $A/\dot{Q}_{e_{opt}} = 2.6$		X = 6 (in) $A/\dot{Q}_{e_{opt}} = 1.75$	
V	C_{oper}	V	C_{oper}	V	C_{oper}
5	68.21	5	70.13	5	79.67
10	66.86	10	62.06	10	64.29
20	53.34	20	51.64	20	51.95
31 opt	51.27	27.5 opt	49.15	28 opt	50.08
$\eta = 9$					
X = 2 *$A/\dot{Q}_{e_{opt}} = 4.0$		X = 4 $A/\dot{Q}_{e_{opt}} = 2.2$		X = 6 $A/\dot{Q}_{e_{opt}} = 1.5$	
V	C_{oper}	V	C_{oper}	V	C_{oper}
5	56.68	5	65.26	5	72.83
10	50.44	10	55.55	10	59.12
20	48.37	20	49.75	20	49.86
24 opt	47.99	24 opt	49.52	24.5 opt	49.34
$\eta = 12$					
X = 2 $A/\dot{Q}_{e_{opt}} = 3.8$		X = 4 $A/\dot{Q}_{e_{opt}} = 1.92$		X = 6 $A/\dot{Q}_{e_{opt}} = 1.26$	
V	C_{oper}	V	C_{oper}	V	C_{oper}
5	53.01	5	63.16	5	74.38
10	47.82	10	53.36	10	59.06
15	46.57	15	50.65	15	54.69
20.8 opt	46.46	22.5 opt	48.11	24 opt	49.48
$\eta = 15$					
X = 2 $A/\dot{Q}_{e_{opt}} = 3.5$		X = 4 $A/\dot{Q}_{e_{opt}} = 1.6$		X = 6 $A/\dot{Q}_{e_{opt}} = 1.0$	
V	C_{oper}	V	C_{oper}	V	C_{oper}
5	52.14	5	66.55	5	83.53
10	47.22	10	54.95	10	63.15
14.2 opt	46.20	18 opt	51.27	15	57.72
				22 opt	51.81

Units: $A/\dot{Q}_{e_{opt}}$ (ft^2/ton); V (ft/sec); C_{oper} ($/ton)

Table 11. Annual Operating Cost for 9.0×10^3 (¢/kw-yr)

η = 6 (fins/in)					
X = 2 (in) *$A/\dot{Q}_{e_{opt}}$ = 4.0		X = 4 (in) $A/\dot{Q}_{e_{opt}}$ = 3.4		X = 6 (in) $A/\dot{Q}_{e_{opt}}$ = 2.3	
V	C_{oper}	V	C_{oper}	V	C_{oper}
5	102.31	5	90.14	5	99.97
10	91.61	10	81.64	10	83.79
20	80.87	20	71.69	20	71.38
31 opt	76.91	23.5 opt	69.62	24 opt	69.92
η = 9					
X = 2 *$A/\dot{Q}_{e_{opt}}$ = 4.0		X = 4 $A/\dot{Q}_{e_{opt}}$ = 3.05		X = 6 $A/\dot{Q}_{e_{opt}}$ = 1.9	
V	C_{oper}	V	C_{oper}	V	C_{oper}
5	90.73	5	81.74	5	94.73
10	75.67	10	72.24	10	79.68
20	72.67	15	68.93	15	72.42
24 opt	71.99	20 opt	67.57	22 opt	69.81
η = 12					
X = 2 *$A/\dot{Q}_{e_{opt}}$ = 4.0		X = 4 $A/\dot{Q}_{e_{opt}}$ = 2.74		X = 6 $A/\dot{Q}_{e_{opt}}$ = 1.5	
V	C_{oper}	V	C_{oper}	V	C_{oper}
5	77.81	5	79.63	5	100.01
10	70.57	10	70.63	10	81.87
20 opt	68.99	15	69.02	15	77.07
		18 opt	66.41	21.5 opt	70.90
η = 15					
X = 2 *$A/\dot{Q}_{e_{opt}}$ = 4.0		X = 4 $A/\dot{Q}_{e_{opt}}$ = 2.4		X = 6 $A/\dot{Q}_{e_{opt}}$ = 1.1	
V	C_{oper}	V	C_{oper}	V	C_{oper}
5	74.22	5	81.19	5	117.00
7	70.52	7	75.18	10	90.26
10	68.23	10	71.43	15	83.37
13 opt	67.68	13.2 opt	70.10	20 opt	76.89

Units: $A/\dot{Q}_{e_{opt}}$ (ft^2/ton); V (ft/sec); C_{oper} (\$/ton)

Table 12. Annual Operating Cost for 1.35x10[4] (¢/kw-yr)

η = 6 (fins/in)					
X = 2 (in) *$A/\dot{Q}_{e_{opt}}$ = 4.0		X = 4 (in) *$A/\dot{Q}_{e_{opt}}$ = 4.0		X = 6 (in) $A/\dot{Q}_{e_{opt}}$ = 3.0	
V	C_{oper}	V	C_{oper}	V	C_{oper}
5	153.47	5	124.79	5	135.62
10	150.44	10	114.49	10	117.65
20	121.31	15	105.63	15	108.46
31 opt	115.36	22 opt	104.33	21 opt	100.46
η = 9					
X = 2 *$A/\dot{Q}_{e_{opt}}$ = 4.0		X = 4 $A/\dot{Q}_{e_{opt}}$ = 3.9		X = 6 $A/\dot{Q}_{e_{opt}}$ = 2.5	
V	C_{oper}	V	C_{oper}	V	C_{oper}
5	136.09	5	110.83	5	123.74
10	113.50	10	100.67	10	108.07
20	108.83	15	97.38	15	100.58
24 opt	107.99	17.5 opt	96.83	19 opt	98.49
η = 12					
X = 2 *$A/\dot{Q}_{e_{opt}}$ = 4.0		X = 4 $A/\dot{Q}_{e_{opt}}$ = 3.2		X = 6 $A/\dot{Q}_{e_{opt}}$ = 2.0	
V	C_{oper}	V	C_{oper}	V	C_{oper}
5	116.72	5	112.24	5	115.09
10	105.85	7	105.67	10	110.33
20 opt	103.48	10	101.52	12	108.06
		13 opt	97.31	16 opt	101.25
η = 15					
X = 2 *$A/\dot{Q}_{e_{opt}}$ = 4.0		X = 4 $A/\dot{Q}_{e_{opt}}$ = 2.64		X = 6 $A/\dot{Q}_{e_{opt}}$ = 1.5	
V	C_{oper}	V	C_{oper}	V	C_{oper}
5	111.32	5	116.99	5	144.55
7	105.38	7	109.09	10	128.81
10	102.34	10	104.38	13	118.51
13 opt	101.52	12.5 opt	102.81	16 opt	107.90

Units: $A/\dot{Q}_{e_{opt}}$ (ft^2/ton); V (ft/sec); C_{oper} ($/ton)

APPENDIX G

CAPITAL COST DATA FOR CONDENSER COILS

Note: Each data point in the following plots represents the cost of an individual condenser coil. The straight line curves have been fitted to the data.

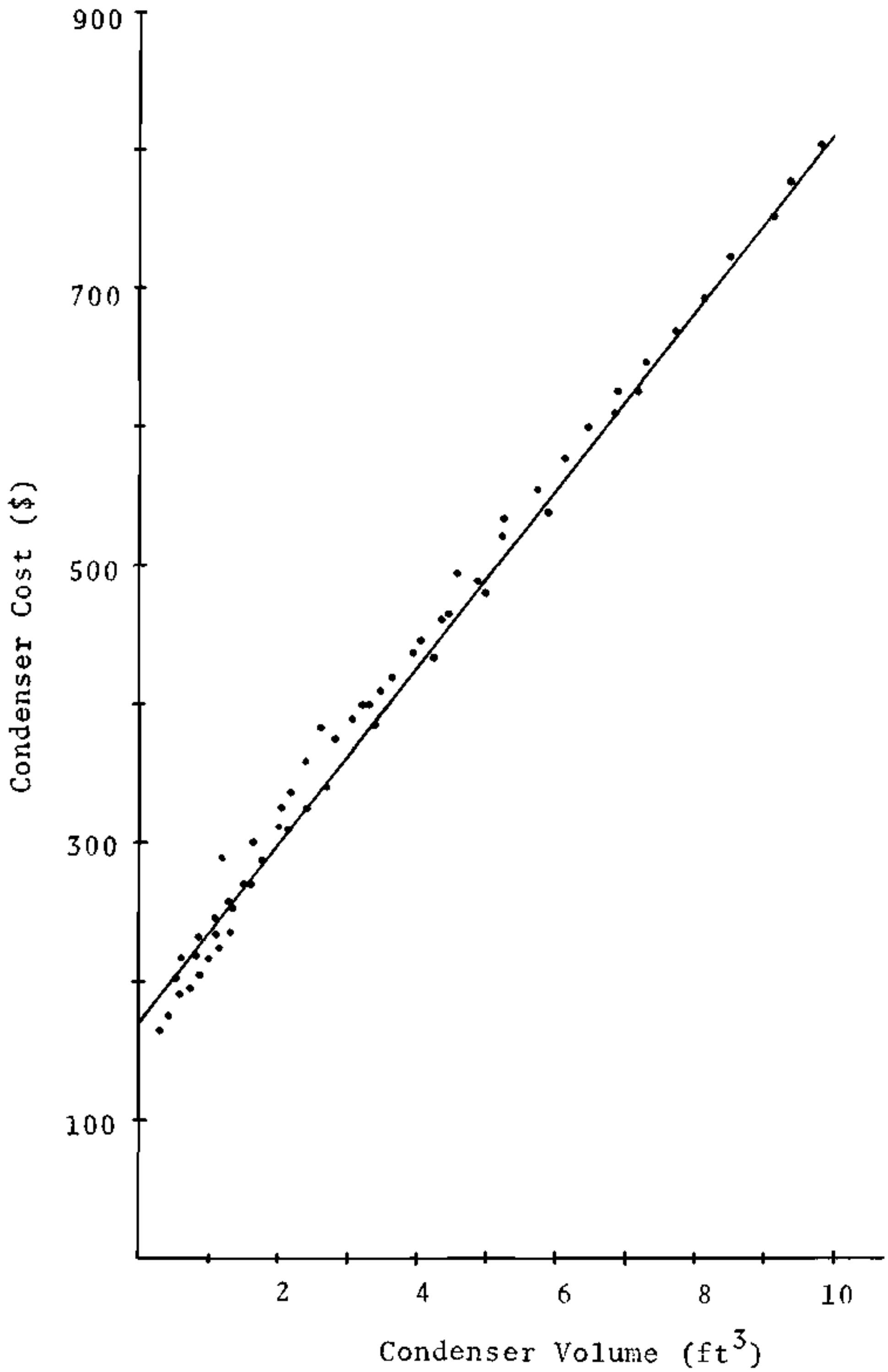

Figure 57. Capital Cost of Condensers with $\eta = 6$ (fins/in)

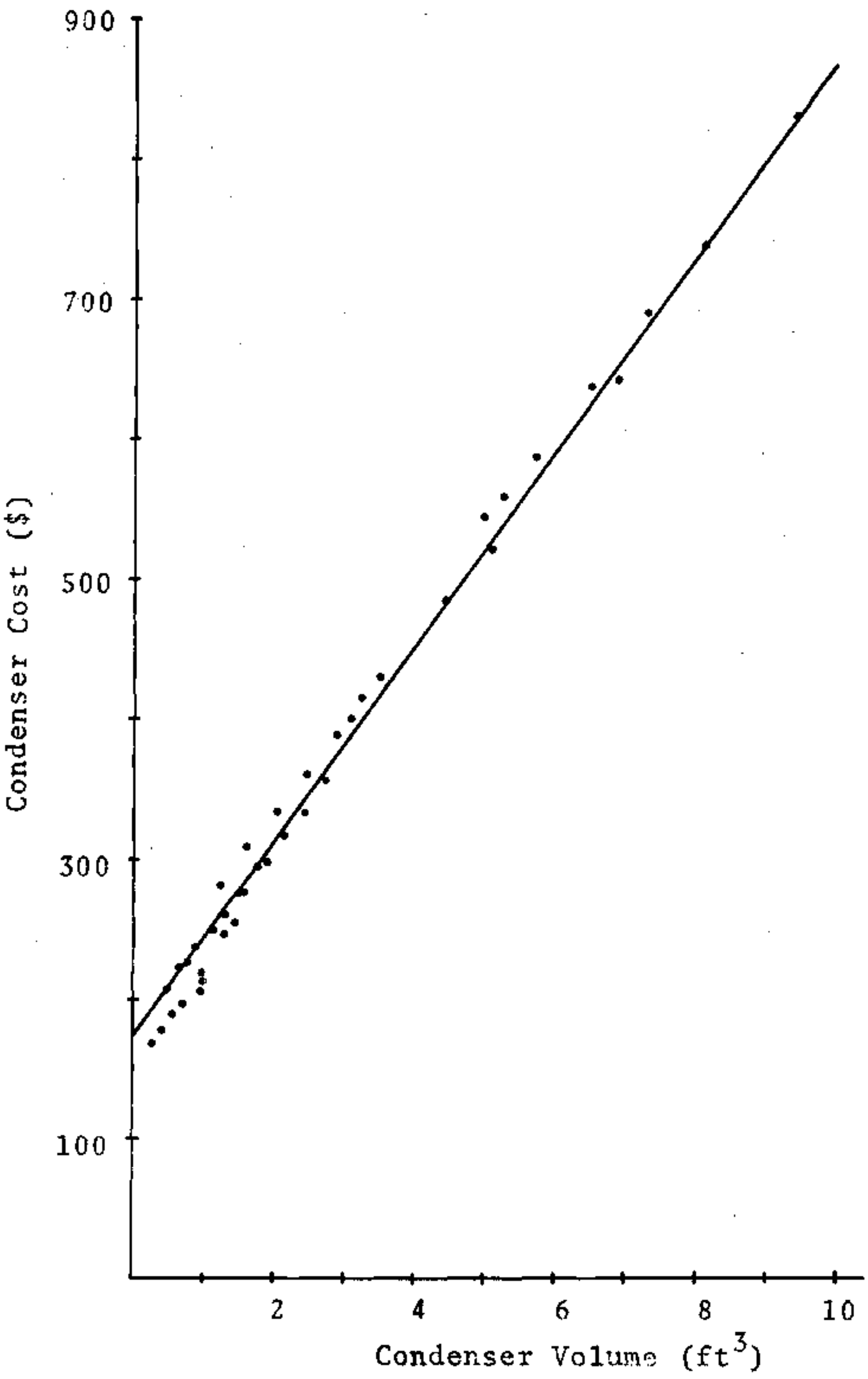

Figure 58. Capital Cost of Condensers with η = 9 (fins/in)

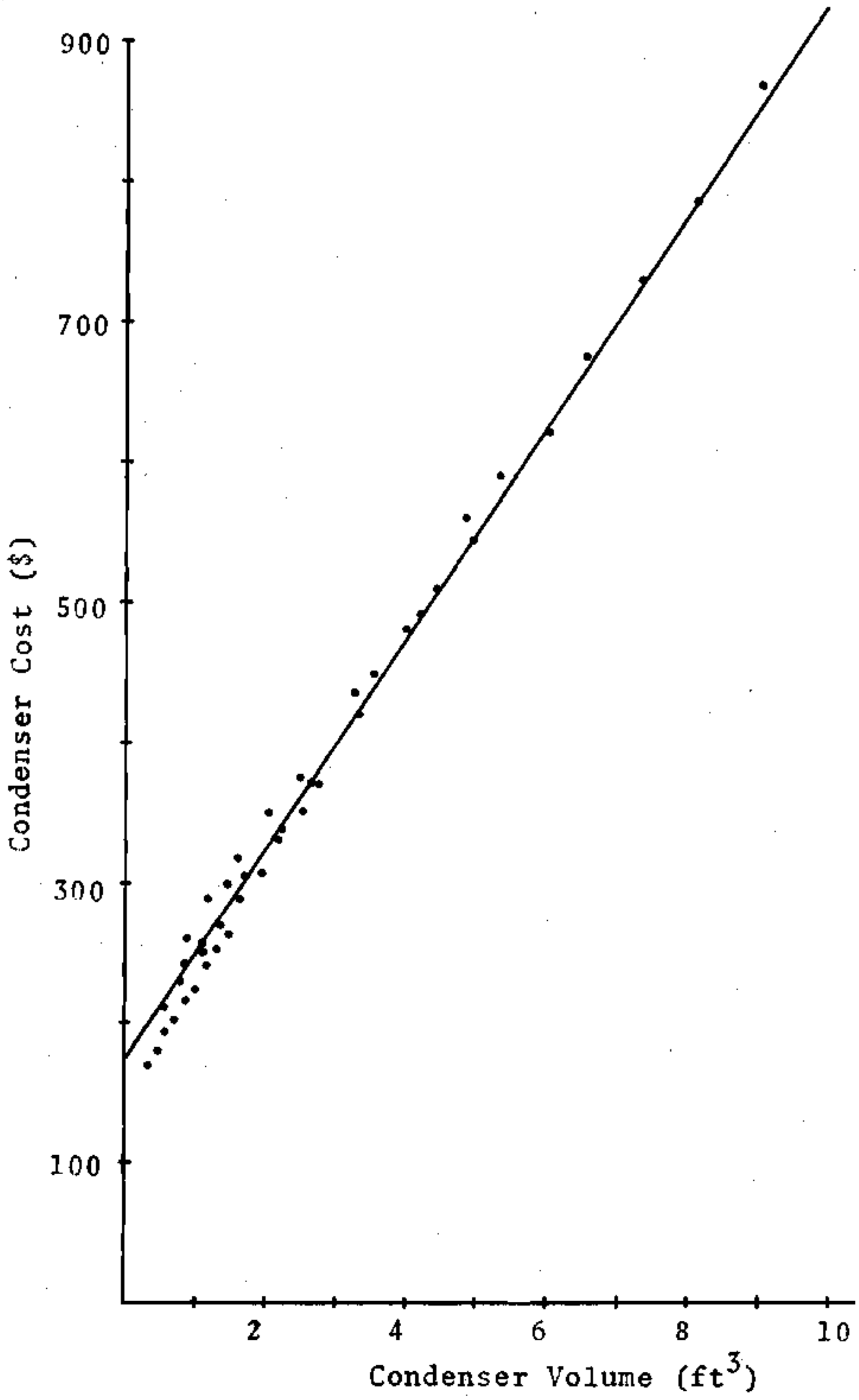

Figure 59. Capital Cost of Condensers with η = 12 (fins/in)

APPENDIX H

DERIVATION OF EXPRESSIONS FOR SYSTEM COEFFICIENT OF PERFORMANCE FROM THE FUNDAMENTAL EQUATIONS

Fundamental Equations

(1) $\dot{Q}_c = \dot{m}C_p\ (T_2 - T_1)$

(2) $T_{rc} - T_2 = (T_{rc} - T_1)\exp\left(\frac{-2U_oAX\eta}{\dot{m}C_p}\right)$

(3) $\dot{m} = \rho VA\ (1 - \eta t)$

(4) $U_o = \left(\frac{1}{\bar{h}} + \frac{A_o}{A_i\bar{h}_r} + \frac{1-\phi}{\bar{h}\left(\frac{A_t}{A_f}+\phi\right)}\right)^{-1}$

(5) $St\ Pr^{2/3} = \frac{\bar{h}\ Pr^{2/3}}{\rho VC_p} = \frac{C_f}{2}$

(6) $C_f = a/Re^b$

(7) $\dot{W}_{fc} = C_f\rho V^3\ X\eta A/E_{fc}$

(8) $COP_{com} = \dot{Q}_e/\dot{W}_{com}$

(9) $COP_{com} = \left(\frac{T_{re}}{T_{rc} - T_{re}}\right) E_{com}$

(10) $\dot{Q}_c = \dot{W}_{com} + \dot{Q}_e$

(11) $\beta_c = \dfrac{\dot{W}_{fc}}{\dot{W}_{com}}$

(12) $\beta_e = \dfrac{\dot{W}_{fe}}{\dot{W}_{com}}$

(13) $COP_s = \dfrac{\dot{Q}_e}{\dot{W}_{com}+\dot{W}_{fc}+\dot{W}_{fe}}$

I. The derivation of Equation (2) of the fundamental equations follows. From an equilibrium energy balance,

$$\left\{\begin{array}{l}\text{Rate of heat rejected}\\ \text{by the refrigerant in}\\ \text{the condenser tubes}\end{array}\right\} = \left\{\begin{array}{l}\text{Rate of heat absorbed}\\ \text{by the air passing}\\ \text{through the condenser}\end{array}\right\}$$

On a differential basis this can be written as,

$$\dot{m}_r \; C_{pr} \; dT_{rc} = \dot{m}_a \; C_p \; dT_a = -dq \qquad \text{(H-1)}$$

where $\dot{m}_r$ is the mass flow rate of refrigerant C_{pr} is the specific heat of the refrigerant, T_a is the temperature of air. From heat transfer theory,

$$dq = U_o \; (T_{rc}-T_a)dA_o \qquad \text{(H-2)}$$

From (H-1),

$$dT_{rc} = -dq/\dot{m}_r C_{pr} \quad \text{and} \quad dT_a = -dq/\dot{m}_a C_p \tag{H-3}$$

or,

$$dT_{rc} - dT_a = d(T_{rc}-T_a) = -\left(\frac{1}{\dot{m}_r C_{pr}} - \frac{1}{\dot{m}_a C_p}\right)dq \tag{H-4}$$

Rearranging (4),

$$dq = -\frac{d(T_{rc}-T_a)}{\dfrac{1}{\dot{m}_r C_{pr}} - \dfrac{1}{\dot{m}_a C_p}} \tag{H-5}$$

Equating (H-2) and (H-5),

$$\frac{-d(T_{rc}-T_a)}{\dfrac{1}{\dot{m}_r C_{pr}} - \dfrac{1}{\dot{m}_a C_p}} = U_o \; (T_{rc}-T_a)dA_o \tag{H-6}$$

Rearranging and integrating (H-6),

$$\int_{T_a=T_1}^{T_a=T_2} \frac{d(T_{rc}-T_a)}{(T_{rc}-T_a)} dT_a = -U_o \left(\frac{1}{\dot{m}_r C_{pr}} - \frac{1}{\dot{m}_a C_p}\right)\int^{A_o} dA_o \tag{H-7}$$

which results in,

$$-\ell n\ (T_{rc}-T_a)\Bigg|_{T_a=T_1}^{T_a=T_2} = -U_oA_o\ [\frac{1}{\dot{m}_aC_p}\ [\frac{\dot{m}_aC_p}{\dot{m}_rC_{pr}} - 1]] \qquad \text{(H-8)}$$

But $\frac{\dot{m}_aC_p}{\dot{m}_rC_{pr}}$ equals zero since C_{pr} is infinite for the condensation process. (H-8) simplifies to,

$$\ell n(\frac{T_{rc}-T_2}{T_{rc}-T_1}) = \frac{-U_oA_o}{\dot{m}_aC_p} \qquad \text{(H-9)}$$

or,

$$T_{rc}-T_2 = (T_{rc}-T_1)\exp(\frac{-U_oA_o}{\dot{m}_aC_p}) \qquad \text{(H-10)}$$

By assumption 5 (page 15) A_o is the total surface area of the fins which is given by,

$$A_o = 2AX\eta \qquad \text{(H-11)}$$

Substituting (H-11) into (H-10),

$$T_{rc}-T_2 = (T_{rc}-T_1)\exp(\frac{-2U_oAX\eta}{\dot{m}_aC_p}) \qquad \text{(H-12)}$$

Equation (H-12) is the same as Equation (2).

II. The fundamental equations are now combined to yield expressions for $1/COP_s$. Solving (10) for $\dot{Q}_e$ and substituting into (8),

$$COP_{com} = \frac{\dot{Q}_c}{\dot{W}_{com}} - 1 \tag{1H}$$

Substituting (11) into (1H), for $\dot{W}_{com}$ and solving for $\dot{W}_{fc}$,

$$\dot{W}_{fc} = \frac{\beta_c \dot{Q}_c}{1+COP_{com}} \tag{2H}$$

Rearranging (9),

$$COP_{com} = \frac{1}{\frac{T_{rc}-T_{re}}{E_{com}T_{re}}} = \frac{1}{\frac{T_{rc}}{E_{com}T_{re}} - \frac{1}{E_{com}}} \tag{3H}$$

Substituting (3H) into (2H),

$$\dot{W}_{fc} = \frac{\beta_c \dot{Q}_c}{1 + \frac{1}{\frac{T_{rc}}{E_{com}T_{re}} - \frac{1}{E_{com}}}} \tag{4H}$$

Substituting (6) into (7),

$$\dot{W}_{fc} = \frac{a\rho V^3 X\eta A}{Re^b\ E_{fc}} \tag{5H}$$

Equating (4H) and (5H) and solving for $\dot{Q}_c$,

$$\dot{Q}_c = a\rho V^3 X\eta A\ (1 + \frac{1}{\frac{T_{rc}}{E_{com}T_{re}} - \frac{1}{E_{com}}})/Re^b \beta_c E_{fc} \tag{6H}$$

Substituting (3) into (2),

$$T_{rc} - T_2 = (T_{rc} - T_1)\exp(\frac{-2U_o X\eta}{\rho V C_p (1-\eta t)}) \tag{7H}$$

Solving (7H) for T_2,

$$T_2 = T_{rc}\ [1-\exp(\frac{-2U_o X\eta}{\rho V C_p (1-\eta t)})] + T_1\ \exp(\frac{-2U_o X\eta}{\rho V C_p (1-\eta t)}) \tag{8H}$$

Substituting (3) into (1),

$$\dot{Q}_c = \rho VAC_p (1-\eta t)(T_2 - T_1) \tag{9H}$$

Solving (9H) for T_2,

$$T_2 = \frac{\dot{Q}_c}{\rho VAC_p (1-\eta t)} + T_1 \tag{10H}$$

Equating (8H) and (10H) and solving for $\dot{Q}_c$,

$$\dot{Q}_c = \rho VAC_p (1-\eta t)(T_{rc} - T_1)[1-\exp(\frac{-2U_o X\eta}{\rho V C_p (1-\eta t)})] \tag{11H}$$

Equating (6H) and (11H) and solving for β_c,

$$\beta_c = \frac{a\rho V^3 X\eta A\left(1 + \dfrac{1}{\dfrac{T_{rc}}{E_{com}T_{re}} - \dfrac{1}{E_{com}}}\right)}{E_{fc}Re^b \rho VAC_p(1-\eta t)(T_{rc}-T_1)\left[1-\exp\left(\dfrac{-2U_oX\eta}{\rho VC_p(1-\eta t)}\right)\right]} \qquad (12H)$$

Dividing the numerator and denominator of (13) by $\dot{W}_{com}$,

$$\frac{\dot{Q}_e/\dot{W}_{com}}{\dfrac{\dot{W}_{com}}{\dot{W}_{com}} + \dfrac{\dot{W}_{fc}}{\dot{W}_{com}} + \dfrac{\dot{W}_{fe}}{\dot{W}_{com}}} \qquad (13H)$$

Substituting (8), (11), and (12) into (13H),

$$COP_s = COP_{com}/(1+\beta_c+\beta_e) \qquad (14H)$$

Substituting (3H) into (14H) and inverting,

$$\frac{1}{COP_s} = \left(\frac{T_{rc}}{E_{com}T_{rc}} - \frac{1}{E_{com}}\right)(1+\beta_c+\beta_e) \qquad (15H)$$

Substituting (12H) into (15H),

$$\frac{1}{COP_s} = \left(\frac{T_{rc}}{E_{com}T_{re}} - \frac{1}{E_{com}}\right) x$$

$$\left[1+\beta_e + \frac{aV^2X\eta\left(1 + \cfrac{1}{\cfrac{T_{rc}}{E_{com}T_{re}} - \cfrac{1}{E_{com}}}\right)}{E_{fc}Re^bC_p(1-\eta t)(T_{rc}-T_1)\left[1-\exp\left(\frac{-2U_oX\eta}{\rho VC_p(1-\eta t)}\right)\right]}\right] \qquad (16H)$$

Rearranging (16H),

$$\frac{1}{COP_s} = \frac{aV^2X\eta\left(1 + \frac{T_{rc}}{E_{com}T_{re}} - \frac{1}{E_{com}}\right)}{E_{fc}Re^bC_p(1-\eta t)(T_{rc}-T_1)\left[1-\exp\left(\frac{-2U_oX\eta}{\rho VC_p(1-\eta t)}\right)\right]}$$

$$+ (1+\beta e)\left[\frac{T_{rc}}{E_{com}T_{re}} - \frac{1}{E_{com}}\right] \qquad (17H)$$

Equation (17H) is equivalent to Equation (14) of Chapter II. U_o in (17H) is now evaluated. Substituting (6) into (5) and solving for $\bar{h}$,

$$\bar{h} = \frac{a\rho VC_p}{2Re^bPr^{2/3}} \qquad (18H)$$

Rearranging (4),

$$U_o = \frac{1}{\frac{1}{\bar{h}}\left[1 + \frac{1-\phi}{\frac{A_t}{A_f}+\phi}\right] + \frac{A_o}{A_i\bar{h}_r}} \qquad (19H)$$

Substituting (18H) into (19H),

$$U_o = \frac{1}{\frac{2Re^b Pr^{2/3}}{a\rho VC_p}\left[1 + \frac{1-\phi}{\frac{A_t}{A_f}+\phi}\right] + \frac{A_o}{A_i \bar{h}_r}} \tag{20H}$$

Multiplying numerator and denominator of (20H) by $a\rho VC_p$,

$$U_o = \frac{a\rho VC_p}{2Re^b Pr\left[1 + \frac{1-\phi}{\frac{A_t}{A_f}+\phi}\right] + \frac{a\rho VC_p A_o}{A_i \bar{h}_r}} \tag{21H}$$

When (21H) is substituted into (17H) the term in brackets associated with exp in Equation (17H) becomes,

$$k = \frac{aX\eta/(1-\eta t)}{Re^b\ Pr^{2/3}\left[1 + \frac{1-\phi}{\frac{A_t}{A_f}+\phi}\right] + \frac{a\rho VC_p A_o}{2\bar{h}_r A_i}} \tag{22H}$$

Equation (22H) is the same as (15) in Chapter II where k is the term associated with exp in (17H), exp(-k).

To obtain Equation (16) in Chapter II T_{rc} is eliminated from (17H). Substituting (9H) into (10)

$$\dot{W}_{com} + \dot{Q}_e = \rho VAC_p(1-\eta t)(T_2-T_1) \tag{23H}$$

Dividing (23H) by $\dot{Q}_e$ and using (8),

$$\frac{1}{COP_{com}} + 1 = \rho VAC_p(1-\eta t)(T_2-T_1)/\dot{Q}_e \tag{24H}$$

Solving (24H) for $A/\dot{Q}_e$,

$$\frac{A}{\dot{Q}_e} = \frac{\frac{1}{COP_{com}} + 1}{\rho VC_p(1-\eta t)(T_2-T_1)} \tag{25H}$$

Substituting (3H) and (8H) into (25H) for COP_{com} and T_2,

$$\frac{A}{\dot{Q}_e} = \frac{\frac{T_{rc}}{E_{com}T_{re}} - \frac{1}{E_{com}} + 1}{\rho VC_p(1-\eta t)(T_{rc}-T_1)[1-\exp(-k)]} \tag{26H}$$

where k is given by (22H). It is seen that in (26H) as $T_{rc} \to T_1$ for fixed T_{re} and $\dot{Q}_e$ that $A \to \infty$. This is used in the fourth conclusion reached in the discussion of the ideal heat exchanger in Chapter II. Solving (26H) for T_{rc},

$$T_{rc} = T_{re}\left[\frac{\frac{\dot{Q}_e}{A(1-\eta t)}(1-E_{com}) - \rho VC_pE_{com}T_1[1-\exp(-k)]}{\frac{\dot{Q}_e}{A(1-\eta t)} - \rho VC_pE_{com}T_{re}[1-\exp(-k)]}\right] \tag{27H}$$

(27H) is now substituted into (17H). In order to simplify the equations define the following,

$S = \frac{aX\eta}{E_{fc}Re^{b}(1-\eta t)}$; $B = 1-\exp(-k)$; $u = \frac{\dot{Q}_e}{A(1-\eta t)}$; $L_1 = \rho C_p E_{com} T_1$; $L_e = \rho C_p E_{com} T_{re}$. Substituting these defined terms into (17H) and (27H) and then substituting (27H) into (17H),

$$\frac{1}{COP_s} = \frac{SV^2[1 + \frac{1}{E_{com}}(\frac{u(1-E_{com})-VL_1B}{u-VL_eB} - 1)]}{BC_pT_1[\frac{T_{re}}{T_1}(\frac{u(1-E_{com})-VL_1B}{u-VL_eB})-1]}$$

$$+ \frac{(1+\beta_e)}{E_{com}}(\frac{u(1-E_{com})-VL_1B}{u-VL_eB}) \qquad (28H)$$

Manipulation of (28H) yields,

$$\frac{1}{COP_s} = \frac{SV^3[L_e(1-E_{com})-L_1]}{C_pT_{re}E_{com}[u(1-E_{com} - \frac{T_1}{T_{re}})+VB(\frac{T_1}{T_{re}}L_e-L_1)}$$

$$+ (1+\beta_e)\frac{BV(L_e-L_1)-uE_{com}}{E_{com}(u-VL_eB)} \qquad (29H)$$

Replacing S, u, B, L_1, L_e with their values several terms will cancel yielding the following expression,

$$\frac{1}{COP_s} = \frac{aX\eta V^3 \rho A}{E_{fc}\ Re^b\ \dot{Q}_e}$$

$$+ (1+\beta_e) \frac{(1-\frac{T_{re}}{T_1})[1-\exp(-k)] + \frac{\dot{Q}_e}{\rho V C_p T_1 A(1-\eta t)}}{E_{com}\frac{T_{re}}{T_1}[1-\exp(-k)] - \frac{\dot{Q}_e}{\rho V C_p T_1 A(1-\eta t)}} \quad (30H)$$

where k is given by (22H). Equation (30H) is the same as Equation (16) of Chapter II.

An expression for β_c can be obtained by substituting (27H) into (12H). Using the same defined quantities S, u, B, L_1, L_e, as before, the following is obtained,

$$\beta_c = (\frac{aX\eta\rho V^3 A}{E_{fc}\ Re^b\ \dot{Q}_e})\ x$$

$$(\frac{E_{com}\frac{T_{re}}{T_1}[1-\exp(-k)] - \frac{\dot{Q}_e}{\rho V C_p T_1 A(1-\eta t)}}{(1-\frac{T_{re}}{T_1})[1-\exp(-k)] + \frac{\dot{Q}_e}{\rho V C_p T_1 A(1-\eta t)}}) \quad (31H)$$

where k is again given by (22H).

Equations (31), (32), (34), and (35) stem from (30H). For the laminar solution, (31) and (32) the value of k changes as $\bar{h}$ is corrected for entrance effects as given by Equation (30), Chapter II. Similarly for the turbulent solution, Equations (34) and (35), where $\bar{h}$ is adjusted for entrance effects by (33).

BIBLIOGRAPHY

1. ARI Standard 410-64, Standard for Forced Circulation Air-Cooling and Air-Heating Coils, Air-Conditioning and Refrigeration Institute, Virginia, 1964.

2. Armstrong, R. J., "Heat Transfer Correlations for: "Freon" 12, "Freon" 22, and "Freon" 502," Freon Technical Bulletin B-45, Published by E. I. DuPont de Nemours and Company, 1968.

3. ASHRAE Handbook of Fundamentals, 1972, Chapter 6.

4. ASHRAE Systems Handbook and Product Directory, 1973, Chapters 35, 43, 44.

5. Beauvais, F. N., "An Aerodynamic Look at Automotive Radiators," SAE Paper No. 650470, May, 1965.

6. Brandis, R., Principles of Economics, Richard D. Irwin, Inc., Illinois, 1968.

7. Carrier, W. H., Cherne, R. E., Grant, W. A., and Roberts, W. H., Modern Air Conditioning, Heating, and Ventilating, Pitman Publishing Corporation, New York, 1959.

8. Chaddock, J. B., "Film Condensation of Vapor in a Horizontal Tube," Refrigerating Engineering, Vol. 65, No. 4, April, 1957, p. 36.

9. Colburn, A. P., "A Method of Correlating Forced Convection Heat Transfer Data and a Comparison with Fluid Friction," Transactions of AICE, Vol. 54, 1933, pp. 174-210.

10. Conklu, O., "Computer Simulation of Automotive Air-Conditioning Condensers," SAE Paper No. 720076, January 10, 1972.

11. Cook, N. A., "Economic Factors in Radiator Selection," SAE Paper No. 720714, September 11, 1972.

12. Davis, G. L., Chianese, F., Jr., and Scott, T. C., "Computer Simulation of Automotive Air Conditioning--Components, System, and Vehicle," SAE Paper No. 720077, January 10, 1972.

13. Dickerson, S., and Robertshaw, J., Planning and Design: The Systems Approach, Copyright, 1973.

14. Fan Engineering (An Engineer's Handbook), Edited by R. Jorgensen, Buffalo Forge Company, New York, 1961.

15. Hamilton, J. F., and Pearson, J. T., "Typical Performance Characteristics of the Basic Vapor-Compression Cooling System," ASHRAE Transactions, Vol. 80, 1974, pp. 271-275.

16. Jennings, B. H., Environmental Engineering--Analysis and Practice, International Textbook Company, Pennsylvania, 1970.

17. Kays, W. M., "Numerical Solutions for Laminar-Flow Heat Transfer in Circular Tubes," Transactions of ASME, Journal of Applied Mechanics, Vol. 177, November, 1955, pp. 1265-1274.

18. Kays, W. M., and London, A. L., Compact Heat Exchangers, McGraw-Hill Book Company, New York, 1964.

19. Kreith, F., Principles of Heat Transfer, 2nd Edition, International Textbook Company, Pennsylvania, 1965.

20. McAdams, W. H., Heat Transmission, 3rd Edition, McGraw-Hill Book Company, New York, 1954.

21. McMurray, S., "Rising Fuel Costs Heighten Interest in Public-, Municipal-Owned Utilities," Air Conditioning Heating and Refrigeration News, November 4, 1974, pp. 1, 6, 7.

22. McQuiston, F. C., and Tree, D. R., "Optimum Space Envelope of the Finned Tube Heat Transfer Surface," ASHRAE Transactions, Vol. 78 (Part 2), 1972, pp. 144-152.

23. Pearson, J. T., Leonard, R. G., and McCutchan, R. D., "Gain and Time Constant for Finned Sperpentine Crossflow Heat Exchangers," ASHRAE Transactions, Vol. 80 (Part 2), 1974, pp. 255-267.

24. Rich, D. G., "The Effect of Fin Spacing on the Heat Transfer and Friction Performance of Multi-Row, Smooth Plate Fin- and-Tube Heat Exchangers," ASHRAE Transactions, Vol. 79 (Part 2), 1973, pp. 137-145.

25. Rohsenow, W. M., and Choi, H. ., Heat, Mass, and Momentum Transfer, Prentice Hall, Inc., New Jersey, 1961.

26. Schlicting, Dr. H., Boundary-Layer Theory, 6th Edition, Translated by Dr. J. Kestin, McGraw-Hill Book Company, New York, 1968.

27. Schoonman, W., "Aircooler Optimization Aided by Computer," Symposium on Air-Cooled Heat Exchangers, Published by ASME, 1964, pp. 86-102.

28. Shepherd, D. G., "Performance of One-Row Tube Coils with Thin Plate Fins," Heating, Piping, and Air Conditioning, Vol. 28, No. 4, April, 1956, pp. 137-144.

29. Smith, M. C., "Performance Analysis and Model Experiments for Louvered Fin Evaporator Core Development," SAE Paper No. 720078, January 10, 1972.

30. Spiegler, K. S., Editor, Principles of Desalination, Academic Press, New York, 1966.

31. Stanford Research Institute, "Patterns of Energy Consumption in the United States," January, 1972.

32. Stoecker, W. F., Refrigeration and Air Conditioning, McGraw-Hill Book Company, New York, 1958.

33. Traviss, D. P., Rohsenow, W. M., and Baron, A. B., "Forced-Convection Condensation Inside Tubes: A Heat Transfer Equation for Condenser Design," ASHRAE Transactions, Vol. 79 (Part 1), 1973, pp. 157-165.

34. Wark, K., Thermodynamics, McGraw-Hill Book Company, New York, 1966.

35. Wrench, J. C., "Factors Affecting RAC Efficiency," ASHRAE Transactions, Vol. 80 (Part 2), 1974, pp. 265-267.

36. Young, D., and Contreras, L., "Expected Present Worth of Cash Flows Under Uncertain Timing," Engineering Economist, Vol. 20, No. 4, 1975, pp. 257-268.

37. Zahn, W. R., "Factors Influencing Automotive Air Conditioning Evaporator Optimization," SAE Paper No. 690131, January 13, 1969.